Time Domain Reflectometry Measurement of Water Content and Electrical Conductivity Using a Polyolefin Coated TDR Probe

by

Gerald Ronald McIsaac

A thesis
presented to the University of Waterloo
in fulfillment of the
thesis requirement for the degree of
Master of Environmental Studies
in
Geography

Waterloo, Ontario, Canada, 2010

AUTHOR'S DECLARATION

I hereby declare that I am the sole author of this thesis. This is a true copy of the thesis, including any required final revisions, as accepted by my examiners.

I understand that my thesis may be made electronically available to the public.

Abstract

The use of time domain reflectometry (TDR) to determine water content (θ_v) from the measurement of the apparent dielectric constant (K_a) or the square root of the apparent dielectric constant ($K_a^{0.5}$) in highly saline environments has been limited due to the dampening effect that electrical conductivity (EC) has on the TDR signal. The objective of this research was to evaluate the use of a three-rod TDR probe with a polyolefin coating on the center-conducting rod (CCRC probe) to simultaneously measure θ_v and EC in saline conditions where standard, non-coated TDR probes (NC probe) are ineffective.

The application of a 0.00053 m thick polyolefin coating on the center-conducting rod of a CS605 TDR probe increased the capability of the probe to measure θ_v at EC levels as high as 1.06 S m^{-1} compared to 0.132 S m^{-1} for a NC CS605 probe. The CCRC probe was found to be incapable of determining any difference in EC levels. A 0.01 m long section or "gap" at the center of the polyolefin coating on the center conducting rod (GAP probe) was cut from the polyolefin coating to expose a section of the stainless steel center-conducting rod to allow direct contact with the material being sampled. The GAP probe was found to be capable of measuring θ_v and EC at EC levels as high as 0.558 S m^{-1}.

Using a water-air immersion method, a comparison between the NC probe and the CCRC and GAP probes was undertaken. The correlation between θ_v vs. $K_a^{0.5}$ was found to be linear for all three probes with the slope (m) of the regressed equation for the NC probe (m = 7.71) being approximately twice that of the CCRC probe (m = 4.25) and the GAP probe (m = 4.36). The intercept values were equivalent for all three probes. The linearity between θ_v vs. $K_a^{0.5}$ for the NC and CCRC probes using the water-air immersion method was also observed when the probes were used to measure $K_a^{0.5}$ of different sand-water mixtures. The slope of regressed equation for the NC probe in the sand-water

mixtures (m = 7.69) was equivalent to the water-air immersion slope for the NC probe, however the intercept values for the sand-water mixtures was lower than the intercept values for the water-air immersion method. Similarly, the slope of the CCRC probe in the sand-water mixtures (m = 5.00) was equivalent to the CCRC probe water-air immersion slope. Calculated $K_a^{0.5}$ values using a water-air dielectric-mixing model (WAMM) were equivalent to measured $K_a^{0.5}$ values for the NC probe. The water air immersion method was found to provide a suitable methodology for TDR research, however a more definitive test of the coated probe response in a series of soils with a range of homogenous water contents should be completed to ascertain the reliability of the water-air immersion method.

The straightforward relationship between the inverse of TDR measured impedance (Z_L^{-1}) and EC provided an effective calibration method for both the NC and GAP probes. The use of the Giese-Tiemann method to establish a calibration curve for EC measurement was limited to a maximum EC level of 0.132 S m^{-1} for the NC probe. The use of the cell constant method was considered to be unacceptable as a means of developing a calibration curve due to the fact that the cell constant K was not a constant value.

$K_a^{0.5}$ values for the CCRC and GAP were consistently less than $K_a^{0.5}$ values for the NC probe at all θ_v levels except θ_v = 0.000 m^3 m^{-3} or 100% air. The difference in $K_a^{0.5}$ ($\Delta K_a^{0.5}$) between the NC probe and the CCRC and GAP probes was seen to increase with increasing water content. Similarly, a measurable effect was found between the TDR waveforms for the NC probe when the probe head was surrounded completely by air when compared to the TDR waveforms for the NC probe when the probe head was completely surrounded by water. Modeled electrostatic fields for the NC and CCRC CS605 TDR probes displayed a decrease in the electric potential and electric field intensity in the region outside of the polyolefin coating of the CCRC probe compared to the NC probe. The decrease

in potential and electric field intensity became greater when the dielectric constant of the material surrounding the CCRC probe increased.

The use of a polyolefin coating on the center-conducting rod with a small section of the coating removed at the midsection of rod provides an effective means of extending the application of TDR θ_v and EC measurement in saline environments where standard TDR probes cannot be used.

Acknowledgements

Thank you to the many people who have given me the great amount of support that has allowed me to complete my work. It has been a very long road with many obstacles to overcome.

Thanks to my supervisor, Dr. Jonathan Price, for patiently walking me through the process.

Thanks to all the friends I have gathered along the way: Marilou Montemayor, Pete Whittington, Sarah Mouneimne. I have enjoyed working and hanging out with you.

Thanks to Ty Ferre for taking the time to provide some necessary perspective on my work.

The great support of my parents, John and Shirley McIsaac, was so important to me during this step in my life. Although they could not stay around long enough to see the final product, I know deep in my heart, they are still with me. Thanks so very much Mom and Dad.

My good buddy and father-in law, Don McConkey and my other mom, Joy Arthurs, gave the same support. Thanks buddy, thanks Joy. I wish you could have been here for this. I know you are in spirit.

The greatest thanks go to my very best friend and all-time sweetheart, Joanne. I wouldn't have finished this if it were not for you Jo. Love you.

Dedication

For Joanne

Whom I Love Dearly

“I love you so much it hurts my soul”

“I’ll protect you from the Hooded Claw”

“Keep the vampires from your door”

Frankie

Table of Contents

List of Figures

List of Tables

Chapter 1
Introduction

1.1 Reason for the Research

Due to a storm surge, a peat bog mining operation in Pokesudie, New Brunswick, was inundated with saltwater from a greater than normal high tide. The saltwater contaminated the peat soil that was being harvested for commercial sales, effectively shutting down the operation resulting in substantial economic loss. Similar situations occur, such as the contamination of landfill sites or the spill of hazardous materials in urban areas, where it would be useful to determine the extent of the contamination and how the contamination could best be mitigated.

To obtain the required information it would be necessary to understand how the hydrological processes of the site affect the movement of the contamination, which in the case of the peat bog mining site would require the capability to simultaneously measure soil water content and electrical conductivity, as an indirect measure of the saltwater contamination, of the soil at several locations and depths over time. Mapping differences in soil water content and electrical conductivity with respect to location and time would provide necessary information to determine the hydrological processes affecting the movement of the contamination.

Attempts to use time domain reflectometry (TDR) with a standard TDR probe to measure soil water content and electrical conductivity at the Pokesudie site were unsuccessful because water content could not be determined due to the high electrical conductivity levels caused by the saltwater intrusion. To overcome this problem a modified TDR probe was developed. A thin polyolefin coating with a small gap was applied to the center rod of a three-rod TDR probe that made it possible to measure water content and electrical conductivity simultaneously. Since the TDR probe had been altered from its original condition, it was not known what the effect of the coating with a gap would

have on the measurements taken. To gain a better understanding of the changes introduced by this modified probe, the present study was undertaken.

1.2 Purpose of the Research

Time domain reflectometry (TDR) has been developed as a nondestructive means to simultaneously measure soil water volumetric content (θ_v) and bulk soil electrical conductivity (EC). Typically, soil water volumetric content and bulk soil electrical conductivity are determined from a TDR waveform that displays the changes in the TDR signal measured from a TDR probe inserted in the soil. TDR measurements of θ_v and EC are determined from different sections of the TDR waveform and are calculated separately.

In highly saline soils, TDR cannot be used to measure θ_v using standard TDR probes because of the adverse effect that high EC levels have on the TDR signal. An increase in soil electrical conductivity reduces the TDR signal to such a point that it is not possible to discern the difference between TDR waveforms collected from soils with different water volume contents. Coating one or more of the TDR probe rods with a nonconductive material has been shown to reduce the effect EC has on the TDR signal, making it possible to measure θ_v at higher EC levels than normally possible with a standard TDR probe. However, the completely coated TDR probe was found to be incapable of measuring EC unless a small section of the coating was removed. To understand the effect that the coating with a small gap had on TDR measurement a calibration of the probe was necessary. The purpose of this research was to evaluate how a polyolefin coating on the center conducting rod of a three-rod TDR probe with and without a small gap affected TDR measurement of 1) θ_v using the water air immersion method and a standard calibration method using sand-water mixtures, 2) TDR measurement of EC using water and salt solutions to give increasing EC levels and 3) identify possible reasons why and how the coating affects the TDR signal.

1.3 Background

TDR has been used to determine θ_v in several types of soil in laboratory settings and field evaluations (Topp et al., 1980; Topp and Davis, 1985). Automated TDR systems have been established to measure θ_v in remote locations using real time monitoring (Heimovaara and Bouten, 1990) to provide high-resolution information on the changes in θ_v at temporal and spatial scales (Herkelrath et al., 1991).

Pepin et al. (1992) determined that TDR could be used to estimate θ_v in peat soils between 0.21 - 0.95 m^3 m^{-3} with a standard deviation of 0.03 m^3 m^{-3}, however substantial variation was found in measured θ_v using the calibration procedure developed, which was considered to be the result of differences in the particle size and heterogeneity of the peat. Paquet et al. (1993) corroborated the findings of Pepin et al. (1992) for TDR peat θ_v determination. Kellner and Lundin (2001) successfully used TDR to determine θ_v in peat soils and state that the degree of humification of peat soils affected TDR θ_v measurement. TDR measured θ_v was found to be insensitive to changes in peat density (Shibchurn et al., 2005).

Dasberg and Dalton (1985) used TDR to measure θ_v and EC simultaneously in fine loamy sand and found TDR EC measurements were comparable to EC measurements obtained using a typical conductivity instrument, i.e. a four-probe electrode. Further study determined that the TDR and four-probe electrode measured EC values were considerably different than originally speculated (Dalton and Van Genuchten, 1986). Similarly, Topp et al. (1988) found differences in TDR EC measurements compared to EC measured using a bridge type conductivity instrument. All the same it was determined that, in principle; TDR provides an accurate method to determine the EC of aqueous solutions and moist soils. However, TDR θ_v measurement has been found to be limited in saline soils because an increase in soil EC affects the resolution of the TDR signal (Wyseure et al., 1997; Or et

al., 2004). Wyseure et al. (1997) found that θ_v measured using TDR was overestimated when soil solution EC was greater than 0.2 S m^{-1}, while Sun et al. (2000) determined that θ_v could not be measured when the saturated soil extract EC exceeded 0.637 S m^{-1}.

To overcome this problem, the application of a nonconductive coating material has been applied to TDR probes. Coatings that have been applied include phenolic fabric or adhesive polyethylene sheeting (Mojid et al., 1998), PVC (Ferre et al., 1996), heat shrink polyolefin tubing (Nichol et al., 2002; Persson et al., 2004), heat shrink Teflon tubing (Miyamoto and Maruyama, 2004) and a polymer-ceramic composite (Fujiyasu et al., 2004). In fact, one manufacturer provides TDR probes with a PVC coating applied to the probe rods (Becker et al., 2006).

In order to use a coated TDR probe, an understanding of the effect the coating has on TDR measurement and calibration is necessary. The basic premise of any calibration method is to measure the responses for a series of known standards, determine the relationship between the responses and the standards, measure the unknown sample response and determine a value for the unknown sample from the measured value. In the case of TDR, the dielectric constant of a sample is the response being measured and correlated.

Different calibration methods have been used to calibrate TDR probes. Standard calibration methods use the material in which the probe is to be used, e.g. mineral or organic soils, where TDR measurements have been obtained in the selected soil with controlled water content and/or electrical conductivity levels. A widely recognized calibration has been developed through the work of Topp et al. (1980) for the determination of water content in mineral soils. Standard calibrations have also been undertaken for organic or peat soils (Pepin et al., 1992; Paquet et al., 1993; Kellner and Lundin, 2001) The dielectric constant of several different soil types of different water contents were measured using TDR and compared to the actual water content of the soils that was determined gravimetrically.

Liquids with known dielectric constants have been used for calibration purposes. Several liquids have been used, including penetrating oil and acetone (Robinson et al., 2003b) as well as rapeseed oil, syrup and ethanol (Persson et al., 2004). Blends of liquids with water have also been used to provide a range of standard dielectric constants by blending measured volumes of the liquid and water. Blends of water and alcohols have been widely used; blends of propanol and water (Robinson et al., 2003a), isopropoxyethanol and water (Jones et al., 2005) and many others.

A water air immersion method has been used to replicate the response of a TDR probe at different water contents by immersing the TDR probe rods to different depths in a column of water (Robinson et al., 2003b; Heimovaara et al., 2004; Becker, 2004). The TDR measured dielectric constant can be correlated to the actual volume of water that the probe rods are immersed in.

The water air immersion method was selected as a calibration method for this study because the method was found to provide accurate and reproducible measurements quickly and efficiently over a range of dielectric constants from 1 to 81. Since one of the objectives of this study was to determine the effect the polyolefin coating has on TDR θ_v measurement, the ability to accurately control the test parameters, i.e. ratio of the probe rods in air and water, allowed the coating on the probe to be isolated as the single variable. Any differences between $K_a^{0.5}$ determined using the non-coated and coated probes would be directly related to the coating applied. Correlation between the coated probe TDR $K_a^{0.5}$ response using the water air immersion method and the coated probe TDR $K_a^{0.5}$ response using sand-water mixtures would indicate that the water air immersion method provides a reasonable means to compare responses for different TDR probe designs.

Chapter 2
Measuring Volumetric Water Content and Electrical Conductivity Using TDR

2.1 Measuring Volumetric Water Content (θ_v) Using TDR

The use of TDR for θ_v measurement has become commonplace. The basic premise for using TDR to measure θ_v is based on the ratio of the velocity of an electromagnetic (EM) wave in a vacuum (c) to the velocity of an EM wave in a given medium (v_p). The ratio of these two velocities represents an indirect measure of the index of refraction (η) of a medium as:

[2.01] $\eta = c / v_p$

The index of refraction is related to the dielectric permittivity (ε) of a material as $\eta = \varepsilon^{0.5}$ where ε can be expressed as the relative dielectric constant (ε_r), which is the dielectric permittivity of a material relative to a vacuum (ε_0), from $\varepsilon_r = \varepsilon / \varepsilon_0$ giving $\eta = \varepsilon_r^{0.5}$. For any material that an EM wave travels through, ε_r can be substituted for η into Eq. [2.01] to give:

[2.02] $\varepsilon_r^{0.5} = c / v_p$

TDR θ_v determination is assessed by measuring v_p for a sample by measuring the travel time (t_t) required for an EM wave to travel the length of a TDR probe (d) immersed in the sample from:

[2.03] $t_t = d / v_p$

And using [2.03] in [2.02] gives:

[2.04] $\varepsilon_r^{0.5} = ct_t / d$

Topp et al. (1980) used Eq. [2.04] to determine θ_v for various soils by measuring t_t to calculate ε_r. The methodology was based on the definitive difference in ε_r between the major soil matrix components: water, air and soil. Nominal ε_r for water (ε_{water}), air (ε_{air}) and soil (ε_{soil}) are 81 (at

18°C), 1 and 1.5-6, respectively. The large difference between ε_{water} and both ε_{air} and ε_{soil} means the v_p in a soil with high θ_v will be considerably slower than the v_p in a soil with low θ_v and the time for the EM wave to travel through the sample will increase with increasing θ_v.

Topp et al. (1980) measured t_t to determine the ε_r for soils of differing θ_v using a coaxial cell that is electrically equivalent to a coaxial cable with the insulating dielectric material replaced by the test soil. A coaxial cable (Fig. 2.01) is commonly used to transmit EM waves, e.g. cable television signals, and is manufactured in the form of a concentric layering of an inner conducting wire, usually copper, encased by an insulating dielectric material such as polyethylene that is then covered with a braided shield wire that acts as a ground. The entire construction is then covered with an insulating jacket, commonly polyvinylchloride (PVC), to protect the internal components of the cable.

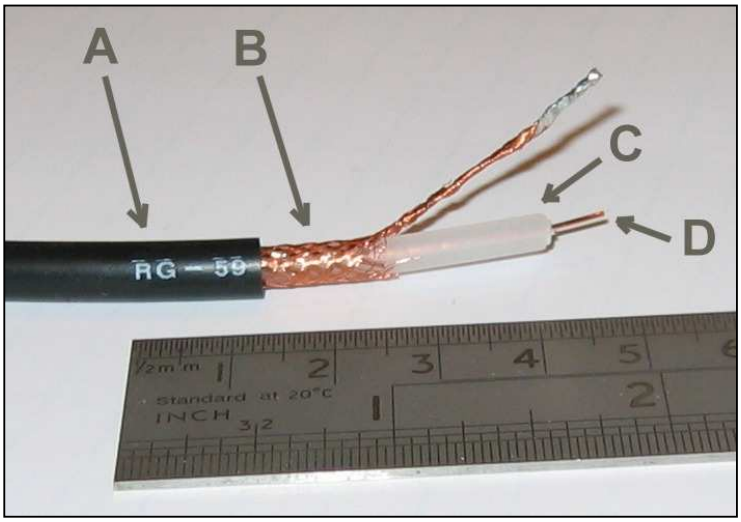

Fig. 2.01 Coaxial Cable Construction
(A) Insulating Jacket (B) Braided Shield Wire (C) Insulating Dielectric Material
(D) Inner Conducting Wire (Source: Belden Cable)

The v_p of an EM wave traveling through a coaxial cable is dependent on the ε_r of the inner insulating material as per Eq. [2.02] and forms the basis for the coaxial cell measurements of Topp et al., (1980). By replacing the inner insulating material with soil at different θ_v, ε_r was determined by

measuring the time required for the EM wave to travel the length of the coaxial cell containing the soil sample.

The dielectric permittivity of a material is a complex parameter consisting of a real part (ε'), an imaginary part (ε''), where ε'' represents the electric loss due to frequency dependent loss mechanisms such as dielectric relaxation and the zero frequency conductivity (σ_{dc}), which is dependent on the angular frequency (ω) of the EM wave and the dielectric permittivity of a vacuum (ε_0 = 8.54E-12 farads per meter (F m^{-1})) with $j = (-1)^{0.5}$ representing the imaginary component as:

[2.05] $\varepsilon = \varepsilon' + j(\varepsilon'' + (\sigma_{dc} / \omega\varepsilon_0))$

For this reason, TDR does not measure an exact value of ε and Topp et al. (1980) assumed that ε' was significantly greater than the electric loss, i.e. $\varepsilon' >> \varepsilon'' + (\sigma_{dc} / \omega\varepsilon_0)$, such that $\varepsilon \approx \varepsilon'$. Even though the electric loss was not measurable, Topp et al. (1980) accounted for the exclusion of this term by representing ε as the apparent dielectric constant K_a, replacing ε_r such that:

[2.06] $K_a^{0.5} = ct_t / d$

The use of a laboratory coaxial cell for θ_v measurement is not easily transferred to field soil measurement of θ_v since it would disrupt the soil structure. For this reason, various field waveguide probes have been designed specifically for field studies. A common design uses a three-rod probe (Zegelin et al., 1989) that is considered to emulate a coaxial cell (Fig. 2.02). This probe consists of three parallel steel rods that are connected to a coaxial cable. The inner conducting wire of the coaxial cable is soldered to the center rod of the three parallel rods and the grounded shield wire is split in half and soldered to both of the two outer rods.

The section where the rods are soldered to the coaxial cable forms the probe head and is typically cast in an epoxy resin to protect the cable connection from the surrounding environment. The exposed rod lengths can then be inserted into the soil such that the soil takes the place of the

inner, insulating dielectric material between the center conducting rod and the two outer ground shield rods. In essence, the coaxial cable transmission line leading to the probe rods has been altered to a parallel three-wire transmission line, which can be considered analogous to a conjoined symmetric twin wire transmission line.

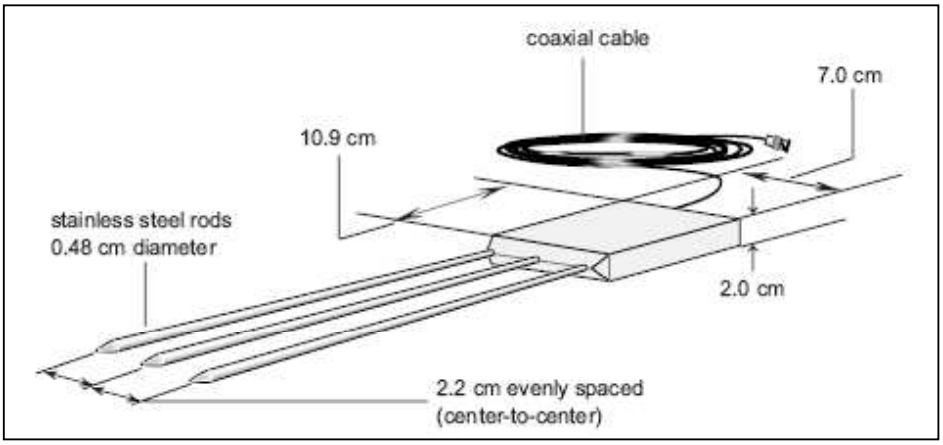

Fig. 2.02 Three-rod CS605 TDR Probe
(Source: Campbell Scientific Inc.)

Typically, a twin wire transmission line is balanced, i.e. the voltage in the two wires are equal in magnitude but different in sign with a positive voltage on one wire and a negative voltage on the other wire. Coaxial cables are different in that the system is unbalanced with a voltage exclusively on the center-conducting rod. This aspect of coaxial cable design means that no voltage is generated along the outer shield wire conductor as long as the current in the center conductor is returned through the shield wire conductor (Dascher, 1996). The connection of the center conducting wire of the coaxial cable to the center-conducting rod of the three-rod TDR probe means that the three-rod probe represents an unbalanced transmission line.

2.2 Measuring K_a Using TDR

The travel time, t_t, for an EM wave to propagate through the sample is commonly measured using a TDR instrument such as the Tektronix 1502B Metallic TDR Cable Tester (Beaver, Oregon,

USA) or the Campbell Scientific Inc. TDR100 (Logan, Utah, USA). The EM wave generated by a TDR instrument comes from a repeated, controlled voltage pulse into a coaxial cable and through to the TDR probe. As the TDR signal travels along the coaxial cable and into the TDR probe the voltage will increase, decrease or remain constant depending on the dielectric properties of the insulating dielectric material of the coaxial cable and the sample medium surrounding the probe. The change in voltage along the coaxial cable and the TDR probe is displayed as a waveform trace on an oscilloscope screen with respect to time.

In practical application, the voltage changes shown on a 1502B waveform are displayed as discrete changes in the measured impedance (Z). Most TDR systems display the magnitude of the voltage changes in terms of the reflection coefficient, which is the ratio of the voltage reflected back from a discrete point divided by the initial voltage going into that point. The reflection coefficient (ρ) is defined as the ratio of the initial or incident voltage (V_i) and the reflected voltage (V_r) as:

[2.07] $\rho = (V_r - V_i) / V_i$

The reflection coefficient is related to impedance of the coaxial cable (Z_0), which is typically 50Ω for most TDR systems, and Z_L of the TDR probe in the soil by:

[2.08] $\rho = (Z_L - Z_0) / (Z_L + Z_0)$

The 1502B plots Z or ρ values as a function of the electrical distance or apparent length on the horizontal axis, which represents the time traveled by the EM wave. The apparent length can be converted to time using the 1502B propagation velocity factor. The 1502B allows for variable propagation velocity factor settings in order to match the v_p of the generated EM wave to the v_p of the insulating dielectric material. Most TDR soil measurements use the propagation velocity factor setting for air, which is 0.99.

When there is no difference between the impedance of the coaxial cable (Z_0) and the impedance of the TDR probe (Z_L), all of the energy traveling along the transmission line is transferred

into the sample. When a difference does exist between Z_0 and Z_L, not all of the energy in the system can be transferred from the coaxial cable to the TDR probe and some of the energy is reflected back through the probe and the coaxial cable to the TDR instrument. Any changes in Z are displayed on the TDR waveform trace and the time at which these changes occur can be determined from the apparent length at which the change occurs.

A typical TDR waveform obtained from a TDR probe inserted into a soil sample (Fig. 2.03) shows as a straight line representing the TDR signal passing through the coaxial cable since $V_r = V_i$ and $Z_0 = Z_L = 50\Omega$ so that $\rho = 0$ from Eq. [2.08]. As the signal enters the probe head, the impedance change gives the case of $Z_0 \neq Z_L$ resulting in a voltage change and subsequent reflection of the EM wave that gives a corresponding change in ρ. The initial change in ρ typically occurs at the soldered connection of the coaxial cable and the probe rods identifying the start point (ρ_1) of the TDR probe. The waveform then increases to a maximum (ρ_{apex}), decreases to a minimum value at ρ_{min} and then increases to a second maximum at ρ_f.

The distance to ρ_1 at the start point of the probe is identified as the first reflection point, which typically corresponds with an inflection in the waveform and an increase in ρ. The distance to the point where the waveform displays another inflection point and a second increase in ρ is identified as the second reflection point (ρ_2) corresponding to the position or distance to ρ_{min}. The total apparent length (l_t) is then the distance between ρ_1 and ρ_2 where l_t can be converted to the time required for the EM wave to travel the length of the probe and back. Since the reflected voltage pulse travels the length of the probe rods and back, the actual distance traveled by the EM wave is twice the length of the probe rods or $d = 2\ l_t$, which when substituted in [6] gives:

[2.09] $K_a^{0.5} = ct_t / 2l_t$

Determining the position of ρ_1 and ρ_2 is commonly done using the flat tangent or the dual tangent method (Heimovaara and Bouten, 1990; Or et al., 2004). Either method determines the position of the reflection point from the intersection point of two tangent lines drawn from ρ values prior to and after either of the points (Fig. 2.03). With the flat tangent method, a tangent line parallel to the x-axis is drawn using the average ρ_{min} just before the beginning of the reflection point, whereas the dual tangent method draws tangent lines leading to the apex of each inflection point.

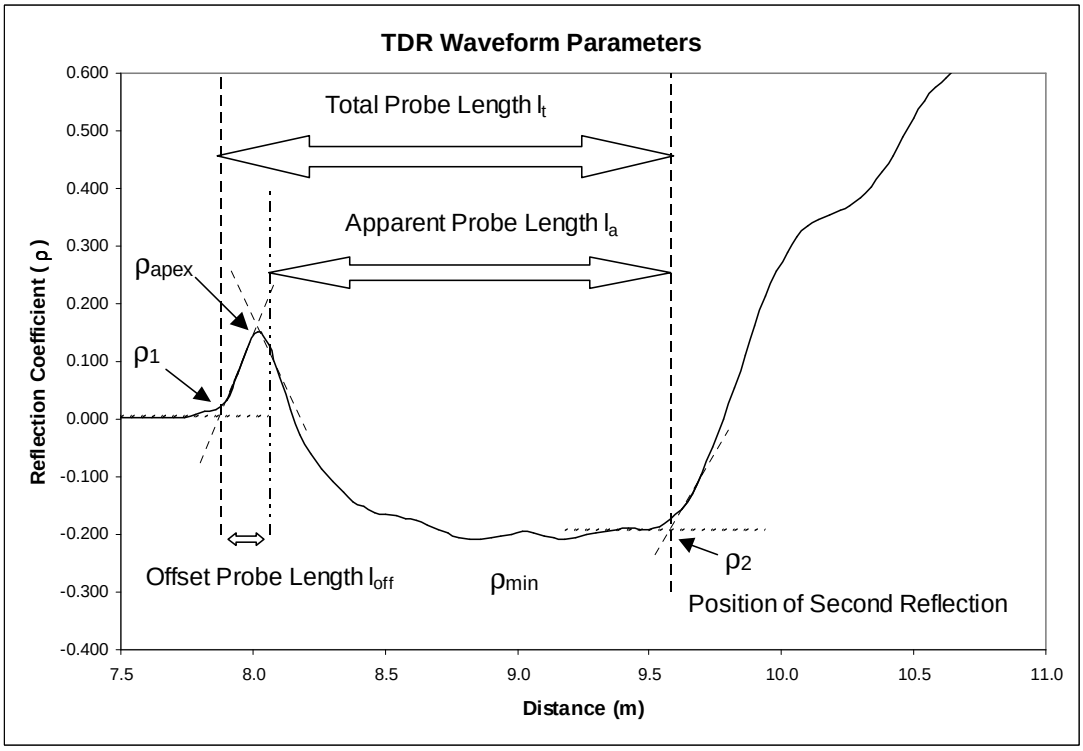

Fig. 2.03 TDR Waveform Parameters Obtained Using A Tektronix 1502B Metallic Cable Tester
Solid Line represents the measured TDR waveform.
Dotted Lines define waveform positions used to determine TDR measurements.

Since the flat tangent method measures the distance from ρ_1 to ρ_2, the measured total apparent length (l_t) includes the rod length encased in the probe head (l_h) and the exposed section of the probe rods (l_r). To obtain the apparent length that is exclusive to the exposed rods (l_a), the apparent length of the rod encased in the probe head has to be accounted for. This correction is

typically termed the probe offset (l_{off}) value and can be determined by measuring K_a for the probe in air where $K_a = 1$ or by immersing the probe in a liquid of known K_a, such as distilled water. The value of l_{off} is then determined by subtracting the measured value of l_t from the expected value of l_a for air or distilled water to get the probe offset from:

[2.10] $l_{off} = l_t - l_a$

The probe offset can also be determined using l_h and the dielectric constant of the material used to form the probe head (K_{head}) that encases that section of the probe rods. Since the TDR signal is applied along the entire length of the probe rods, the TDR waveform includes the change in Z that is contributed by the probe head material. If there is a change in Z due to the probe head material and the change is specific to the material comprising the probe head only, l_{off} can be calculated from l_h and K_{head} by rearranging Eq. [2.11] to:

[2.11] $l_{off} = l_h K_{head}^{0.5}$

Using l_t in place of t_t (Campbell Scientific Inc (CSI), 2005) provides a more efficient method to determine K_a directly from the TDR waveform since most TDR instruments use apparent length as the unit of measurement. Using l_t in place of t_t eliminates the operational step of computing t_t by replacing $ct/2$ in Eq. [2.09] with l_a and the one way distance of the exposed rod length (l_r) such that:

[2.12] $K_a^{0.5} = l_a/l_r$

The dual tangent method uses the position of ρ_{apex} to determine the starting point of the exposed probe rod length (Fig. 2.03) and effectively eliminates the need to determine l_{off}. An inherent error is introduced using this methodology since the time or distance to ρ_{apex} changes with a variation in θ_v (Robinson et al., 2003a). Robinson et al. (2003b) examined the problem of determining an accurate l_{off} value that is caused by the moving apex of a TDR waveform using a water air immersion method. Incremental insertion of a TDR probe to greater depths in water caused the position of the apex to occur at longer apparent lengths when the TDR probe was exposed to an increased volume of

water (Fig. 2.04). The error in K_a measurement due to this lateral movement of the apex with an increase in the volume of water surrounding the TDR probe lead to the decision to use the flat tangent method to determine l_t in this study.

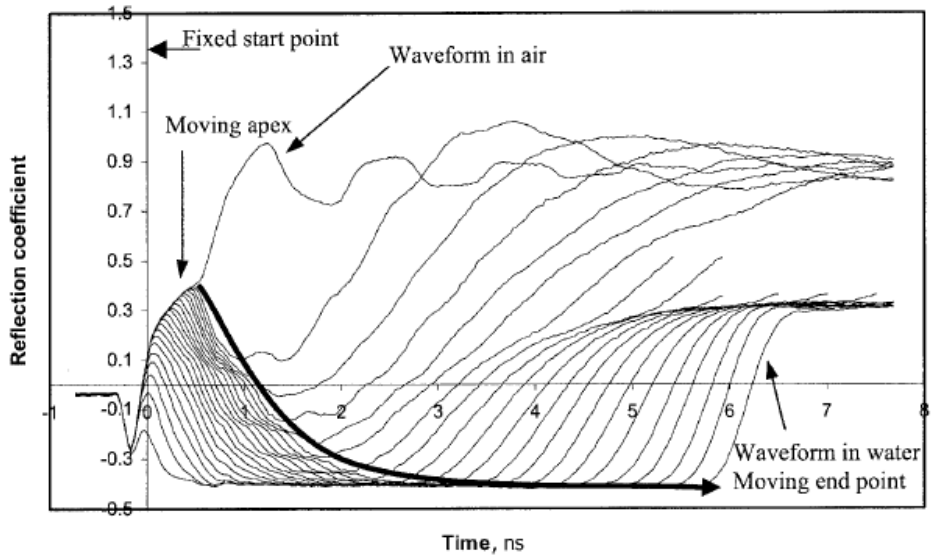

Fig. 2.04 Effect of Increasing Water Content on Position of TDR Waveform Apex
The position of the Moving Apex increases with the increase in Time due to an increase in water content. (From Robinson et al. (2003b))

2.3 Measuring Electrical Conductivity (EC) Using TDR

Fellner-Feldeg (1969) proposed that the derivative of ρ measured by TDR could be related to the EC of an electrolytic solution with respect to time. Dalton and van Genuchten (1986) determined that EC could be calculated from a TDR waveform (Fig. 2.05) using the voltage pulse entering a parallel transmission line (V_T) and the reflected voltage pulse (V_R) from:

[2.13] $EC = K_a^{0.5}/120\pi \ln (V_T/V_R)$ (Siemens [S] m^{-1})

Determining the position of V_R has proven to be difficult and at times impossible (Noborio, 2001). To overcome this problem Topp et al. (1988) combined the thin sample analysis of Giese and Tiemann (1975) with the work of Clarkson et al. (1977) to derive a method to determine EC that took

into account the multiple reflections found in the TDR waveform. This approach is commonly referred to as the Giese-Tiemann method and EC_{GT} is calculated as:

[2.14] $EC_{GT} = (\varepsilon_0 c/l_r)\,(Z_{TDR}/Z_0)\,[(2V_0/V_{inf}) - 1]$ $(S\ m^{-1})$

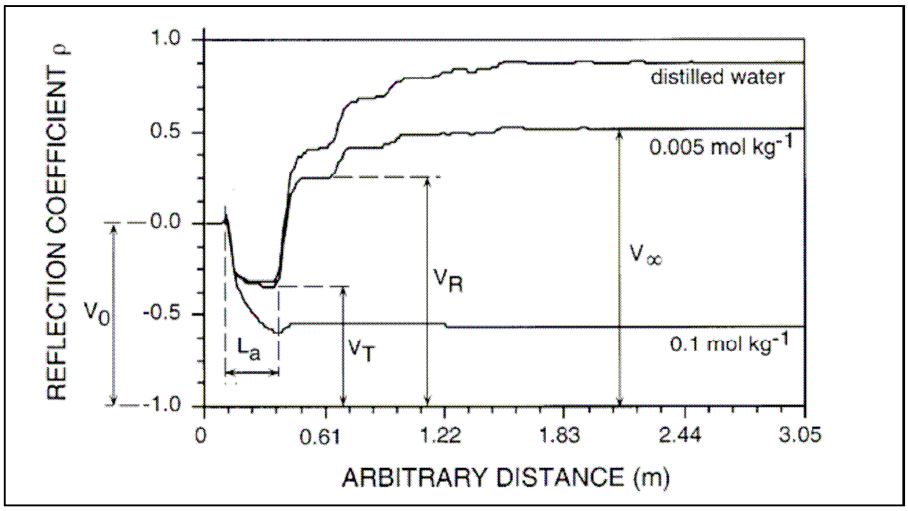

Fig. 2.05 TDR Waveform Parameters for Measuring EC
(From Noborio, 2001)

Where Z_{TDR} is the characteristic probe impedance, Z_0 is the cable tester impedance (usually 50Ω), V_0 is the incident pulse voltage and V_{inf} is the return pulse voltage after the multiple reflections have ceased (Fig. 2.06). Z_{TDR} is usually determined by immersing the TDR probe in deionized water, where K_{water} (for a known temperature) provides a reference dielectric constant and Z_0 is calculated from:

[2.15] $Z_{TDR} = Z_0\, K_a^{0.5}\, [V_1/(2V_0/V_1)]$ (Ω)

Where V_1 is the minimum voltage at the position of ρ_2, which is equivalent to ρ_{min}, so that V_1 is equivalent to ρ_{min}.

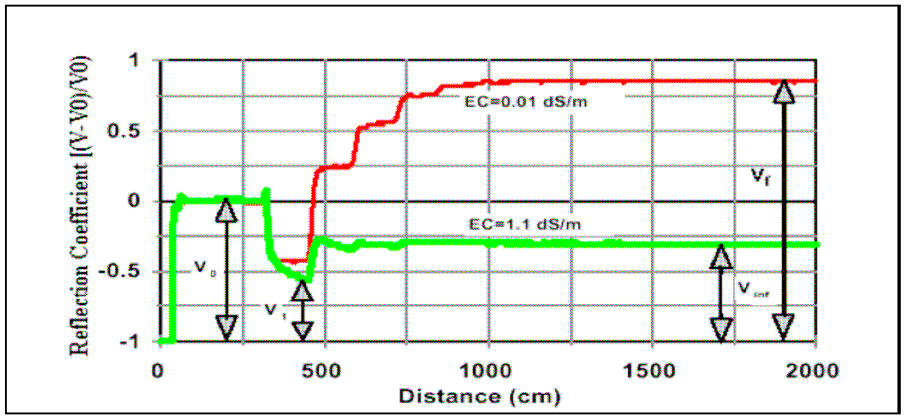

Fig. 2.06 TDR Waveform Parameters V_0, V_1, V_{inf} and V_f for Measuring EC
(From Or et al., 2004)

Voltage values (V_T, V_R, V_0, V_1 and V_{inf}) cannot be acquired directly from the Tektronix 1502B or the TDR100 instruments because these instruments report ρ values only. However, the relationship between ρ and V (Eq. 2.07) can be used to convert V to ρ values to allow direct application of ρ measurements from the 1502B and TDR100 instruments. The relationship between ρ and V from Eq. [2.07] gives:

[2.16] $(1 - \rho_x)/(1 + \rho_x) = (2V_0/V_x)/V_x = 2V_0/V_x - 1$

Where the subscript "*x*" applies to the location or apparent distance where ρ or V is read from the TDR waveform. Similarly, the inverse form gives:

[2.17] $(1 + \rho_x)/(1 - \rho_x) = V_x / (2V_0/V_x)$

Substituting Eq. [2.17] into Eq. [2.15] with $\rho_x = \rho_{min}$ yields:

[2.18] $Z_{TDR} = Z_0 K_a^{0.5} [(1 + \rho_{min})/(1 - \rho_{min})]$

And replacing Z_{TDR} from Eq. [2.18] into Eq. [2.14] gives the same result determined by Zegelin et al. (1989), which when combined with the ρ conversion of Eq. [2.16] yields:

[2.19] $EC_{GT} = (\varepsilon_0 c/l_r) K_a^{0.5} [(1 + \rho_{min})/(1 - \rho_{min})] [(1 - \rho_{inf})/(1 + \rho_{inf})]$ (S m^{-1})

Nadler et al. (1999) used a similar method and replaced the voltage measurements with ρ values from the TDR waveform to determine EC. This method has been designated as the cell constant method (EC_{cell}) and EC_{cell} is determined from:

[2.20] $EC_{cell} = (K/Z_c)\,[(1-\rho_{inf})/(1+\rho_{inf})]$ (S m^{-1})

Where K is the geometric constant of the probe (m^{-1}) and Z_c is the characteristic impedance of the coaxial cable (usually 50Ω). The solution for EC_{cell} is based on the premise that the correlation between EC_{cell} and $(1/Z_c)\,[(1-\rho_{inf})/(1+\rho_{inf})]$ is linear with K as the slope of the regression line of the two variables. Essentially, Eq. [2.20] is the inverted form of Eq. [2.08] that has been rearranged to solve for Z_L, i.e. $Z_L = Z_c\,[(1+\rho)/(1-\rho)]$ as $Z_L^{-1} = Z_c^{-1}\,[(1-\rho)/(1+\rho)]$, with the insertion of K as the probe constant term. This effectively reduces Eq. [2.20] to the simpler form of:

[2.21] $EC_{cell} = K\,Z_L^{-1}$ (S m^{-1})

Such that:

[2.22] $K = EC_{cell}\,Z_L$ (m^{-1})

It is not necessary to use ρ_{inf} to obtain an accurate measure of EC. Although ideally, the use of ρ_{inf} insures that all waveform reflections have ceased, it is possible to use a ρ value at a shorter distance (ρ_f) where the amplitude of the reflections have decreased significantly and the waveform flattens enough that ρ_f can be considered equivalent to ρ_{inf} and ρ_f can be used in place ρ_{inf} for the calculation of EC. The value of ρ_f can be determined visually from the waveform or the position of ρ_f can be selected as a specific distance past the measured value of l_a, e.g. Noborio (2001) considered that the position of ρ_f should be ten times longer than l_a.

All of the EC measurement methods described here use the electrical relationship between resistance (*R*) and impedance (*Z*), where *R* and *Z* can be considered equivalent for the purpose of this study. The relationship between *R* and the conductance (*G*) is $G = R^{-1}$, so that the reciprocal of

impedance is related to conductance by $G = Z^{-1}$. EC is then proportional to G and the cross sectional area of the probe rods and inversely proportional to the length of the probe rods (Jackson, 1976) as:

[2.23] $EC = A/(Gl)$

Where A and l are the respective cross sectional area and length of the conductor, which in this case would be analogous with the TDR probe rods. Since EC is dependent upon the probe dimensions, a separate calibration procedure would be required for any specific TDR probe design. However, for a given probe design EC (S m^{-1}) represents the G (S) of the medium being measured relative to the spatial dimensions of the probe.

The TDR waveform equations and their derivation used in this study are presented in Appendix A.

Chapter 3
Coated TDR Probes

3.1 Background

Problems are encountered when TDR is used to measure θ_v in saline soils with soil water of high electrical conductivity (EC). As the EC of the soil increases, the zero frequency conductivity (σ_{dc}) increases and the electric loss increases (see Eq. [2.05]). If σ_{dc} is large enough, then $\varepsilon'' + (\sigma_{dc} / \omega\varepsilon_0)$ becomes significant and the assumption that $\varepsilon \approx K_a$ is no longer valid. Essentially, the highly conductive soil matrix between the TDR probe rods is analogous to the formation of an electrical short circuit and all of the energy passes directly from the center-conducting rod to the outer shield rods with little or no interaction with the surrounding soil. As the soil EC increases, the ability to identify the location of the second reflection point on the TDR waveform is diminished to the point where it becomes impossible to accurately measure l_a. Dalton et al. (1984) determined that θ_v could not be measured using TDR when the soil EC exceeded 0.36 S m^{-1}. To extend the use of TDR in saline soils, the use of shorter length probes has been recommended (Robinson et al., 2003a), however there is a loss of resolution in the measurement of K_a because the shorter probes result in reduced t_t. The use of three-rod probes was found to be more suitable in saline soils than two rod probes, however three-rod probes were still not capable of measuring θ_v in highly saline soils (Whalley, 1993).

The application of a nonconductive coating material to the TDR probe rods has been successfully used to extend the capability of TDR θ_v measurement in saline soils. The nonconductive coating acts as a barrier between the probe rods and the soil preventing direct contact of the metal rods with the soil reducing the energy loss due to electrical conduction (Mojid et al., 1998). TDR

probe rods have been coated with phenolic fabric or adhesive polyethylene sheeting (Mojid et al., 1998), PVC (Ferre et al., 1996), heat shrink polyolefin tubing (Nichol et al., 2002; Persson et al., 2004) or heat shrink Teflon tubing (Miyamoto and Maruyama, 2004). TDR probes with a PVC coating are commercially available (Becker et al., 2006).

When a coating is applied to a TDR probe, the relationship between K_a and θ_v is affected. At least three factors have an effect on this relationship: the thickness of the coating applied, the dielectric constant of the coating material (K_{coat}) and the number of TDR probe rods that are coated. Analytical solutions have shown that increasing the thickness of the coating material resulted in a decrease in K_a (Annan, 1977a, 1977b; Knight et al., 1997; Ferre et al., 1996) and experimental results for a TDR probe immersed in water using coatings of an epoxy ceramic ($K_{coat} \approx 63$-77), enamel spray paint ($K_{coat} \approx 5$-8) and heat shrink polyolefin ($K_{coat} \approx 3$-4) showed a decrease in measured K_a with a decrease in K_{coat}. K_a was seen to decrease from 82.5 for the uncoated probe to 73.1, 47.1 and 28.0, for each of the respective coating materials (Fujiyasu et al., 2004).

Mojid et al. (1998) measured the effect on measured K_a for a three-rod TDR probe with different rod coating configurations. The coating configurations studied included coating of the center-conducting rod only, coating just the outer two rods coated and coating all three rods. Coating the center conducting rod or all three rods made it possible to measure θ_v in saline soils with EC levels as high as 7.88 S m^{-1}, while coating just the outer two rods limited θ_v measurement to soils with EC < 0.49 S m^{-1}. Measured K_a for all of the coated rod configurations was found to be lower than the measured K_a for the TDR probe with no coating with the greatest reduction in K_a occurring when all three rods were coated (Mojid et al., 1998). A similar reduction in measured K_a was found to occur using a TDR probe with non-coated rods when the center conducting rod and ground shield rods were separately inserted into dry or wet sand in the same configurations as the different coatings (Mojid and Cho, 2002). Measured K_a was found to be considerably lower when the center-conducting rod

was placed in dry sand and the ground shield rods were placed in wet sand compared to the center conducting rod in wet sand and the ground shield rods in dry sand, i.e. the center conducting rod had the greater effect on measured K_a.

Knight et al. (1997) determined that the effect of an air gap along the length of the center-conducting rod of a three-rod probe would be greater than the effect of an air gap along the length of the outer shield rods. In these cases, the air gap completely enveloped the TDR probe rods and could be considered analogous to a coating of air around a TDR probe rod such that $K_{coat} = 1$. The reason for the air gap around the center-conducting rod having a greater effect on K_a than an air gap around both of the two ground rods was based on the spatial weighting associated with the sensitivity of the TDR probe (Knight, 1992).

Ferre et al. (1996) considered a square root averaging model with uniform weighting factors for axially varying coating materials and an inverse averaging model with non uniform spatial weighting for transversely varying coating materials. Persson et al. (2004) used this approach for calibrating a coated-uncoated TDR probe design using a two-phase dielectric-mixing model.

3.2 Measuring θ_v and EC with a Coated TDR Probe

The application of a coating to the TDR probe rods was primarily intended to extend the capability of a TDR probe to measure θ_v in highly saline conditions. For the most part, research has been limited to determining the measurement of θ_v only and investigation into the effect that a coated TDR probe has on EC measurement is limited. Nichol et al. (2002), using a three-rod TDR probe with a 0.0004 m thick polyolefin coating applied to the center-conducting rod coated reported a nonlinear decrease in ρ_f with an increase in solution EC from 0.1 S m^{-1} to 7.0 S m^{-1}. A small decrease was seen in ρ_f from 0.1 S m^{-1} to 2.0 S m^{-1} while substantial differences in ρ_f occurred between successive EC levels for EC > 3.0 S m^{-1}. However, Nichol et al. (2002) noted a failure with the probe head seal that

led to the probe head rod sections being directly exposed to the EC solutions, which could adversely affect the measurement of ρ_f since the probe head center-conducting rod was not coated. Persson et al. (2004) determined EC measurement was not possible when the center-conducting rod was coated with their coated-uncoated probe design adaptation.

A TDR probe with the center-conducting rod coated with polyolefin was found to be incapable of discerning differences in soil and solution EC compared to a non-coated TDR probe for investigative lab and field studies (*pers. comm.* J. Price). However, by cutting out a section of the coating and leaving a section or "gap" in the coating where the center conducting probe rod was still in direct contact with the soil yielded a measurable decrease in ρ_f with increasing EC.

There are conflicting reports in the literature regarding the effect that changes in EC have on TDR measurement of θ_v. An overestimation of soil θ_v with increasing EC was found using non-coated probes (Wyseure et al., 1997; Sun et al., 2000; Persson et al., 2004), while Nichol et al. (2002) found no difference in θ_v for EC < 0.5 S m^{-1}. Nichol et al. (2002) and Persson et al. (2004), both report finding no difference in measured θ_v with increasing EC using a TDR probe with the center-conducting rod coated (Nichol et al., 2002; Persson et al., 2004).

To effectively use coated TDR probes for the measurement of θ_v in saline soils it would be necessary to determine the effect that EC would have on the TDR waveform collected using a coated TDR probe to measure θ_v. As noted above, past research has reported conflicting results regarding the effect that coatings have on TDR θ_v measurement with changes in sample EC and the present study was undertaken to evaluate and ascertain the effect that a polyolefin coating on the center conducting rod of a three rod TDR probe (CCRC probe) and a polyolefin coating with a "gap" on the center conducting rod of a three rod TDR probe (GAP probe) had on the measurement of θ_v and EC.

3.3 TDR θ_v Calibration

3.3.1 Standard Calibration Methodology

TDR measurements of soil θ_v are normally done using calibration curves derived by plotting K_a determined from TDR waveforms for TDR probes inserted in soils of known θ_v. Using the measured l_a from the TDR waveform for soils at different θ_v levels, K_a can be calculated using Eq. [2.12]. The most renowned calibration for mineral soils was derived by Topp et al. (1980) and uses a third order polynomial to relate K_a to θ_v as:

[3.01] $\theta_v = -0.053 + 0.0292K_a - 0.00055K_a^2 + 0.0000043K_a^3$

Eq. [3.01] was derived by forcing the regressed third order polynomial through K_a for water at 20°C, well outside of the data collected for the mineral soils tested. Considering that a third order polynomial mathematically includes an inflection point that generally occurs at the midpoint of the regression curve, using this calibration function for peat soils would not be prudent. The inflection point found with the calibration function of Topp et al. (1980) occurs over the region of $\theta_v = 0.450$ m^3 m^{-3} to 0.600 m^3 m^{-3}, which is generally well below the water content of most peat soils.

Calibration curves have been derived for use in peat soils and are listed below. A second order polynomial function (Eq. 3.02) was developed by Pepin et al. (1992) for peat from a forested bog, while third order polynomial functions were derived by Paquet et al. (1993) for peat mixed with sand and bark (Eq. 3.03) and Kellner and Lundin (2001) for peat from bog hummocks and hollows (Eq. 3.04). Shibchurn et al. (2005) derived a logarithmic regression calibration for peat used in biological filtering (Eq. 3.05).

[3.02] $\theta_v = 0.085 + 0.0192K_a - 0.00009545K_a^2$ Pepin et al. (1992)

[3.03] $\theta_v = -0.0055 + 0.0425K_a - 0.000975K_a^2 + 0.0000097K_a^3$ Paquet et al. (1993)

[3.04] $\theta_v = 0.039 + 0.0317K_a - 0.00045K_a^2 + 0.0000026K_a^3$ Kellner and Lundin (2001)

[3.05] $\theta_v = 0.2667 \ln K_a - 0.1405$ Shibchurn et al. (2005)

A comparison of the four peat soil calibration curves and the calibration curve from Topp et al. (1980) is presented in Fig. 3.01. The calibration curves display a wide variety of configurations indicating a high degree of variation in soil θ_v vs. TDR measured K_a. All of the peat soil calibration curves yielded θ_v values that were greater than θ_v values determined using the Topp et al. (1980) equation at equivalent K_a values.

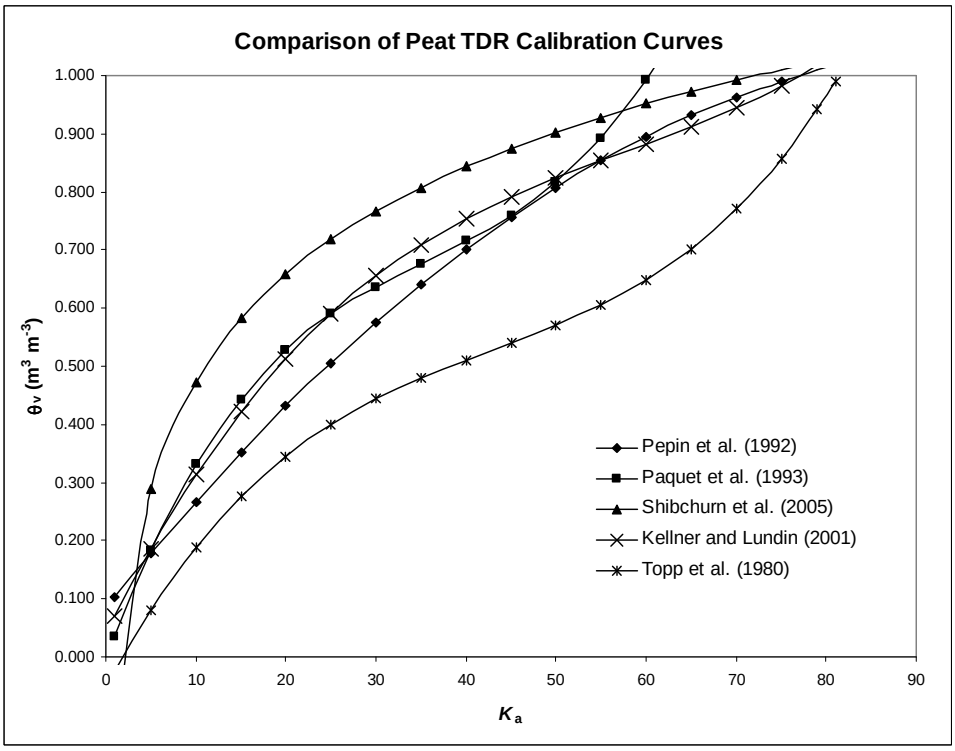

Fig. 3.01 Comparison of TDR Calibration Curves for Peat Soils

The problem of using a third order polynomial function for calibration is highlighted in the calibration curve of Paquet et al. (1993) where a substantial inflection point from $\theta_v = 0.400$ m^3 m^{-3} to 0.600 m^3 m^{-3} occurs in the same manner as the Topp et al. (1980) calibration curve. A similar pattern is seen with the Kellner and Lundin (2001) calibration curve, however the inflection point happens from $\theta_v = 0.650$ m^3 m^{-3} to 0.850 m^3 m^{-3}, which coincides with the average θ_v range for peat soils. The

pattern of the Shibchurn et al (2005) logarithmic calibration curve shows a rapid change in θ_v with increasing K_a for $K_a < 25$ with a gradual change in θ_v for $K_a > 25$ suggesting that a logarithmic function does not provide an optimum fit for calibration purposes.

3.3.2 Calibration Curves Using Liquids of Known K_a and Water Liquid Blends

Many studies have been conducted using liquids of known dielectric constant to provide TDR waveforms that provide a measured l_a value that can be correlated to a known K_a value. The types of liquids that have been used include alcohols, oil, paraffin and glycerol, where the majority of the materials have dielectric constants in the range between that of air and water. Other studies have used blends of a liquid of a known dielectric constant with water to yield calibration curves.

Two concerns are prevalent when calibration curves are derived using either of these two methods. Caution must be exercised to account for the effects on the TDR signal that would occur due to the dielectric loss (ε'') or imaginary permittivity and the electrical conductivity (σ_{dc}) of any particular liquid over the frequency range measured with the TDR system as described in Eq. [2.05]. If the liquid used exhibits a sizeable ε'' or is substantially conductive, the supposition that $\varepsilon' >> \varepsilon'' + (\sigma_{dc} / \omega\varepsilon_0)$ is no longer valid and the effect of either ε'' or σ_{dc}, or both, becomes significant. For the most part, many liquids are available that do not have any appreciable conductivity and the selection of a nonconductive liquid is not a concern for calibration purposes.

Robinson et al. (2003a) discuss the effect that dielectric relaxation has on the TDR measurement of ε' at frequencies within the TDR bandwidth of 0 .001 to 1.75 GHz. Measurements of ε' for propanol were found to decrease from 19.0 at a frequency of 0.2 GHz to 8.4 at 1.0 GHz, which means the signal at the lower frequency travels at a lower velocity relative to the signal at the higher frequency. Since the TDR signal comprises the frequencies between 0 .001 to 1.75 GHz, the TDR waveform represents the combined response of all frequencies within this frequency range.

Water exhibits dielectric relaxation at frequencies in the range of 17 GHz (Robinson et al. 2003a), which is well beyond the frequency range of TDR. However, when the liquid being measured by TDR exhibits dielectric relaxation within the frequency range imposed and an increase in ε'' occurs, TDR measured K_a is affected. Jones et al. (2005) determined ε' and ε'' for various liquids over the frequency range of 0 .001 to 1.0 GHz (Fig. 3.02). For propanol ($\varepsilon' = 22.7$) and glycerol ($\varepsilon' = 46.5$), dielectric relaxation was seen to occur over the frequency ranges of 0.01 to 1.0 GHz and 0.001 to 1.0 GHz, respectively. The increase in ε'' was substantial for each material indicating that ε' measured using TDR would result in a considerably lower K_a value than the expected value.

An exploratory examination of the effect that the dielectric relaxation of these two materials had on TDR measured K_a was undertaken using a Tektronix 1502B metallic cable tester and a 0.30 m three rod TDR probe. Measured K_a for propanol was 14.6 and 20.1 for glycerol (Fig. 303). Both materials had lower K_a values than expected ε' values with K_a for glycerol being substantially lower at less than half the expected ε'. Based on this example, it is clearly seen that the dielectric relaxation properties of a material must be taken into consideration when used to calibrate a TDR probe.

Liquids that have little to no dielectric relaxation within the frequency range of TDR have been identified. Jones et al. (2005) and Blonquist et al. (2005) have used 2-isopropoxyethanol and water blends, however 2-isopropoxyethanol does exhibit an increase in ε'' at 1.0 GHz. White paraffin has been used by Schaap et al. (2003) and acetone and penetrating oil have been used by Robinson et al. (2003).

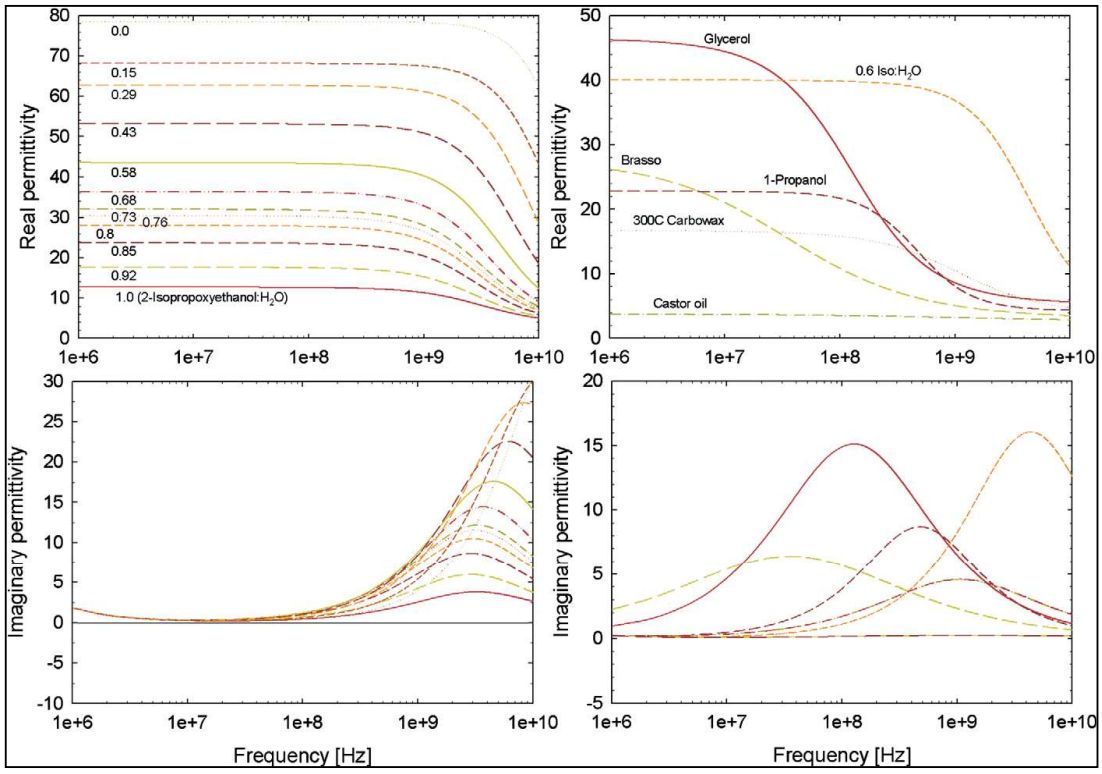

Fig. 3.02 Real Permittivity (ε′) and Imaginary Permittivity (ε″) for Various Liquids
In the bottom, right hand graph, Glycerol (solid red line) and 1-Propanol (dotted red line) display a substantial increase in ε″ over the TDR measurement frequency range. (From Jones et al., 2005)

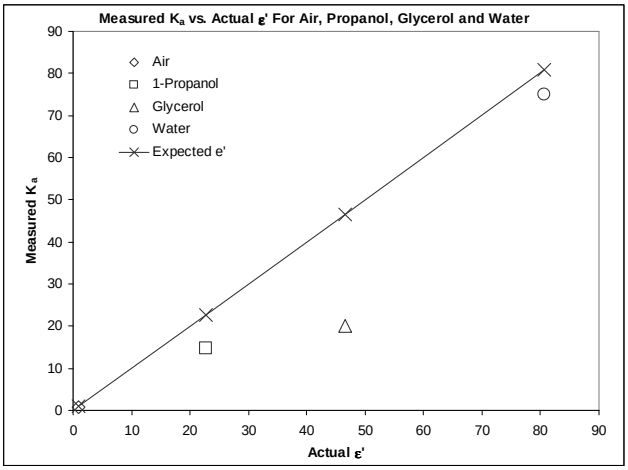

Fig. 3.03 Effect of Dielectric Relaxation on Measured K_a of 1-Propanol and Glycerol
Measured K_a is lower than Expected ε′ for both 1-Propanol and Glycerol due to increase in ε″ over the TDR measurement frequency range.

Blends of liquids with water have been used to calibrate TDR probes (Jones et al. 2005, Blonquist et al. 2005). However the same precaution of selecting a liquid that has no appreciable dielectric relaxation over the TDR frequency range still applies.

3.3.3 Water Air Immersion Method

The water air immersion method simply involves the incremental immersion of a TDR probe into a container of water. The length of the TDR probe immersed in water is then equal to the volume of water measured by the TDR probe while the length of the TDR probe immersed in air equals the volume of air measured by the TDR probe. The sum of the respective water and air volumes represents the total volume measured by the TDR probe (Fig. 3.04).

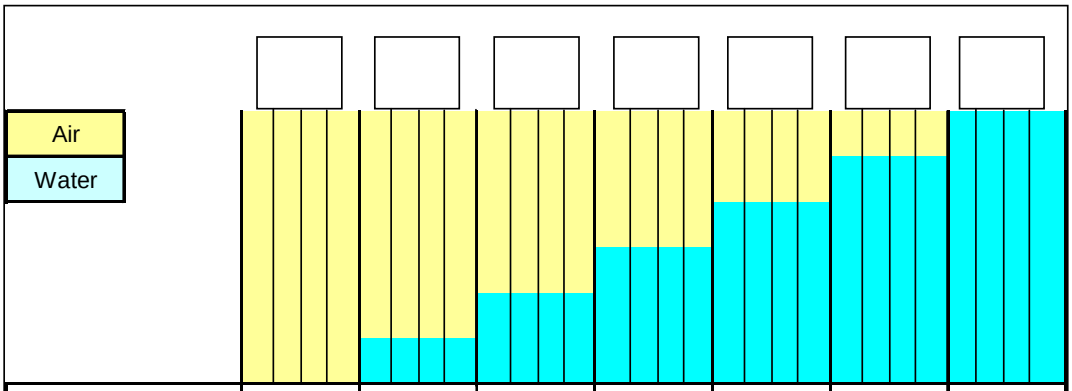

Length of Rods in Water - l_w (m)	0.00	0.05	0.10	0.15	0.20	0.25	0.30
Length of Rods - *lr* (m)	0.30	0.30	0.30	0.30	0.30	0.30	0.30
Fractional Volume of Water (θ_v) Sampled By Rods	0.000	0.167	0.333	0.500	0.667	0.833	1.000

Fig. 3.04 Water-Air Immersion Method
Based on a 0.030 m CS605 Three-rod TDR probe

The water air immersion method has been used as a straightforward technique to calibrate TDR probes. Robinson et al. (2003b) used the water air immersion method to emulate the effect of

changes in water content along the length of a three-rod TDR probe to examine the effect of a low dielectric constant layer over a high dielectric constant layer to emulate a dry soil over moist soil scenario. Schaap et al. (2003) used a similar approach to the water air immersion method by adding white paraffin as a third layer to study the effect on TDR signal propagation through layered media. Heimovaara et al. (2004) determined the dielectric constant profile along the length of a TDR probe using the water air immersion method as well as layered soils. Becker (2004) used the water air immersion method to determine the wave velocity in water and air along the length of a three-rod TDR probe coated with PVC. Herkelrath et al. (1991) and Hook and Livingston (1995) have shown that the series addition of each individual soil matrix component can be summed to obtain the same K_a as a heterogeneous soil matrix.

The basis for using the water air immersion method can be attributed to the work of Topp et al. (1982) where TDR was used to measure the average soil water content along the length of the TDR probe even when large differences in water content existed in the region being measured. Ferre et al. (1996) referred to this as the length weighted average for the measured apparent relative dielectric constant, i.e. K_a. For two sequential materials along the exposed probe rod length (l_r) with apparent dielectric permittivities of K_{a1} and K_{a2} covering the probe rods for sequential lengths of l_1 and l_2 where the exposed probe rod length $l_r = l_1 + l_2$, the length-weighted average $K_a^{0.5}$ becomes:

[3.06] $$K_a^{0.5} = (l_1/l_r)\, K_{a1}^{0.5} + (l_2/l_r)\, K_{a2}^{0.5}$$

Robinson et al. (2003b) described the total time of propagation of the TDR signal for a two-layered medium, i.e. water and air, as a form of a refractive index or dielectric mixing model where t_1 and t_2 represent the time for the TDR signal to travel through each of the sequential materials and f_1 and f_2 represent the volume fractions of each material, respectively as:

[3.07] $$t_t = t_1 + t_2 = K_a^{0.5} = f_1\, K_{a1}^{0.5} + f_2\, K_{a2}^{0.5}$$

Dielectric constant values calculated as a function of immersion length were found to yield accurate values compared to values determined using the dielectric-mixing model with the respective volume fractions of air and water.

One concern of using the water air immersion method to evaluate a coated TDR probe was the effect the coating has on the determination of $K_a^{0.5}$ along the length of the TDR probe rods or in the axial direction. Annan (1977b) based the solution for the effect of an air gap along the length of a transmission line by representing the air gap and the soil between the lines as a series capacitance yielding the total capacitance of the air and the soil as:

[3.08] $C_g = C_{air}\, C_{soil} / (C_{air} + C_{soil})$

Where C_g is the series capacitance between the rods due to the air gap and the soil sample and C_{air} and C_{soil} are the capacitances due to the air gap and the soil between the rods, respectively.

In the case of the water air immersion method, C_{air} is replaced by the capacitance of the polyolefin coating (C_{coat}) while C_{soil} is replaced by some combination of C_{air} and the capacitance of water (C_{water}) to give $C_{water\text{-}coating}$ and $C_{air\text{-}coating}$ as:

[3.09] $C_{water\text{-}coating} = C_{water}\, C_{coating} / (C_{water} + C_{coating})$

[3.10] $C_{air\text{-}coating} = C_{air}\, C_{coating} / (C_{air} + C_{coating})$

Since the water and air layers are distinct and aligned axially along the probe rods, the water-coating and air-coating layers represent two capacitances in parallel and as such, the total capacitance (C_t) along a non-coated probe rod would be the sum of the capacitances or:

[3.11] $C_t = C_{water\text{-}coating} + C_{air\text{-}coating}$

For a coated probe, both conditions represented by Eq. [3.09] and [3.10] exist, i.e. the coated probe immersed in two separate layers of air and water represent two sets of two capacitors (air-coating and water-coating) as two capacitors in parallel along the length of the TDR probe in the axial direction giving a total capacitance of:

[3.12] $C_t = [C_{air}\, C_{coat} / (C_{air} + C_{coat})] + [C_{water}\, C_{coat} / (C_{water} + C_{coat})]$

The fractional contribution of each of the two sets of the two capacitors in series is correlated the to cross-sectional area of the probes and as such, are directly proportional to the respective length of the probe rod immersed in either air or water. Given that the coating thickness and the separation between the TDR probe rods are constant, for any given fractional length of air and water, the total capacitance with respect to the length of the probe rod immersed in water or air would be expected to conform to a linear correlation.

3.3.4 Dielectric Mixing Model

A dielectric mixing model (DMM) provides an alternative method to establish a functional relationship between θ_v and K_a using TDR. The premise for development of a DMM for a soil matrix is based on the respective contribution of the dielectric constant of each material to the actual K_a of the soil matrix. Roth et al. (1990) developed a DMM to determine θ_v using TDR measurements of K_a based on the fractional volumes of water (θ_v), soil ($1 - \phi$), where ϕ represents the porosity of the soil, and air ($\phi - \theta_v$), and the respective dielectric constants of the constituent parts of the soil matrix such as water (K_{water}), soil (K_{soil}) and air (K_{air}).

The modular arrangement of a DMM into the respective volume fractions and material dielectric constants provides the opportunity to derive specific information regarding θ_v or ϕ of a soil matrix. Temperature correction can also be incorporated for any of the individual parameters that are temperature dependent.

A three-component system for wet soils (Roth et al., 1990) is given as:

[3.13] $K_a = [\theta_v\, K_{water}{}^{\alpha} + (1 - \phi)\, K_{soil}{}^{\alpha} + (\phi - \theta_v)\, K_{air}{}^{\alpha}]^{1/\alpha}$

Where α represents the geometry of the medium relative to the applied electric field. For layered soils, α is considered to range from –1 for soil layered perpendicular to the electric field of

the TDR probe to +1 for soil that is layered parallel to the electric field (Birchak et al., 1974; Ansoult et al., 1984). Roth et al. (1990) determined the best fit of the mixing model for several soil types occurs when $\alpha \approx 0.5$, while Kellner and Lundin (2001) arrived at α values ranging from 0.28 to 0.38 for peat soils and Dobson et al. (1985) found $\alpha = 0.65$ for sandy loam to silty clay soils. Changing α to fit a DMM conflicts with the theoretical relationship between η and ε of Eq. [2.01] (Whalley, 1993).

To conform with the relationship between η and ε from Eq. [2.01] the value of $\alpha = 0.5$ would be expected mathematically and substituting $\alpha = 0.5$ into Eq. [3.06] gives:

[3.14] $$K_a = [\theta_v K_{water}^{0.5} + (1 - \phi) K_{soil}^{0.5} + (\phi - \theta_v) K_{air}^{0.5}]^2$$

Using average values of $K_{soil} = 5$, $\phi = 0.96$ and $K_{water} = 79.4$ as reported by Kellner and Lundin (2001), a comparison between the DMM of Eq. [3.07] and the calibration curves of Kellner and Lundin (2001) and Topp et al. (1980) provides a graphic example of the problem encountered using a third order polynomial (Fig. 3.05). The difference in θ_v between the DMM and the two third order polynomial calibration functions for $K_a = 1$ to 80 is as high as 16% for the Topp equation and 13% for the Kellner and Lundin equation. The inflection range of both third order polynomial calibration curves suggest the change in θ_v with the change in K_a is considerably less over the inflection range than the change in θ_v at other points along the calibration curve, which seems questionable as there is no physical reason given to explain such a relationship. In effect, the use of a third order polynomial incorporates measurement error into the regression curve.

From the DMM, the relationship between K_a and θ_v is seen to be directly proportional to the exponent of 2 from Eq. [3.09], suggesting that a second order polynomial would provide a more accurate representation of the correlation between K_a and θ_v. In fact, the correlation can be described with θ_v directly proportional to $K_a^{0.5}$, which is the same as l_a/l_r from Eq. [2.12]. Plotting θ_v vs. l_a/l_r

results in a straightforward linear regression providing the optimum correlation between K_a and θ_v and is essentially the same as using the linear form of θ_v vs. t_t of Ledieu et al. (1986) and others.

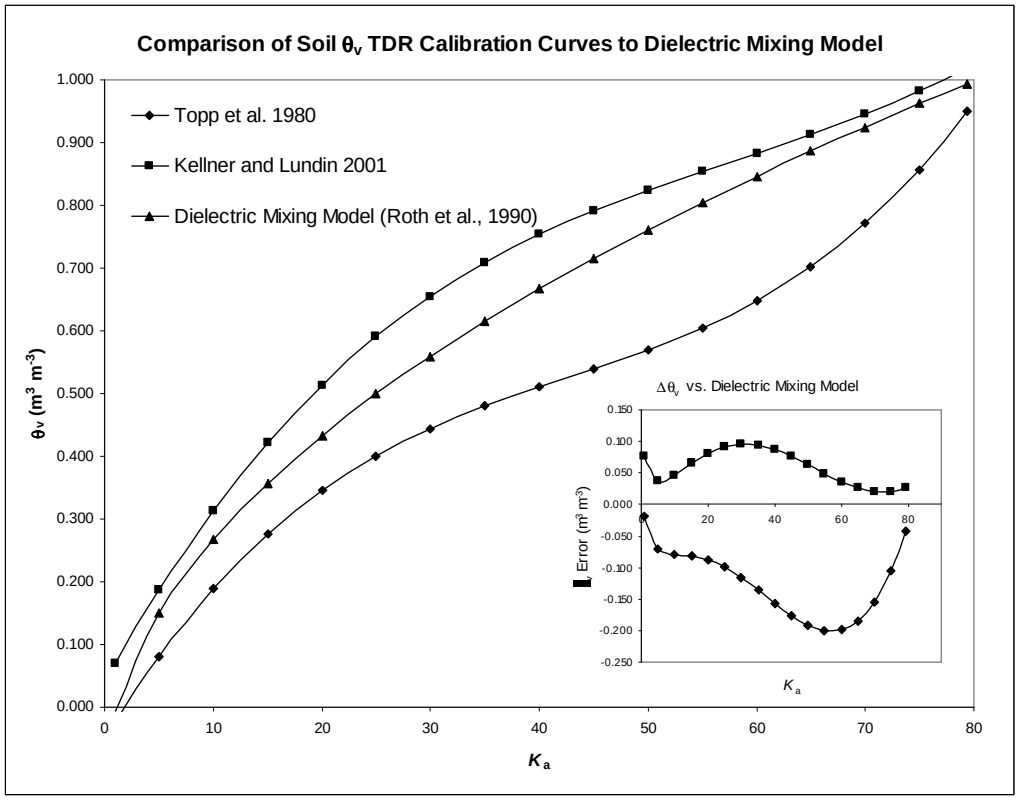

Fig. 3.05 Comparison of TDR Soil θ_v Calibration Curves to Dielectric Mixing Model
Inset shows the deviation in θ_v of the Topp (♦) and Kellner-Lundin (■) regression equations from the Dielectric Mixing Model (▲) regression equation.

3.3.5 Water-Air Dielectric Mixing Model (WAMM)

The DMM can be simplified to a two-phase mixing model using only water and air by eliminating the soil and porosity terms in Eq. [3.07] as:

[3.15] $K_a^{0.5} = \theta_v K_{water}^{0.5} + (1 - \theta_v) K_{air}^{0.5}$

The water-air DMM (WAMM) of Eq. [3.10] can be used to calculate expected $K_a^{0.5}$ values that can be compared to actual $K_a^{0.5}$ values measured by a TDR probe using the water air immersion

method. The water volume fraction (θ_v) of the WAMM would then be equivalent to the ratio of the length of the TDR probe immersed in water (l_{water}) to the exposed rod length, l_r, as $\theta_v = l_{water} / l_r$ and the air fraction then becomes the length of the probe immersed in air (l_{air}) to l_r as $(1 - \theta_v) = l_{air} / l_r$.

3.3.6 Effect of Temperature on K_a Measurement

The value of K_{water} is temperature dependent and K_{water} decreases with increasing temperature. Pepin et al. (1995) found an absolute measurement error of 2.1% in θ_v for peat soil over a temperature range of 15° C, while Persson and Berndtsson (1998) determined a correction factor of –0.002690 θ_v $°C^{-1}$ for sandy soils or a 4% θ_v measurement error. Since it is common for temperature to vary within a 25 °C range under normal field conditions, consideration should be given to the effect that temperature variation has on TDR measurement of K_a.

The effect that temperature (T) has on measured K_a can then be accounted for by calculating a temperature corrected value of K_{water} using the correlation between T and K_{water} of Weast (1986):

[3.16] $K_{water} = 78.54*[1 - 4.5791E\text{-}03(T\text{-}25) + 1.19E\text{-}5(T\text{-}25)^2 - 2.8E\text{-}08(T\text{-}25)^3]$

Chapter 4
Experimental

4.1 θ_v and EC Measurement Using NC, CCRC and GAP TDR Probes

4.1.1 Method and Materials for θ_v Measurement - Water-Air Immersion

The water air immersion method was used to obtain calibration curves for $K_a^{0.5}$ vs. θ_v using a CS605 TDR probe (Fig. 4.01) that had no coating applied to the center-conducting rod (NC probe), the center-conducting-rod coated with polyolefin (CCRC probe) and the center-conducting rod coated with polyolefin with a 0.01 m gap in the coating at the midpoint of the center-conducting rod (GAP probe).

The CS605 TDR 3-rod stainless steel probe (Fig. 4.01) had a total rod length (l_p) of 0.385 m, a head rod length (l_h) of 0.085 m and an exposed rod length (l_r) of 0.30 m. The center-to-center distance between the rods of the CS605 probe rods was 0.022 m and the diameter of the individual probe rods was 0.00475 m. The probe head was made of an epoxy material with K_h = 4.5 to 4.6 (*pers. comm.* J. Bilskie, CSI) giving a median value of K_h = 4.55. The probe offset calculated using these values gives l_{off} = 0.181 m from Eq. [2.11]. The probe head dimensions are 0.108 m long, 0.07 m wide and 0.019 m thick. The CS605 probe was attached to a 15 m Belden 9907 RG58A/U cable that had a rated cable impedance of 50Ω.

The CCRC and GAP probe (Fig. 4.01) were coated using 0.019 m I.D. thin wall, heat shrink polyolefin tubing (NTE Electronics Inc.). The dielectric constant of the polyolefin tubing was K_{coat} = 3.3 based on technical data sheets for similar polyolefin tubing products. The polyolefin heat shrink coating was applied using a thermal heat gun with caution taken to insure that no air gaps were formed between the coating and the probe rod. Using micrometer calipers, the average thickness of

the applied polyolefin coating was measured at 0.00053 m. The GAP CS605 TDR probe was prepared by removing a 0.01 m section of the polyolefin coating from the CCRC probe at a distance of 0.145 m to 0.155 m from the junction of the probe head placing the GAP at the direct center of l_r.

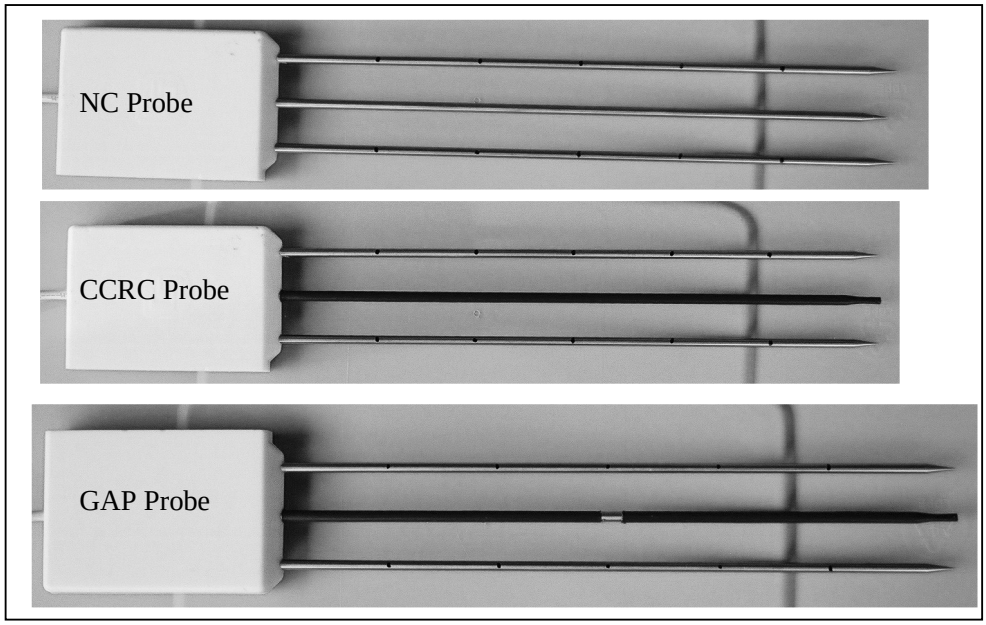

Fig. 4.01 Polyolefin Coating Applications for the CS605 TDR Probe
No rods coat (NC), center-conducting rod coated (CCRC) and center-conducting rod coated with gap (GAP)

The NC, CCRC and GAP probes were immersed in deionized water at incremental depths of 0.05 m from 0.00 m to 0.30 m in a 100 mm I.D. PVC cylinder with a total depth of 0.60 m. The immersion depths were selected to obtain l_w/l_r ratios corresponding to θ_v levels of 0.000, 0.167, 0.333, 0.500, 0.667, 0.833 and 1.000 $m^3\ m^{-3}$. The CS605 TDR probe was centered in the middle of the PVC cylinder to ensure a minimum distance of 0.05 m between the probe rods and the cylinder wall. The temperature of the deionized water was 22.5 °C at the time the TDR readings were taken, which corresponds with K_{water} = 79.45 from Eq. [2.22].

TDR waveforms were obtained using a Tektronix 1502B metallic cable tester and WinTDR software (Or et al., 2000). Ten separate waveforms were collected at each θ_v level for the NC, CCRC

and GAP probes in order of lowest to highest θ_v. The waveform data points were transferred to an Excel worksheet to determine the first and second reflection points (ρ_1 and ρ_1) and calculate l_a for the three probes from Eq. [2.10]. Average values of K_a for each θ_v level were calculated using Eq. [2.12].

4.1.2 Method and Materials for θ_v Measurement - Sand-Water Mixtures

A standard calibration method using sand and deionized water mixtures, to represent the condition of a sandy soil, was used to obtain a comparison between the calibration curves of $K_a^{0.5}$ vs. θ_v for the non-coated (NC) probe and center-conducting rod coated with heat shrink polyolefin (CCRC).

The NC and CCRC probe were inserted vertically into the sand-water mixtures to a depth of 0.30 m so that only the TDR probe rods (l_r) were exposed to the sand-water sample leaving the probe head exposed to air to represent the same condition of the probe head in the water-air immersion method. The NC and CCRC probes were inserted at the center of a glass cylinder containing the sand-water mixture to ensure a minimum distance of 0.05 m between the probe rods and the cylinder wall. The glass cylinder was 0.54 m deep with an I.D. of 0.110 m. The temperature of the sand-water mixtures was 20 °C at the time the TDR readings were taken, which corresponds with $K_{water} = 77.56$ from Eq. [2.22].

The sand used was a commercially available grade (PlaySand from Sil Industrial Minerals Inc.). The sand was dried at 100 °C for 48 hours prior to use. The weight of sand necessary to cover the NC and CCRC probe rods was measured in the glass cylinder, removed to a polyethylene pail and thoroughly mixed with three different volumes of deionized water to obtain three θ_v calibration samples. A fourth sample using only dried sand was included in the sample regimen. Each sand-water mixture was then packed into the glass cylinder and compacted to obtain a level surface that was

aligned at the interface of the probe rods and probe head of the NC and CCRC probes. The bulk density of the dry sand sample was calculated to be 1.818 g cm^{-3}.

TDR waveforms were obtained using a Tektronix 1502B metallic cable tester and WinTDR software (Or et al., 2000). Ten separate waveforms were collected for each sand-water θ_v mixture and the sand only sample for each probe. The waveform data points were transferred to an Excel worksheet to determine the first and second reflection points (ρ_1 and ρ_1) and calculate l_a for each of the samples from Eq. [2.10]. Average values of K_a for each sand-water θ_v level were calculated using Eq. [2.12].

Drying the sand-water mixtures for 48 hours at 100° completed gravimetric determination of θ_v for the sand-water mixtures. The volume water content for the sand-water mixtures was 0.086, 0.183 and 0.306 $m^3\ m^{-3}$ for the NC probe and 0.096, 0.202 and 0.324 $m^3\ m^{-3}$ for the CCRC probe, respectively.

4.1.3 Method and Materials for EC Measurement

The NC, CCRC and GAP CS605 TDR probes were calibrated using 11 EC control solutions (EC_{soln}) that ranged from 0.00002 S m^{-1} (deionized water) to 1.06 S m^{-1}. The NC, CCRC and GAP probes were completely immersed in the EC control solutions to obtain measured EC calibration values. The incremental immersion of the probes to different depths in the water column used in the water air immersion method was not used for EC calibration of the probes.

The EC solutions were prepared by adding quantities of commercially available sea salt to emulate the same chemical composition as that of seawater and then each solution was transferred to the same PVC cylinder used in the θ_v studies. EC_{soln} and temperature were measured using a WTW LF 330 Conductivity Hand Held Meter. The temperatures of the EC solutions were found to be very

consistent with a temperature range during testing of 22.2 °C to 22.9 °C. No temperature correction was applied to the measured EC values.

The NC, CCRC and GAP TDR probes were completely immersed in each EC solution and TDR waveforms were obtained using a Tektronix 1502B metallic cable tester and WinTDR software (Or et al., 2000). Ten separate waveforms were collected for each EC_{soln} in a random order. The waveform data points were then transferred to an Excel worksheet to determine the required ρ values. For each EC_{soln}, measured ρ_f represents the average of the last 10 ρ values from the waveform. To evaluate the effect of EC on $K_a^{0.5}$ measurement, l_a values were also determined for each EC_{soln}.

4.2 Results

4.2.1 θ_v Measurement Using NC, CCRC and GAP TDR Probes – Water-Air Immersion

Waveforms for the CCRC and GAP probes were essentially the same for corresponding θ_v levels, while both the CCRC and GAP waveforms were considerably different then the NC waveforms (Fig. 4.02a to 4.02f). There was a noticeable separation between the CCRC and GAP waveforms when θ_v exceeded 0.333 $m^3\ m^{-3}$ and the degree of separation appeared to increase as θ_v increased. The distance to ρ_{apex} and the amplitude of ρ_{apex} was the same for each TDR probe at corresponding θ_v levels but increased with increasing θ_v for each probe.

$K_a^{0.5}$ values for the CCRC and GAP probes were less than $K_a^{0.5}$ values for the NC probe (Table 4.01). A small difference ($\Delta K_a^{0.5}$) was found between CCRC and GAP $K_a^{0.5}$ values for $\theta_v \geq$ 0.167 $m^3\ m^{-3}$ with the maximum difference occurring at θ_v = 0.667 $m^3\ m^{-3}$. A very strong linear correlation was found for the standard $K_a^{0.5}$ vs. θ_v calibration curves for the NC, CCRC and GAP probes with respective r^2 values of 0.999, 0.997 and 0.996 (Fig. 4.03). The difference in the slope of the NC and CCRC $K_a^{0.5}$ vs. θ_v calibration curves combined with their equivalent *y*-intercept values

indicated that the difference in measured $K_a^{0.5}$ between the NC and CCRC probes increased with increasing θ_v.

WAMM $K_a^{0.5}$ values (Table 4.01) were calculated using Eq. [3.10] with $K_{water} = 79.45$ calculated using Eq. [3.11] with $T = 22.5$ °C. NC probe $K_a^{0.5}$ values were consistently lower than WAMM $K_a^{0.5}$ values with the exception of $\theta_v = 0.167$ m^3 m^{-3}. This exception was considered to be the result of the difficulty encountered in determining an accurate distance to the position for the second reflection point for $\theta_v = 0.167$ m^3 m^{-3} (Fig. 4.01a). In general, the difference ($\Delta K_a^{0.5}$) between WAMM and NC $K_a^{0.5}$ values was the same at each θ_v level, suggesting that a common factor may be intrinsic in the measurement of $K_a^{0.5}$ using the NC probe. $K_a^{0.5}$ values for the CCRC and GAP probes were all consistently less than WAMM $K_a^{0.5}$ values as expected, since CCRC and GAP NC $K_a^{0.5}$ values were consistently less than NC $K_a^{0.5}$ values.

A very strong linear correlation was found between NC $K_a^{0.5}$ vs. CCRC and GAP NC $K_a^{0.5}$ values with $r^2 = 0.994$ and 0.992, respectively (Fig. 4.04).

Table 4.01 $K_a^{0.5}$ vs. θ_v for NC, CCRC and GAP TDR Probes

θv (m^3 m^{-3})	$K_a^{0.5}$				$\Delta K_a^{0.5}$	$\Delta K_a^{0.5}$
	WAMM	NC Probe	CCRC Probe	GAP Probe	NC - WAMM	GAP - CCRC
0.000	1.000	0.860	0.895	0.895	-0.140	0.000
0.167	2.319	2.330	1.321	1.333	0.011	-0.012
0.333	3.638	3.435	2.191	2.218	-0.203	-0.027
0.500	4.957	4.727	2.892	3.034	-0.229	-0.142
0.667	6.276	6.044	3.595	3.778	-0.231	-0.183
0.833	7.595	7.301	4.335	4.456	-0.293	-0.121
1.000	8.913	8.675	5.025	5.080	-0.239	-0.055

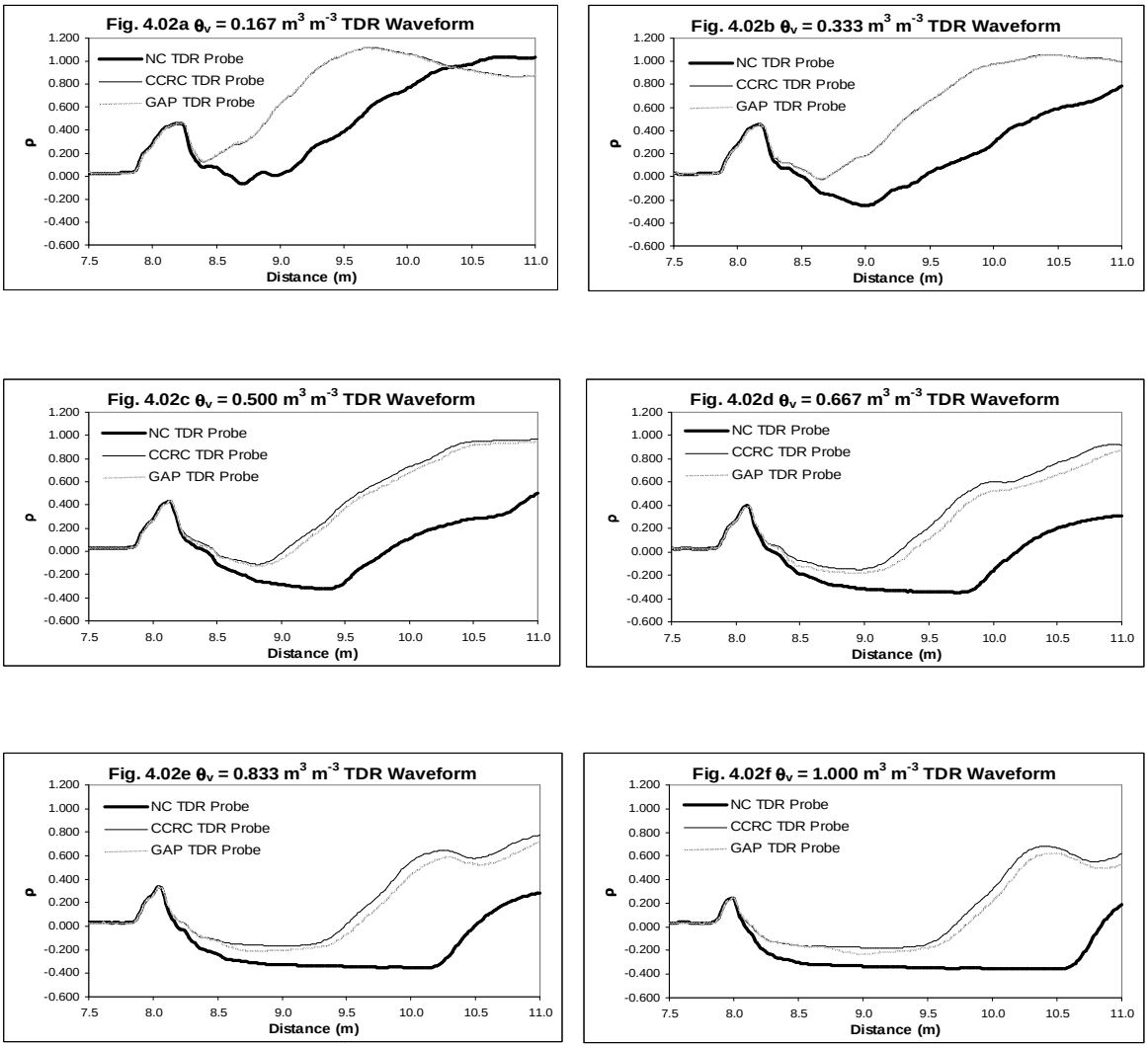

Fig. 4.02 a-f TDR Waveforms for the NC, CCRC and GAP Probes
Water immersion depth of TDR probe increases 0.05 m to 0.30 m from Fig. 4a to Fig. 4f.

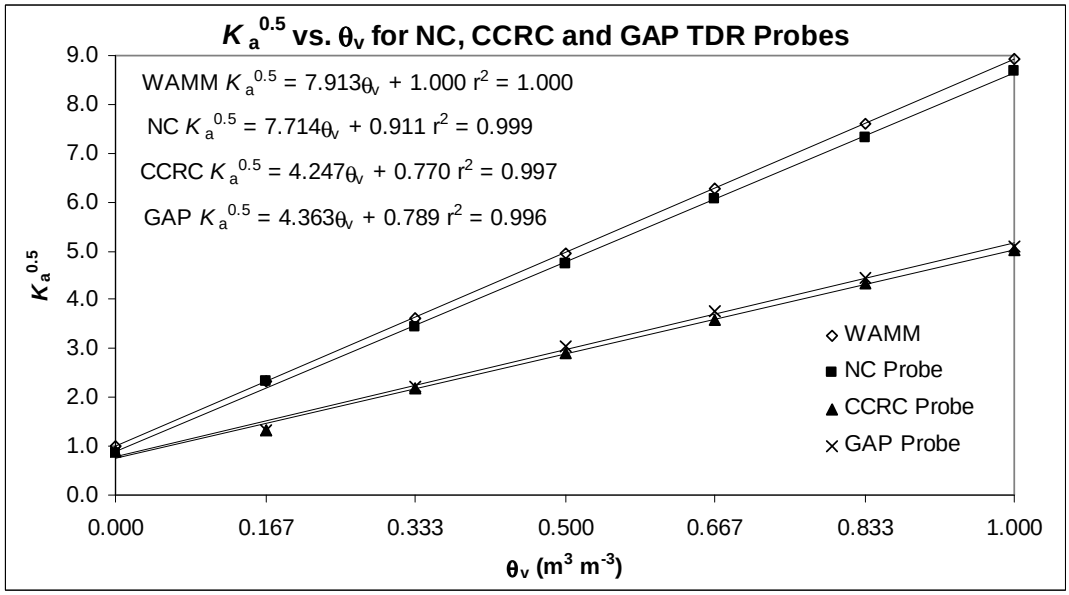

Fig. 4.03 $K_a^{0.5}$ vs. θ_v Standard Calibration Curves for NC, CCRC and GAP TDR Probes
Solid lines represent calculated regression curves.

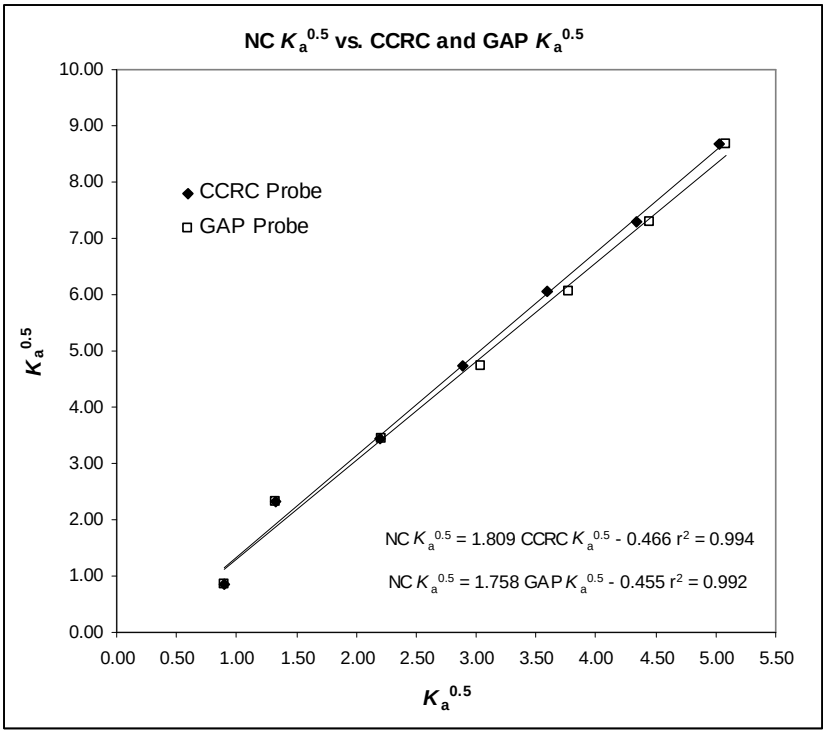

Fig. 4.04 NC $K_a^{0.5}$ vs. CCRC and GAP $K_a^{0.5}$
1:1 correlation between the NC probe and the CCRC and GAP probes, respectively.

4.2.2 θ_v Measurement Using NC and CCRC TDR Probes - Sand-Water Mixtures

Waveforms for the NC and CCRC probes for the different sand-water mixture θ_v levels are presented in Fig. 4.05a to Fig. 4.05d. The shape of ρ_{apex} was not discernable for either the NC or CCRC TDR waveforms at θ_v levels of 0.086 and 0.096 $m^3\ m^{-3}$, respectively. The distance to ρ_{apex} and the amplitude of ρ_{apex} was the same for all θ_v levels for both probes. The distance to the second reflection was reduced using the CCRC probe in place of the NC probe for all equivalent θ_v levels.

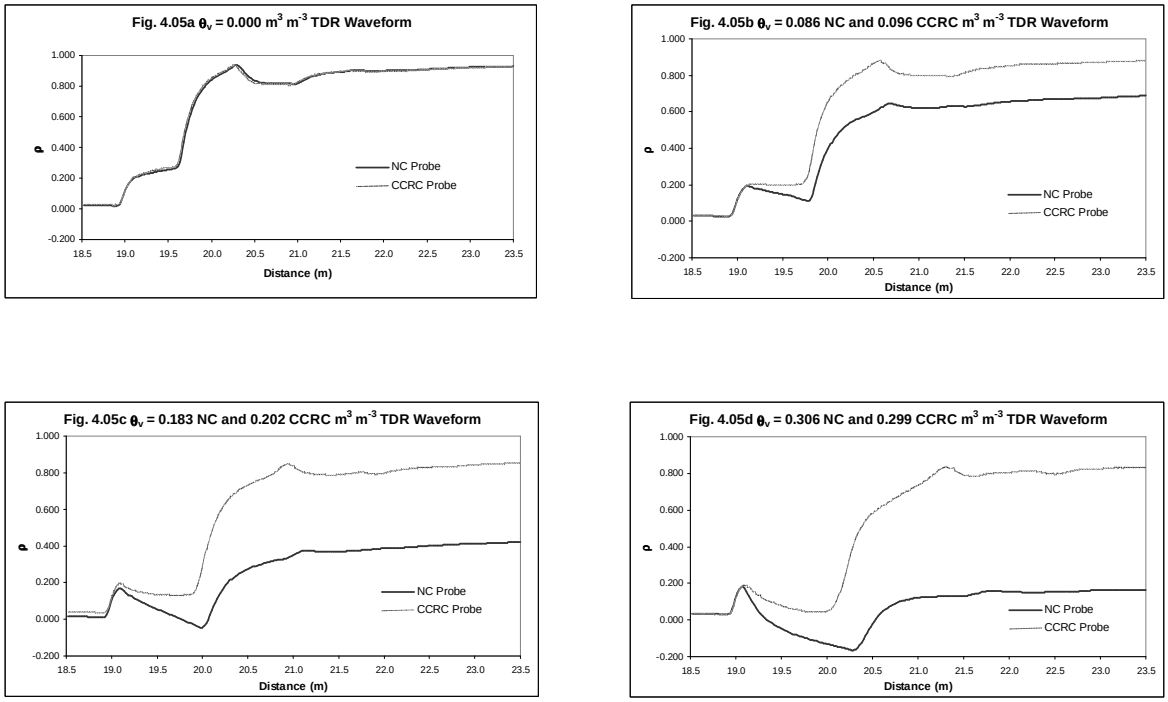

Fig. 4.05 a-d TDR Waveforms for the NC and CCRC Probes – Sand-Water Mixtures

A very strong linear correlation was found between $K_a^{0.5}$ vs. θ_v for both the NC and CCRC probes with an r^2 of 0.997 for both probes (Fig. 4.06). The slopes of the NC probe $K_a^{0.5}$ vs. θ_v for the sand-water mixtures (m = 7.687) and water-air immersion method (m = 7.714) were equivalent while the y-intercepts for the NC probe for the sand-water mixtures and the water-air immersion method were 0.911 and 1.673, respectively (Fig. 4.07). Slopes for the CCRC probe $K_a^{0.5}$ vs. θ_v for the sand-water mixtures (m = 5.000) and the water-air immersion method (m = 4.247) were comparable while

the *y*-intercepts for the CCRC probe for the sand-water mixtures and the water-air immersion method were 0.770 and 1.629. The difference in the y-intercepts of the regressed lines found for both probes in the sand-water mixtures vs. the water-air immersion method reflected the difference in the dielectric constant of 100% air ($\varepsilon_r = 1.0$) vs. 100% sand ($\varepsilon_r \approx 3.0$ or $K_a^{0.5} \approx 1.7$).

The difference in the slope of the NC and CCRC $K_a^{0.5}$ vs. θ_v calibration curves for the sand-water mixtures combined with their equivalent *y*-intercept values indicated that the difference in measured $K_a^{0.5}$ between the NC and CCRC probes increased with increasing θ_v in the same manner observed for both probes using the water-air immersion method.

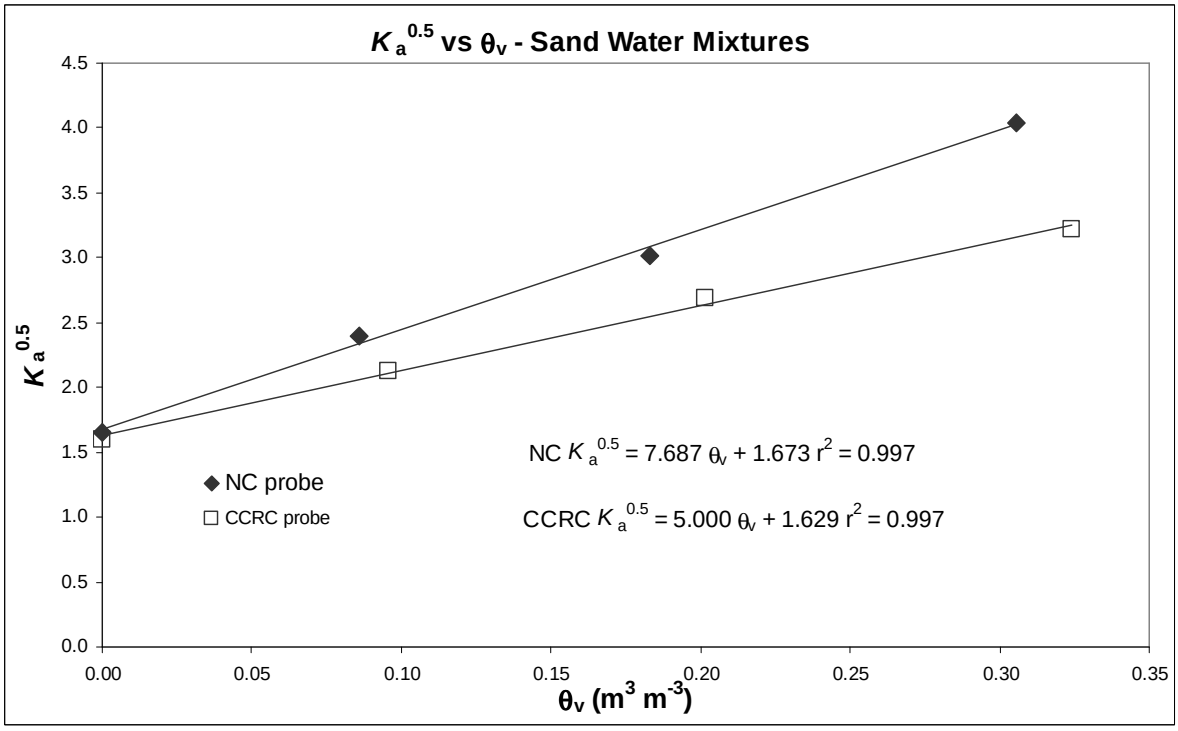

Fig. 4.06 $K_a^{0.5}$ vs. θ_v Sand-Water Calibration Curves for NC and CCRC TDR Probes
Solid lines represent calculated regression curves.

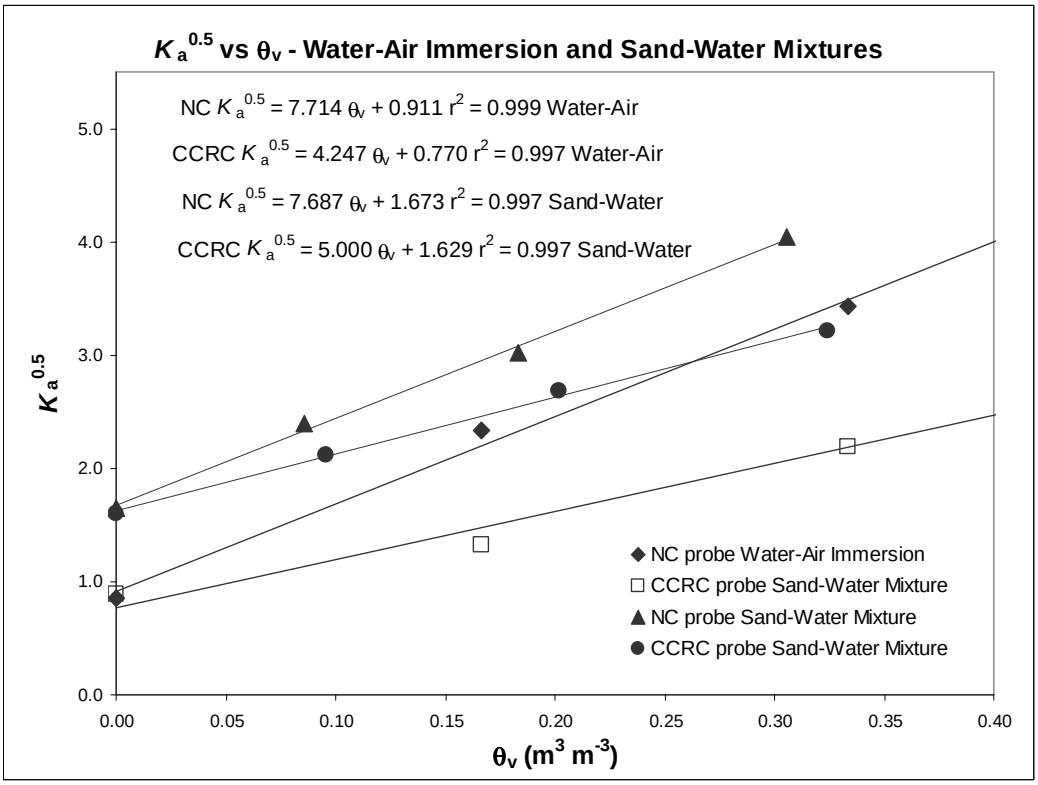

Fig. 4.07 Comparison of Water-Air Immersion and Sand-Water Calibration Curves
Solid lines represent calculated regression curves.

4.2.3 EC Measurement Using NC, CCRC and GAP TDR Probes

The effect of increasing EC_{soln} was clearly evident in the NC TDR waveforms (Fig. 4.08). All of the waveforms had leveled out or had become flattened at an apparent distance of 30.0 m and valid ρ_f values to correlate with EC_{soln} were obtained at this distance. A different pattern was found in the TDR waveforms for the CCRC TDR probe, as there was virtually no difference in ρ_f values with increasing EC_{soln} (Fig. 4.09). There was also a reduced number of multiple reflections in the CCRC waveforms compared to the NC waveforms and any reflections that were discernable were difficult to distinguish when $EC_{soln} \geq 0.132$ S m^{-1}. TDR waveforms for the GAP TDR probe (Fig. 4.10) showed the same pattern of decreasing ρ_f with increasing EC_{soln} as witnessed in the NC TDR waveforms. As

with the CCRC TDR waveforms, there were fewer multiple reflections in the GAP waveforms compared to the NC waveforms.

Three distinct patterns were found in the calculated EC_{GT} values for the NC, CCRC and GAP probes (Fig. 4.11). A response between EC_{soln} and calculated EC_{GT} was nonlinear using Eq. [2.19] with NC probe ρ_{min} and ρ_f values. NC probe EC_{GT} reached a maximum at $EC_{soln} \geq 0.236$ S m^{-1}. No discernable relationship was found between EC_{soln} and EC_{GT} for the CCRC probe, as there was no correlation between the decrease in ρ_f with increasing EC_{soln}. The CCRC probe was found to be incapable of discerning differences in EC_{soln}. A nonlinear response was found between EC_{soln} and EC_{GT} with the GAP probe and a very strong correlation was found for EC_{GT} vs. EC_{soln} using a second order polynomial regression ($r^2 = 1.000$). A one to one relationship was not found between EC_{GT} and EC_{soln} values for any of the three probes tested, i.e. EC_{GT} values were not equivalent to EC_{soln} values.

A second reflection point was not evident in NC probe waveforms for $EC_{soln} \geq 0.236$ S m^{-1} resulting in a situation where $\rho_{min} = \rho_{inf}$ (Table 4.02), which effectively reduced the term $[(1 + \rho_{min})/(1 - \rho_{min})]$ $[(1 - \rho_{inf})/(1 + \rho_{inf})]$ in Eq. [2.19] to unity. As an alternate approach, ρ_{min} was replaced by ρ_0, i.e. the cable impedance Z_0, to determine the effect on the calculated EC_{GT} values. With the change to ρ_0 in place of ρ_{min}, a substantial error still resulted in calculated values of EC_{GT} for the NC probe (Table 4.03). However, EC_{GT} vs. EC_{soln} for the NC probe using ρ_0 displayed a similar pattern to EC_{GT} vs. EC_{soln} using ρ_0 with the GAP probe. In this approach, for both the NC and GAP probes, a very strong correlation between EC_{GT} vs. EC_{soln} was found using a second order polynomial regression with $r^2 = 0.999$ and 1.000 for the NC and GAP probe, respectively (Fig. 4.12). Values of EC_{GT} for the NC probe were generally an order of magnitude greater than EC_{GT} for the GAP probe.

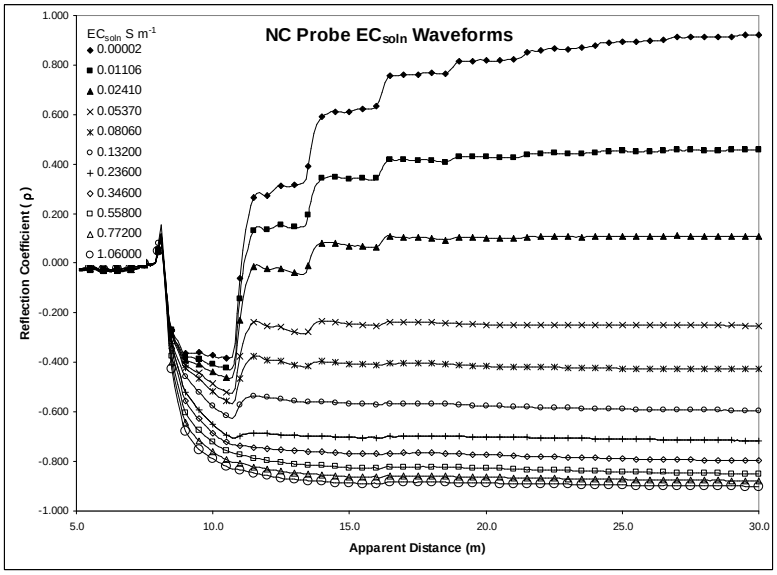

Fig. 4.08 NC Probe EC_{soln} Waveforms

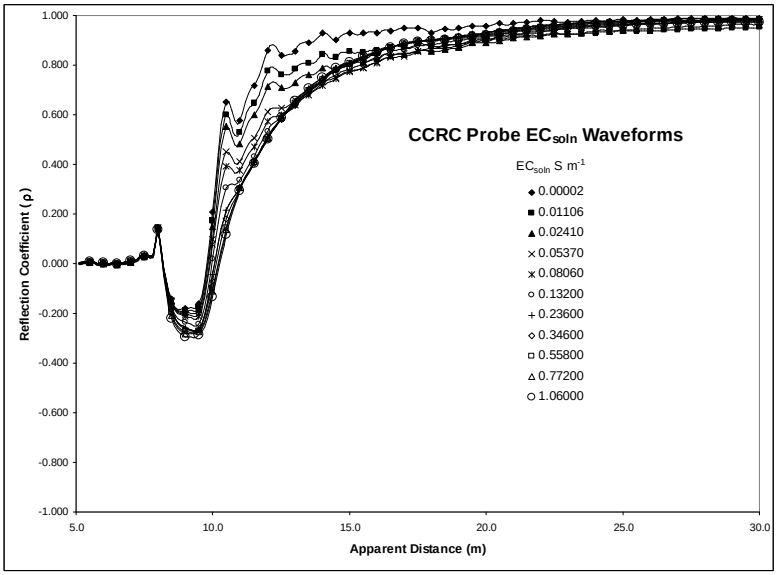

Fig. 4.09 CCRC Probe EC_{soln} Waveforms

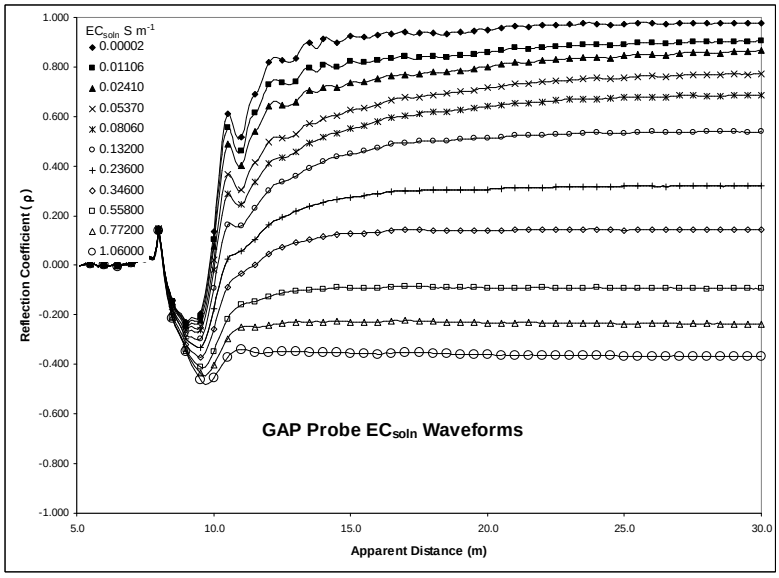

Fig. 4.10 GAP Probe EC_{soln} Waveforms

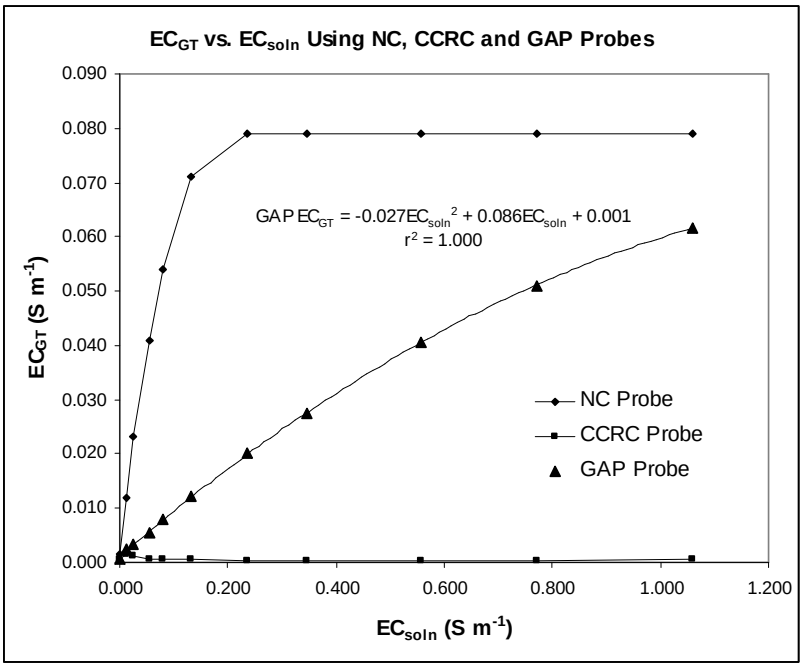

Fig. 4.11 EC_{GT} vs. EC_{soln} Using NC, CCRC and GAP TDR Probes

For the case of EC_{cell}, calculated K values for the NC, CCRC and GAP probe using Eq. [2.22] were found to increase with increasing EC_{soln} (Table 4.04) demonstrating that K was not a constant

value for either of the probes. As such, the use of Eq. [2.21] to obtain EC_{cell} was determined to be of little value and using the direct correlation between Z_L^{-1} and EC_{soln} would be more effective.

Table 4.02 EC_{soln} TDR Waveform Parameters ρ_{min} and ρ_f

TDR Waveform EC_{soln} Parameters ρ_{min} and ρ_f						
EC_{soln} (S m^{-1})	ρ_{min}			ρ_f		
	NC Probe	CCRC Probe	Gap Probe	Noncoat	Coat	Gap
0.00002	-0.385	-0.184	-0.228	0.920	0.984	0.975
0.01106	-0.429	-0.193	-0.236	0.457	0.950	0.903
0.02410	-0.466	-0.201	-0.242	0.109	0.962	0.861
0.05370	-0.526	-0.214	-0.257	-0.252	0.981	0.769
0.08060	-0.568	-0.223	-0.270	-0.428	0.977	0.685
0.13200	-0.626	-0.252	-0.301	-0.595	0.982	0.538
0.23600	-0.716	-0.272	-0.331	-0.716	0.989	0.319
0.34600	-0.798	-0.273	-0.371	-0.798	0.989	0.142
0.55800	-0.851	-0.279	-0.416	-0.851	0.984	-0.095
0.77200	-0.878	-0.284	-0.444	-0.878	0.983	-0.239
1.06000	-0.900	-0.296	-0.480	-0.900	0.973	-0.369

Table 4.03 NC Probe EC_{GT} Values Using ρ_{min} and ρ_0

EC_{soln} (S m^{-1})	NC Probe		CCRC Probe		GAP Probe	
	EC_{GT} using ρ_{min}	EC_{GT} using ρ_0	EC_{GT} using ρ_{min}	EC_{GT} using ρ_0	EC_{GT} using ρ_{min}	EC_{GT} using ρ_0
0.00002	0.00154	0.00328	0.00049	0.00071	0.00053	0.00085
0.01106	0.01177	0.02828	0.00145	0.00213	0.00235	0.00382
0.02410	0.02309	0.05984	0.00111	0.00166	0.00338	0.00556
0.05370	0.04087	0.12515	0.00058	0.00089	0.00563	0.00955
0.08060	0.05414	0.18689	0.00064	0.00102	0.00800	0.01393
0.13200	0.07096	0.29213	0.00051	0.00085	0.01224	0.02273
0.23600	0.07887	0.45319	0.00026	0.00046	0.02028	0.04000
0.34600	0.07887	0.65306	0.00026	0.00046	0.02751	0.05911
0.55800	0.07887	0.91041	0.00038	0.00068	0.04055	0.09572
0.77200	0.07887	1.13431	0.00038	0.00069	0.05090	0.12759
1.06000	0.07887	1.41643	0.00060	0.00112	0.06175	0.16703

Using the reciprocal of the impedance, Z_L^{-1} vs. EC_{soln}, two distinct patterns were found for the NC, CCRC and GAP probes (Fig. 4.13). A nonlinear response was found between Z_L^{-1} and EC_{soln} for the NC and GAP probes with a very strong second order polynomial correlation between Z_L^{-1} and

EC_{soln} for the NC and GAP probes with $r^2 = 0.999$ and 1.000, respectively. NC probe Z_L^{-1} values were greater than GAP probe Z_L^{-1} values for all EC_{soln}, and in general, NC probe Z_L^{-1} values were an order of magnitude greater than GAP probe Z_L^{-1} values. The response between Z_L^{-1} vs. EC_{soln} with increasing EC_{soln} was similar to EC_{GT} vs. EC_{soln} for the CCRC probe, i.e. no correlation could be determined between Z_L^{-1} and EC_{soln} with increasing EC_{soln}.

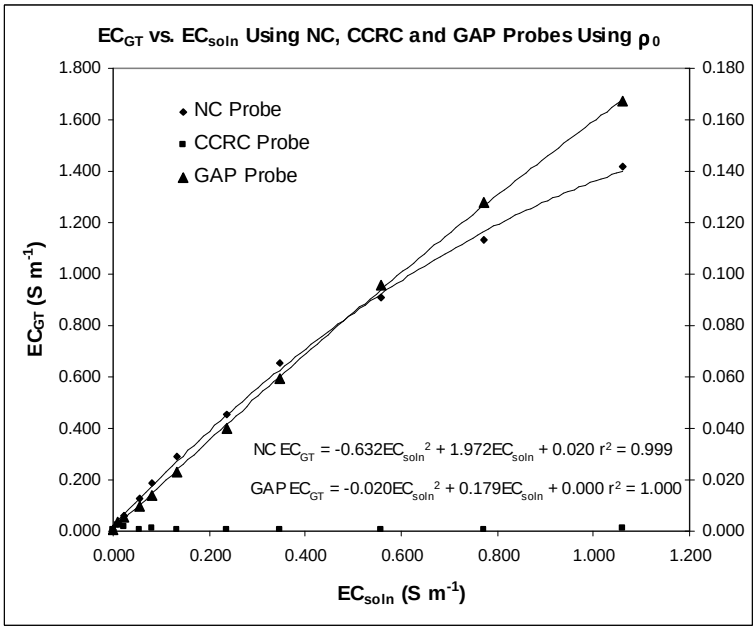

Fig. 4.12 EC_{GT} vs. EC_{soln} Using ρ_0

Table 4.04 Cell Constant K vs. EC_{soln}

EC_{cell} Cell Constant K (m^{-1})			
EC_{soln} ($S\ m^{-1}$)	NC Probe	CCRC Probe	GAP Probe
0.00002	0.02	0.11	0.09
0.01106	1.48	20	11.7
0.02410	1.50	57	17.6
0.05370	1.61	238	23.4
0.08060	1.62	315	24.6
0.13200	1.69	615	25.3
0.23600	1.97	2016	27.0
0.34600	1.98	2982	27.7
0.55800	2.29	3285	28.9
0.77200	2.55	4439	30.6
1.06000	2.83	3782	33.1

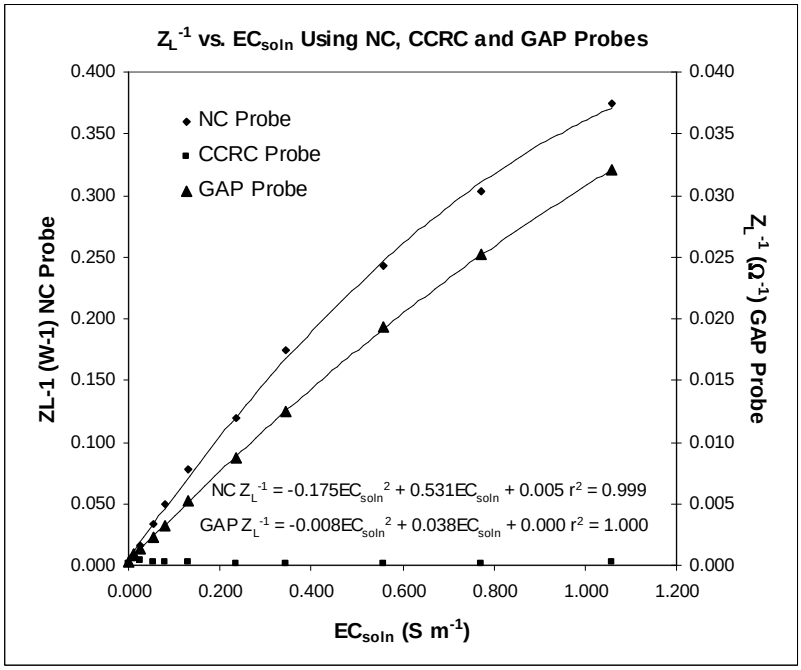

Fig. 4.13 Correlation Between Z_L^{-1} and EC_{soln}

As with EC_{GT}, EC_{cell} values were not equivalent to EC_{soln} values (Table 4.05). EC_{cell} values were consistently less than EC_{soln} values.

Table 4.05 EC_{cell} Values for NC, CCRC and GAP TDR Probes

EC_{soln} (S m^{-1})	ρ_f			Z_L^{-1} (S m^{-1})		
	NC Probe	CCRC Probe	GAP Probe	NC Probe	CCRC Probe	GAP Probe
0.00002	0.916	0.982	0.979	0.00088	0.00018	0.00021
0.01106	0.456	0.947	0.909	0.00746	0.00054	0.00095
0.02410	0.109	0.959	0.872	0.01607	0.00042	0.00137
0.05370	-0.251	0.978	0.794	0.03340	0.00023	0.00229
0.08060	-0.427	0.975	0.718	0.04981	0.00026	0.00328
0.13200	-0.593	0.979	0.587	0.07830	0.00021	0.00521
0.23600	-0.714	0.988	0.392	0.11990	0.00012	0.00874
0.34600	-0.795	0.988	0.231	0.17488	0.00012	0.01250
0.55800	-0.848	0.983	0.017	0.24362	0.00017	0.01931
0.77200	-0.876	0.983	-0.115	0.30286	0.00017	0.02521
1.06000	-0.899	0.972	-0.231	0.37501	0.00028	0.03203

There was no effect on the measurement of $K_a^{0.5}$ with increasing EC_{soln} (Table 4.06). $K_a^{0.5}$ could not be determined for the NC probe at $EC_{soln} \geq 0.236$ S m^{-1}, all $K_a^{0.5}$ values were equivalent for

the CCRC probe and the slight increase in $K_a^{0.5}$ for the GAP probe at $EC_{soln} \geq 0.558$ S m^{-1} was considered to be the result of increasing difficulty in identifying the second reflection in the GAP probe TDR waveforms.

Table 4.06 $K_a^{0.5}$ vs. EC_{soln} for the NC, CCRC and GAP TDR Probes

EC_{soln} (S m^{-1})	$K_a^{0.5}$		
	NC Probe	CCRC Probe	GAP Probe
0.00002	9.09	5.77	5.79
0.01106	9.02	5.83	5.79
0.02410	9.06	5.77	5.77
0.05370	9.09	5.79	5.81
0.08060	9.06	5.68	5.76
0.13200	8.97	5.45	5.74
0.23600	n/d	5.61	5.78
0.34600	n/d	5.65	5.87
0.55800	n/d	5.74	6.08
0.77200	n/d	5.77	6.31
1.06000	n/d	5.78	6.46

4.3 Discussion

4.3.1 θ_v Measurement Using NC, CCRC and GAP TDR Probes – Water-Air Immersion

The application of a polyolefin coating to the center-conducting rod of the CS605 probe improved the capability of a CS605 probe to measure θ_v at higher EC_{soln} concentrations than a CS605 probe with no coating. The CCRC TDR probe was effectively insulated from any energy loss caused by the increase in EC_{soln} such that the CCRC probe was capable of measuring θ_v for $EC_{soln} > 1.06$ S m^{-1}. The NC and GAP probes were both affected with increasing EC_{soln} concentration with the NC probe exhibiting the most pronounced effect. The NC probe could effectively measure θ_v for $EC_{soln} \leq 0.132$ S m^{-1}, while the GAP probe was capable of measuring θ_v for $EC_{soln} \leq 0.558$ S m^{-1}.

The linearity seen between NC $K_a^{0.5}$ values vs. CCRC and GAP $K_a^{0.5}$ values (Fig. 4.04) is in agreement with the results reported in soil by Mojid et al. (1998) and Persson et al. (2004) while the

linearity seen between $K_a^{0.5}$ vs. θ_v (Fig. 4.03) is in agreement with results reported by Staub et al. (2008) for gravel, soil and water samples.

Overall, measured NC $K_a^{0.5}$ values were in good agreement with WAMM predicted $K_a^{0.5}$ values; supporting the tenet that dielectric mixing models can be used as an accurate calibration method to determine θ_v using measured $K_a^{0.5}$. NC $K_a^{0.5}$ values were less than all WAMM $K_a^{0.5}$ values except for $\theta_v = 0.167$ m^3 m^{-3}. Determining an accurate position of the second reflection in the TDR waveform for the $\theta_v = 0.167$ m^3 m^{-3} was a contributing factor for this deviation. CCRC and GAP $K_a^{0.5}$ values were considerably lower than WAMM and NC $K_a^{0.5}$ values and the difference between the coated probes and the NC and WAMM $K_a^{0.5}$ values increased with increasing θ_v. This differential in $K_a^{0.5}$ was evident in the regression slopes of the NC probe compared to the CCRC and GAP probes. At the same time, there was a very strong linear relationship between NC vs. CCRC $K_a^{0.5}$ values and NC vs. GAP $K_a^{0.5}$ values. The coating appears to dampen the TDR signal, more so with increasing θv, but still maintain a linear correlation with respect to $K_a^{0.5}$ measured by a non-coated probe.

Implied by the fact that $K_a^{0.5}$ values for the NC probe were consistently lower than WAMM $K_a^{0.5}$ values was the possibility that the calculated value of $l_{off} = 0.181$ may be inaccurate. Using the method described in Section 2.2 and Eq. [2.10], it was possible to determine l_{off} for the NC probe with the probe immersed completely in air (PICA, $\theta_v = 0.000$ m^3 m^{-3}) or deionized water (PICW, $\theta_v = 1.000$ m^3 m^{-3}). Since $K_{air} = 1$ and $K_{water} = 79.45$ at 22.5 °C, the expected l_a values for the PICA and PICW would be 0.300 m and 2.674 m, respectively. Subtracting PICA and PICW l_a values from measured l_t values using Eq. [2.10], PICA and PICW l_{off} values were determined to be 0.139 m and 0.151 m, respectively. PICA l_{off} was less than PICW l_{off} and both of these l_{off} values were lower than the calculated l_{off} value of 0.181 m. Of note, the above calculated and measured l_{off} values are all greater than the probe offset factor of 0.085 m determined empirically by the manufacturer of the CS605 probe (Campbell Scientific Inc., 2005).

The discrepancy in l_{off} values could possibly be related to the dielectric constant of the material surrounding the probe head of the CS605 probe, which is always air in this case, using the water air immersion method. This line of thought suggests that the rod length encased in the probe head epoxy coating has measured some fractional volume of material external to the dimensions of the probe head. In effect, the probe head epoxy coating could be considered analogous to the polyolefin coating applied to the CCRC and GAP probes. This also suggests that the probe head dimensions or the volume of the probe head may be a significant factor on TDR $K_a^{0.5}$ measurement, i.e. the smaller the volume of the probe head, the greater the effect the material surrounding the probe head has on the TDR measurement. The smallest dimension of the CS605 probe is the thickness at 0.019 m, which means the thickness of the epoxy coating above and below the circumference of the probe rods would be 0.0095m or 18 times the thickness of the polyolefin coating.

The effect that materials with considerably different permittivities surrounding the probe head had on TDR measurements was examined using the water air immersion method and the results are provided in Chapter 5. There was a substantial difference in the TDR waveforms collected with the NC probe when the probe head was surrounded by air compared to being surrounded by water.

4.3.2 θ_v Measurement Using NC and CCRC TDR Probes - Sand-Water Mixtures

The linear response between $K_a^{0.5}$ vs. θ_v observed for the NC and CCRC probes using the water-air immersion method was also evident when the NC and CCRC probes were used for the sand-water mixtures as a valid representation of a sandy soil at different water contents. The linearity seen between $K_a^{0.5}$ vs. θ_v for the CCRC probe (Fig. 4.06) was in agreement with the results reported for coated TDR probes when used in different soils by Mojid et al. (1998). Linearity was also established between $K_a^{0.5}$ vs. θ_v for coated probes used in sand (Persson et al., 2004) and gravel, soil and water mixtures (Staub et al., 2008) using data transposed from their research results (See Appendix B).

The substantial discrepancy between the $K_a^{0.5}$ vs. θ_v calibration curves for the water-air immersion and sand-water mixtures method highlights the fact that a separate calibration step would be required when a TDR probe is used to determine the water content of different materials when a polyolefin coating is applied to the center-conducting rod of a TDR probe. Of significant note, the water-air immersion method cannot be used as a surrogate for other mediums, however the water-air immersion method does provide an effective methodology to measure and determine any differences that may result from design changes to a TDR probe.

4.3.3 EC Measurement Using NC, CCRC and GAP TDR Probes

Increasing EC_{soln} resulted in decreasing ρ_{min} and ρ_f values for the NC and GAP probe while ρ_{min} values decreased and ρ_f values were equivalent for the CCRC probe. No direct correlation was evident between EC_{soln} and ρ_f for the CCRC probe. The NC and GAP probes were capable of measuring EC_{soln} up to 1.06 S m^{-1} and the CCRC probe was incapable of measuring EC_{soln} at any level. These observations clearly indicate that there must be direct contact between the medium being measured and the metal surface of the center-conducting rod of the CS605 probe before any effect on the TDR signal is caused by an increase in EC_{soln}. This finding indicates that the effective soil volume being measured for EC has to be contained within the area of the 0.01 m gap and does not represent the EC along the entire length of the probe.

The low conductance polyolefin coating on the CCRC and GAP probes has effectively reduced the length and cross sectional area of the conductive metal TDR rod exposed to EC_{soln} and altered the measurement of conductance and conductivity. The effect of reducing the exposed metal surface of the center conducting rod from 0.30 m to 0.01 m for the GAP probe resulted in EC_{GT} and Z_L^{-1} values for EC_{soln} that were at least a magnitude lower than EC_{GT} and Z_L^{-1} vs. EC_{soln} for the NC probe.

The fact that NC probe EC_{GT} values using ρ_{min} (or ρ_0) were not equal to EC_{soln} values (Table 4.03) clearly demonstrates that the EC_{GT} method does not accurately explain the relationship between EC and TDR ρ_{min} and ρ_f values. As well, the EC_{GT} method effectively reduces the maximum EC concentration that can be measured with TDR as was evident from the results shown in Fig. 4.08 where $EC_{soln} \geq 0.132$ S m^{-1} could not be resolved. By definition, this result would be expected since $\rho_{min} = \rho_f$ for $EC_{soln} \geq 0.132$ S m^{-1} thereby reducing $[(1 + \rho_{min})/(1 - \rho_{min})]$ $[(1 - \rho_{inf})/(1 + \rho_{inf})]$ of Eq. [2.19] to unity such that $EC_{GT} = (\varepsilon_0 c/l_r) K_a^{0.5}$. This will be a constant value at any given θ_v level and essentially identifies the maximum EC_{soln} concentration that can be calculated using the EC_{GT} method. The same limitation for the EC_{GT} method will occur with the GAP probe since ρ_{min} will eventually be equivalent to ρ_f for an EC_{soln} concentration greater than 1.06 S m^{-1} (Fig. 4.08).

Since EC_{cell} values were not equal to EC_{soln} values for the NC and GAP probes and the cell constant K increased as EC_{soln} increased, the cell constant method was considered to be invalid as a means of determining EC using TDR in highly saline soils: especially in light of the fact that K was variable and not a constant value. The relatively minor change in slope of the second order polynomial regression curve for $EC_{soln} \leq 0.132$ S m^{-1} supports the use of a linear correlation between EC_{cell} and EC_{soln}, however calculated EC_{cell} values are still not equivalent to EC_{soln} values. The EC_{cell} method does not accurately explain the relationship between EC and ρ_f values. The straightforward relationship between Z_L^{-1} vs. EC_{soln} was found to perform just as effectively as a calibration method for the determination of EC_{soln} using TDR.

No change in $K_a^{0.5}$ was found to occur with increasing EC_{soln} (Table 4.06) for $\theta_v = 1.000$ m^3 m^{-3}. The only noticeable effect of EC_{soln} on the measurement of $K_a^{0.5}$ was the suppression of the second reflection in the TDR waveform. Interestingly, $K_a^{0.5}$ values for all three probes in Table 4.01 were lower than $K_a^{0.5}$ values in Table 4.06 and this discrepancy was considered to be a function of the resolution of the 1502B TDR instrument. To obtain a valid ρ_f value for EC measurement, the distance

scale was increased from the 0.5 m per division that was used for the $K_a^{0.5}$ measurements in Table 4.01 to 2.5 m per division.

4.3.4 Applying the WAMM to θ_v Measurement

$K_a^{0.5}$ values measured for the CCRC and GAP probes were not equal to $K_a^{0.5}$ values calculated using the WAMM. The slope for the NC $K_a^{0.5}$ vs. θ_v regression line was approximately twice the slope of the CCRC and GAP $K_a^{0.5}$ vs. θ_v regression lines. This difference indicated that the effect on $K_a^{0.5}$ caused by the polyolefin coating became more pronounced as θ_v increased. The effect of the polyolefin coating appears to be substantially greater than would be expected based on the 0.00053 m thickness of the coating. The thickness of the polyolefin coating (pc_t) relative to the 0.002375 m radius of the probe rods (r_p) was pc_t/r_p = 22.5%, while the thickness of the polyolefin coating relative to the separation distance between the probe rods (s_p) was pc_t/s_p = 3.0%.

The difference in $K_a^{0.5}$ between the CCRC and GAP probes and the WAMM means that $K_a^{0.5}$ cannot be calculated using the WAMM unless modifications are made to the WAMM to account for the effect of the polyolefin coating. The coating material has become an integral part of the sample volume being measured by the TDR such that the volume of the coating material (V_{coat}) and the dielectric constant of the coating material (K_{coat}) would have to be included in the WAMM of Eq. [3.08]. As well, the volume fractions of water and air would have to be adjusted to account for V_{coat} as a portion of the total volume of the sample, effectively reducing the sample volume being measured. Modifying the WAMM to derive a coated probe water air dielectric model for water and air (CWAMM) was found to be very involved technically.

The fact that the electrical insulating properties of the polyolefin coating may have had a greater effect on the TDR signal than the volume of the coating, consideration was given to the effect the coating material had on the electric fields generated by the TDR probe. Annan (1977a) considered the dependence of the sample volume to be related to the proximity to the center-conducting rod and a

result of the TDR signal being more sensitive to the region closest to the center rod of the TDR probe. The spatial sensitivity of K_a measured using TDR has been related to the electrostatic potential distribution (Φ) for a TDR probe and considered analogous to the sample area measured by a TDR probe (Zegelin et al., 1989; Knight, 1992; Ferre et al., 1998).

Two-dimensional electrostatic field models of the electric potential field (Φ) and the electric field intensity (E) were generated for the NC and CCRC probes in air, water and polyolefin to evaluate the effect the polyolefin coating had on the electrostatic properties created with a three rod TDR probe. The results of this study are presented in Chapter 6.

To estimate the effect of the spatial sensitivity on TDR measured $K_a^{0.5}$, the volume of the polyolefin coating was increased radially by adding successive, concentric layers of the polyolefin heat shrink tubing (Fig. 4.14). A total of 20 layers of the polyolefin tubing were applied to the center-conducting rod of the CS605 TDR probe to obtain a final coating thickness of 0.011379 m. The effect of increasing the thickness of the polyolefin coating on TDR measured $K_a^{0.5}$ was determined using the water air immersion method.

Due to the large number of waveforms collected, i.e. twenty layers times six θ_v levels, only the waveforms for $\theta_v = 1.000$ m^3 m^{-3} have been presented here (Fig. 4.15). As the thickness of the polyolefin coating increases, the distance to the position of the second reflection (ρ_2) decreases. When the coating thickness exceeded 0.011 m, there was little separation between the TDR waveforms and the position of ρ_2.

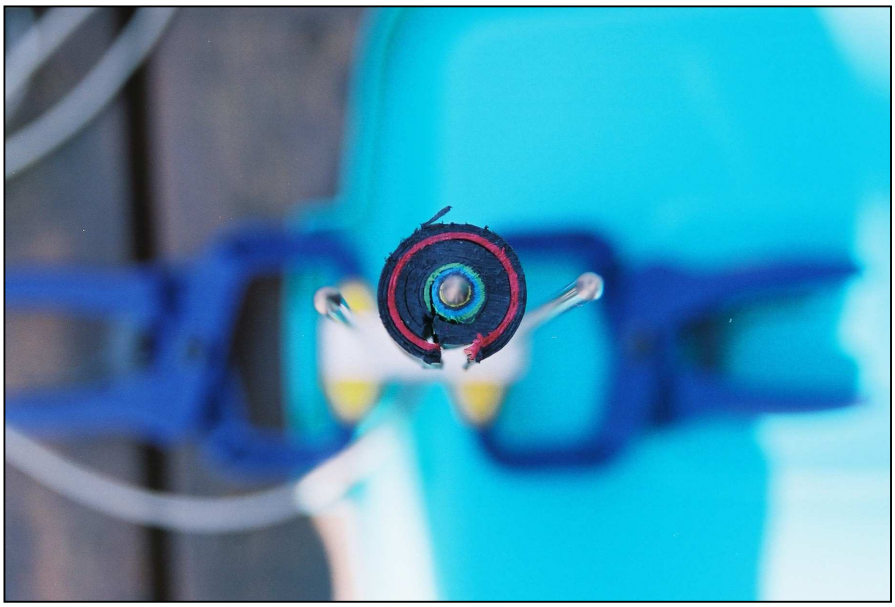

Fig. 4.14 Increasing Thickness of the Polyolefin Coating on the Center Conducting Rod
Shows the successive layers of polyolefin heat shrink tubing added to center conducting rod.

Due to the large number of waveforms collected, i.e. twenty layers times six θ_v levels, only the waveforms for θ_v = 1.000 m^3 m^{-3} have been presented here (Fig. 4.15). As the thickness of the polyolefin coating increases, the distance to the position of the second reflection (ρ_2) decreases. When the coating thickness exceeded 0.011 m, there was little separation between the TDR waveforms and the position of ρ_2.

The expected value of $K_a^{0.5}$ = 1.82 for 100% polyolefin was not reached at the maximum polyolefin coating thickness of 0.011328 m at θ_v = 1.000 m^3 m^{-3} with measured $K_a^{0.5}$ = 2.13 or 17% greater than expected $K_a^{0.5}$. In effect, the small change in measured $K_a^{0.5}$ past 0.011 m polyolefin coating thickness indicated that the contribution of any material outside of the 0.011 m coating thickness was minimal. The thickness of the polyolefin coating relative to the separation distance between the probe rods (s_p) was pc_t/s_p = 66%, leaving 34% open to be filled by any material.

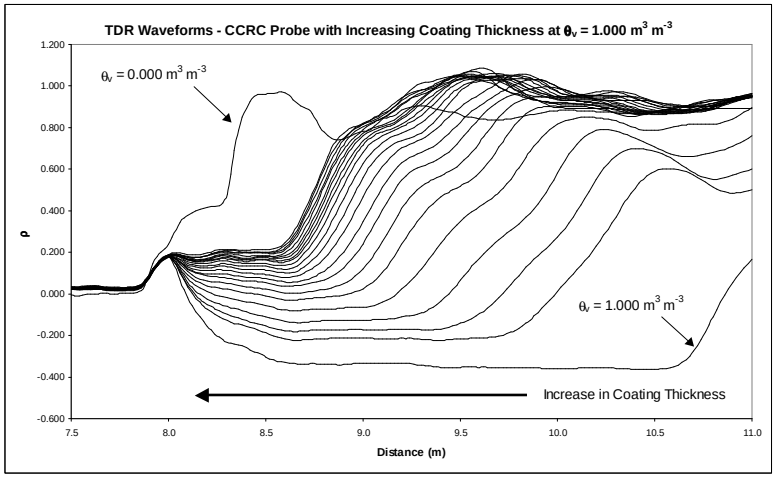

Fig. 4.15 CCRC Probe TDR Waveforms for Increasing Coating Thickness at θ_v = 1.000 m^3 m^{-3}
(NC probe TDR waveforms for θ_v = 0.000 m^3 m^{-3} and θ_v = 1.000 m^3 m^{-3} are included for reference)

Regressing measured $K_a^{0.5}$ vs. thickness of the polyolefin coating determined that a very strong, log-log (power) correlation existed, r^2 = 0.993 (Fig. 4.16). This was not the case when the radius of the center-conducting rod was added to give the total thickness of the center conducting rod plus the polyolefin coating, a correlation could not be determined between $K_a^{0.5}$ vs. thickness of the polyolefin coating + the radius of the center conducting rod.

Regression of $K_a^{0.5}$ vs. θ_v for each increase in coating thicknesses determined that a strong, linear correlation was evident at all thicknesses, with an $r^2 \geq 0.980$ for all thicknesses. As with the TDR waveforms, only selected thicknesses of $K_a^{0.5}$ vs. θ_v regressions are presented here (Fig. 4.17). The slope of all regressed $K_a^{0.5}$ vs. θ_v lines decreased with increasing coating thickness. As well, the difference between measured $K_a^{0.5}$ values for the NC probe and measured $K_a^{0.5}$ values for all coating thicknesses increased with an increase in θ_v. However, the difference between NC and coated $K_a^{0.5}$ values decreased with increasing coating thickness.

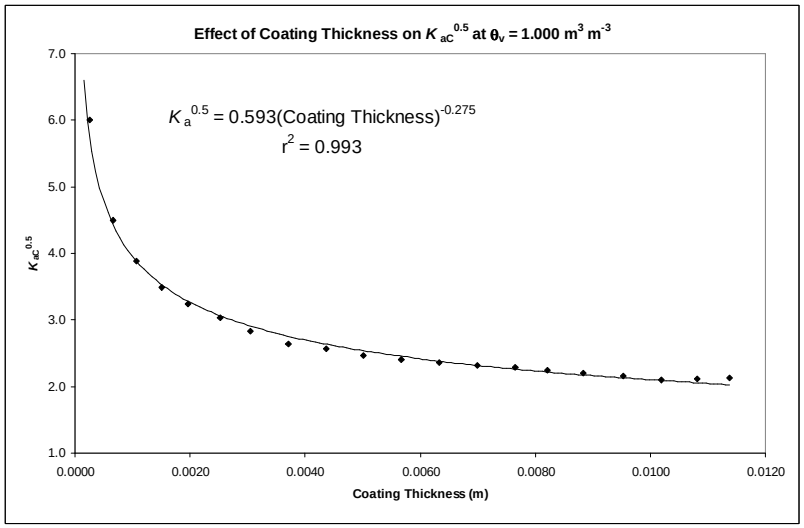

Fig. 4.16 Effect of Increasing Coating Thickness on $K_a^{0.5}$ at θ_v = 1.000 m^3 m^{-3}

The substantial change in the slope of the regressions for coating thicknesses of 0.000254 m and 0.000660 m (Fig. 4.17) corresponded with a $\Delta K_a^{0.5}$ of 1.80 at θ_v = 1.000 m^3 m^{-3} for a 0.00041 m change in the thickness of the coating. A 160% increase in coating thickness resulted in an absolute change of 28% in measured $K_a^{0.5}$. This suggests that any deviations in the thickness of the coating along the length of the probe rod would affect the measured value of $K_a^{0.5}$ and the thinner the coating, the greater the influence that a change in coating thickness will have. Cursory measurements of the polyolefin coating after removal from the CCRC probe were made with a micrometer determined an approximate range of ± 0.00012 m or a 14% variation. Based on these observations, the best practice would be to calibrate the TDR probe after the application of the polyolefin coating**.**

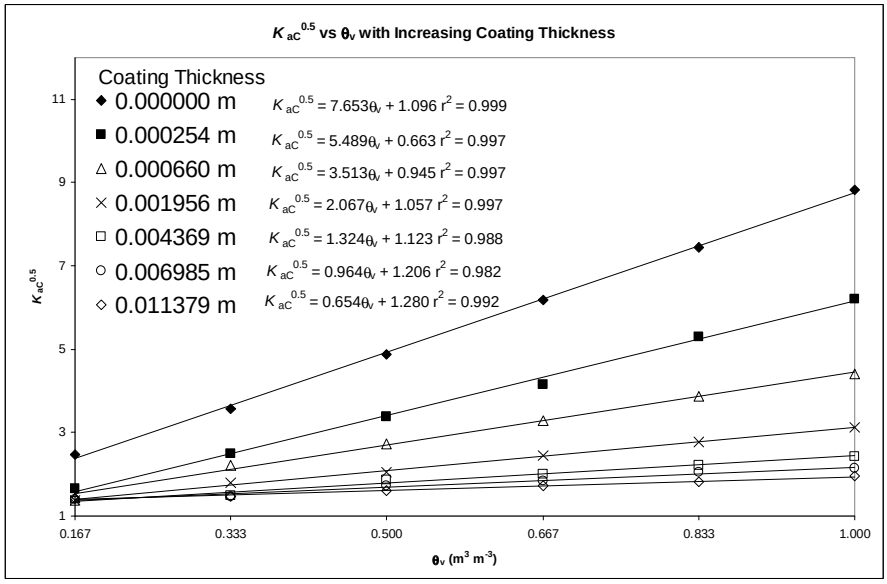

Fig. 4.17 $K_a^{0.5}$ vs. θ_v with Increasing Coating Thickness
For six of twenty different coating thicknesses evaluated

Chapter 5
Determining the Probe Head Offset l_{off}

5.1 Background

The fact that $K_a^{0.5}$ values were consistently lower than WAMM $K_a^{0.5}$ values suggested the possibility that the calculated value of l_{off} = 0.181 was inaccurate, especially since measured PICA and PICW l_{off} values were 0.139 m and 0.151 m, respectively, and l_{off} reported by the manufacturer was 0.085 m. Since the methodology called for the probe head to be immersed downward into deionized water, the probe head was surrounded by air (PHSA) for all θ_v measurements.

To determine the effect that the material surrounding the probe head had on l_{off} and, subsequently $K_a^{0.5}$, it would be necessary to immerse the probe head in such a way that the ratio of l_w/l_h was equal to l_w/l_r. This would require the TDR probe head to be exposed to water and air at the same length ratio as the probe rods, which would be very difficult to carry out. However, it was possible to follow the water air immersion methodology with water replacing air as the material surrounding the probe head (PHSW), which increased the dielectric constant surrounding the probe head from K_{air} = 1 to K_{water} = 79.45. This range in the dielectric constant corresponds with the minimum and maximum dielectric constant that the probe would be exposed to.

5.2 Method

Using a second CS605 TDR probe, $K_a^{0.5}$ measurements were taken with the TDR NC probe at the previously established θ_v levels for the PHSA and PHSW conditions. To acquire NC probe PHSW measurements, the CS605 probe was clamped into a position at a distance of 0.035 m from the bottom of a large polyethylene container using a plastic clamp. Deionized water was then added to give l_w/l_r

ratios corresponding to the same θ_v levels as the PHSA condition but with the probe head completely surrounded by water, i.e. the PHSW condition.

The CS605 probe was clamped along the sides of the probe head (width = 0.075 m) at the end of the probe head where the coaxial cable was inserted into the probe head. This insured that the clamp was at the maximum distance possible from the rod sections within the probe head to minimize any interference on the TDR measurement by the clamp material. No significant difference was found between PICA l_t values ($p = 0.300$) with and without the clamp attached, demonstrating that the clamp had no affect on the TDR measurements.

TDR waveforms were obtained using a Tektronix 1502B metallic cable tester and WinTDR software (Or et al., 2004). Ten separate waveforms were collected at each θ_v level for the NC probe in order of lowest to highest θ_v. The waveform data points were then transferred to an Excel worksheet to determine the first and second reflection points (ρ_1 and ρ_2) and calculate l_a for the three probes from Eq. [2.10]. Average values of K_a for each θ_v level were calculated using Eq. [2.12].

All statistical tests were completed at a confidence level of 95% unless otherwise stated.

5.3 Results

There were substantial differences in the NC probe PHSA and PHSW TDR waveforms at corresponding θ_v levels (Fig. 5.01 a-f). Distance to and amplitude of ρ_{apex} decreased with increasing θ_v for the PHSA while there was no change in ρ_{apex} with the PHSW. The fact that ρ_{apex} was constant for the PHSW condition (Fig. 5.02 b) was a complete departure from that seen in Fig. 2.04 (Robinson et al., 2003b) and results for the PHSA condition (Fig. 5.02 a). The increase in the dielectric constant of the material surrounding the probe head had a distinct effect on the TDR waveform response, which was seen to extend along the entire length of the TDR probe.

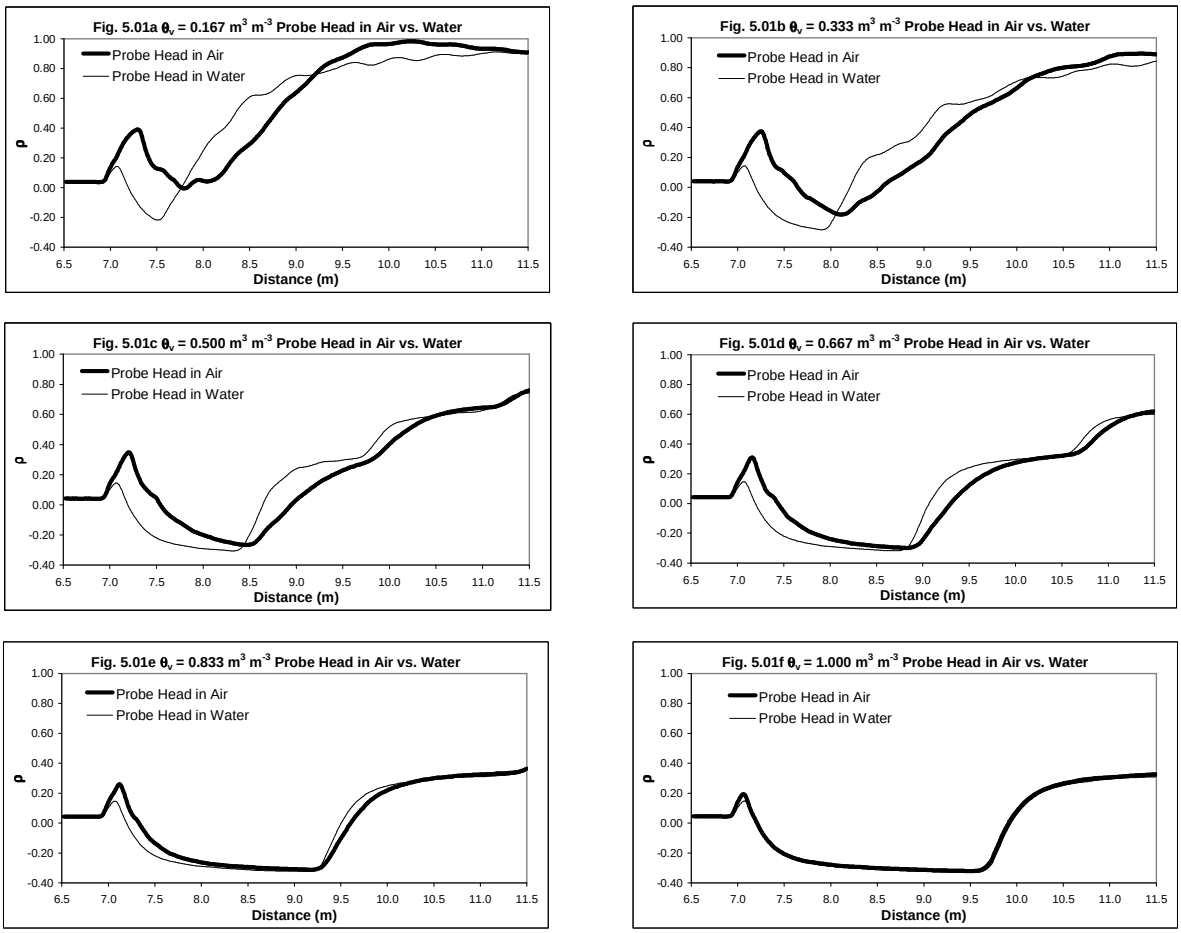

Fig. 5.01 a-f NC Probe TDR Waveforms for PHSA and PHSW Conditions
(PHSA = Probe head surrounded in air, PHSW = Probe head surrounded in water)

There was a significant difference in PHSA and PHSW ρ_{min} at all θ_v levels ($p < 0.000$) based on a difference between means analysis using a 95% confidence interval, but the difference decreased as θ_v increased (Table 5.01). The definition of the PHSW waveforms was enhanced with a noticeably steeper slope evident in the rise in ρ following ρ_2 and the position of ρ_2 was more easily distinguished. All PHSW l_t values were significantly less than PHSA l_t values with the exception of

$\theta_v = 0.000\ m^3\ m^{-3}$ and $\theta_v = 1.000\ m^3\ m^{-3}$, which were equivalent for the PHSA and PHSW conditions, respectively (Table 5.01).

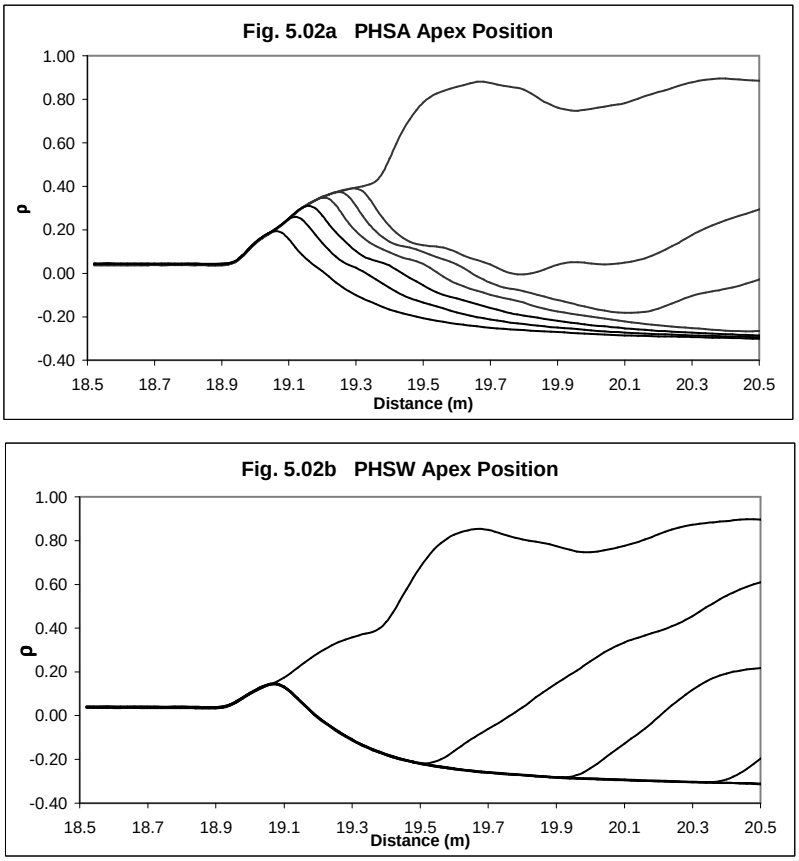

Fig. 5.02 a-b Position of ρ_{apex} for the PHSA and PHSW Condition
Probe head is surrounded by air in Fig. 5.02a and water in Fig. 5.02b

Table 5.01 PHSA and PHSW ρ_{min} and l_t vs. θ_v

	ρ_{min}		l_t	
θ_v	PHSA	PHSW	PHSA	PHSW
0.000	0.330	0.335	0.426	0.449
0.167	-0.005	-0.218	0.885	0.615
0.333	-0.181	-0.284	1.238	1.032
0.500	-0.267	-0.306	1.613	1.502
0.667	-0.299	-0.317	2.007	1.917
0.833	-0.312	-0.322	2.370	2.334
1.000	-0.320	-0.330	2.742	2.762

The design of the methodology included two $K_a^{0.5}$ TDR measurements where the material surrounding the probe head had substantially different K_a values: PHSA at $\theta_v = 0.000$ m^3 m^{-3} with the probe head and exposed rods surrounded by air ($K_{air} = 1$) and PHSW at $\theta_v = 0.000$ m^3 m^{-3} with the probe head surrounded by water ($K_{water} = 79.45$) and the probe rods exposed to air. A significant difference was found between PHSA and PHSW l_t values at $\theta_v = 0.000$ m^3 m^{-3} ($p < 0.000$) based on a difference between means analysis using a 95% confidence interval which is clearly seen in their respective TDR waveforms (Fig. 5.03).

Measurements taken to determine l_{off} using PICA and PICW conditions for this second probe were compared to PICA and PICW l_{off} values for the first probe. Using Eq. [2.10], PICA $l_{off} = 0.126$ m for $\theta_v = 0.000$ m^3 m^{-3} and $K_{air} = 1$ with PICW $l_{off} = 0.149$ m for $\theta_v = 1.000$ and $K_{water} = 79.45$. Both values were different than the respective PICA and PICW l_{off} values of 0.139 m and 0.151 m for the first probe. There was no statistical difference between PICA l_t values ($p = 0.300$) for the two probes based on a difference between means analysis using a 95% confidence interval, but there was a statistically significant difference between PICW l_t values ($p < 0.000$) for the two probes. However, the difference in PICW l_t values was very small (< 0.2%) and the two values were considered equivalent. Measured PICA and PICW l_{off} values for the probes were notably less than the calculated l_{off} value of 0.181 m from Eq. [2.11].

Using the respective l_{off} values, $K_a^{0.5}$ vs. θ_v calibration curves were constructed (Fig. 5.04). PHSW $K_a^{0.5}$ values were consistently less than PHSA $K_a^{0.5}$ values at all θ_v levels except for $\theta_v = 0.000$ m^3 m^{-3} and $\theta_v = 1.000$ m^3 m^{-3}. The greatest variation between $K_a^{0.5}$ values occurred at $\theta_v = 0.167$ m^3 m^{-3}. A very strong linear correlation for $K_a^{0.5}$ vs. θ_v was found for the PHSA ($r^2 = 0.999$) and PHSW ($r^2 = 0.992$) conditions.

The results indicate that the material surrounding the probe head affects the measured TDR waveform of a CS605 TDR probe and that l_{off} varies with the ε of the material surrounding the probe head. $K_a^{0.5}$ of the material surrounding the probe head also affects measured ρ or Z values as witnessed by the significant difference in ρ_{min} values of the TDR waveforms ($p < 0.000$), based on a difference between means analysis using a 95% confidence interval.

In field applications the entire TDR probe is typically inserted into the soil. The probe head and the probe rods would in all probability be surrounded by a material that had the same K_a and the large difference in K_a between air and water surrounding the probe head used here would not be experienced. However, a variation in l_{off} and ρ_{min} would still occur with a large deviation in water content, which would introduce an error in the TDR measurement of θ_v.

The effect that the dielectric constant of the material surrounding the probe head has on subsequent TDR measurements was marginal due to the relatively large dimensions of the CS605 probe head epoxy coating. However, TDR probes with smaller probe head dimensions would be affected to a greater extent. In order to determine an accurate, constant l_{off} value the dimensions of the probe head coating material should be sized such that the encased rod sections measure the dielectric constant of the probe head coating material only. Selection of a probe head material with a high dielectric constant, i.e. that of water, would significantly reduce, if not eliminate the variation in the position of ρ_{apex}.

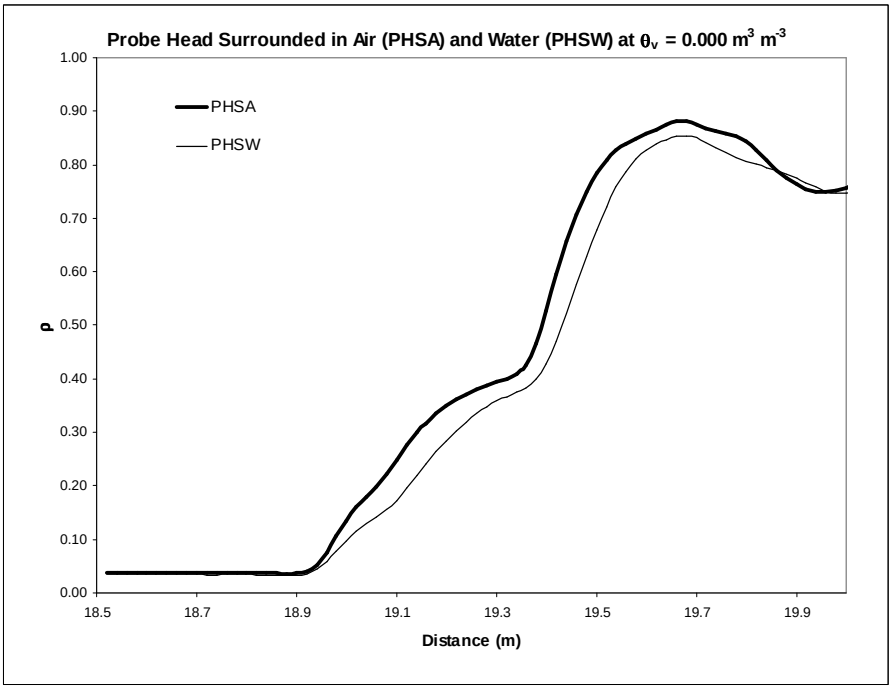

Fig. 5.03 PHSA and PHSW TDR Waveforms at θ_v = 0.000 m^3 m^{-3}

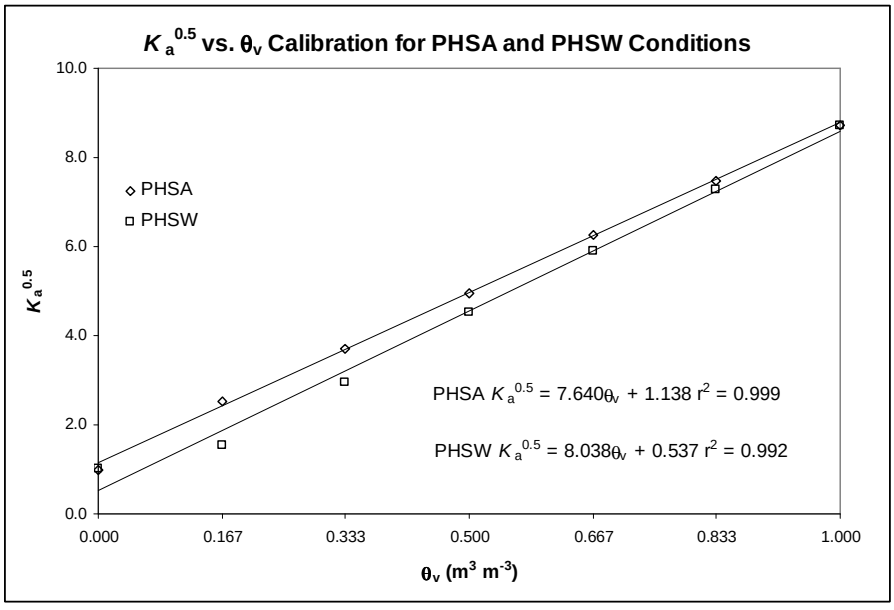

Fig. 5.04 $K_a^{0.5}$ vs. θ_v Calibration Curves for PHSA and PHSW Conditions

Chapter 6
The Electrostatic Field of Non-coated and Coated TDR Probes

6.1 Application of Electrostatic Theory

The ability to determine the relationship between K_a and θ_v for a coated TDR probe is complicated by the effect the coating material has on the TDR signal. If the coating is an integral part of the composite sample there should be very little effect on measured K_a when a thin coating is applied to the TDR probe. Annan (1977a) considered the dependence of the sample volume to be related to the proximity to the center-conducting rod and a result of the TDR signal being more sensitive to the region closest to the center rod of the TDR probe.

The spatial sensitivity of K_a measured using TDR has been related to the electrostatic potential distribution (Φ in V) for a TDR probe and considered analogous to the sample area measured by a TDR probe (Zegelin et al., 1989; Knight, 1992; Ferre et al., 1998). A greater interaction with the nearer surrounding dielectric materials is found within the higher relative energy density resulting in an increased sensitivity (Becker et al., 2006). The effective sampling area or volume was considered to conform to the area of greatest spatial sensitivity within the electrostatic potential distribution, which in turn, is controlled by the diameter (*d*) and separation (*s*) of the rods (Ferre et al., 1998). This approach associates the heterogeneous variations in dielectric constant surrounding the probes to be directly dependent on Φ, where Φ is determined from the source voltage applied to the probe.

The electric field intensity (E) is the space surrounding an electric charge or electric force per unit charge (V m^{-1}) and is dependent upon potential differences within an electric field. The organization or charge density of potential differences within the electric field, which includes charge migration and electric dipole reorientation, is termed the electric displacement field or electric flux

density (D). The electric displacement field is related to the electric field intensity by the ε or K_a of the material the electric field is formed within (Frohlich, 1986; Jackson, 1976) and defined as:

[6.01] $D = K_a E$ (C m^{-2})

Electric fields store energy (U) and for normal substances:

[6.02] $U = 0.5(ED + HB)$ (J m^{-3})

Where H is the magnetic field and B is the magnetic induction. For most soils the magnetic properties cannot be established due to the short time interval of the exciting TDR pulse (Roth et al., 1992). Therefore, $HB << ED$ and the stored electric energy is represented by half the product of E and D. The relationship between E, D and U is dependent upon the dielectric constant of the sample volume and changes in K_a will directly affect D and U corresponding to a specific ratio. Over the very short time interval in which the TDR measurement is taken, i.e. nanoseconds, θ_v and ϕ can be considered constant, effectively making the sample volume homogenous in terms of sample dielectric constant even though the separate soil components are heterogeneous in make up.

By determining the spatial pattern of E within the region of the TDR probe it could be possible to define the sample volume by determining the position where the TDR receiver can detect the minimum E created by the TDR voltage pulse. The maximum distance to which the difference in voltage due to E can be differentiated by the instrument will define the volume measured.

6.2 Method

Two-dimensional electrostatic field models of the electric potential field (Φ) and the electric field intensity (E) were developed using Ansoft Maxwell 2D Version 3.1.04 Electrical Engineering Simulation Software. The models were derived using a basic template to represent a CS605 TDR three-rod probe inserted into materials of different dielectric constants.

The modeled fields were generated within a 0.007 m^2 area using the dimensions of 0.10 m in a parallel orientation to the probe rods and 0.07 m in a perpendicular orientation to the probe rods (Fig. 6.01). The origin of the model at x = 0 m and y = 0 m was set at the center of the center-conducting rod. It was possible to extend the area beyond 70 cm^2 by setting a 'balloon' boundary. The balloon boundary extends the model area to infinity based on the assumption that the fields generated by the TDR probe in the balloon boundary are isolated from other electric field sources.

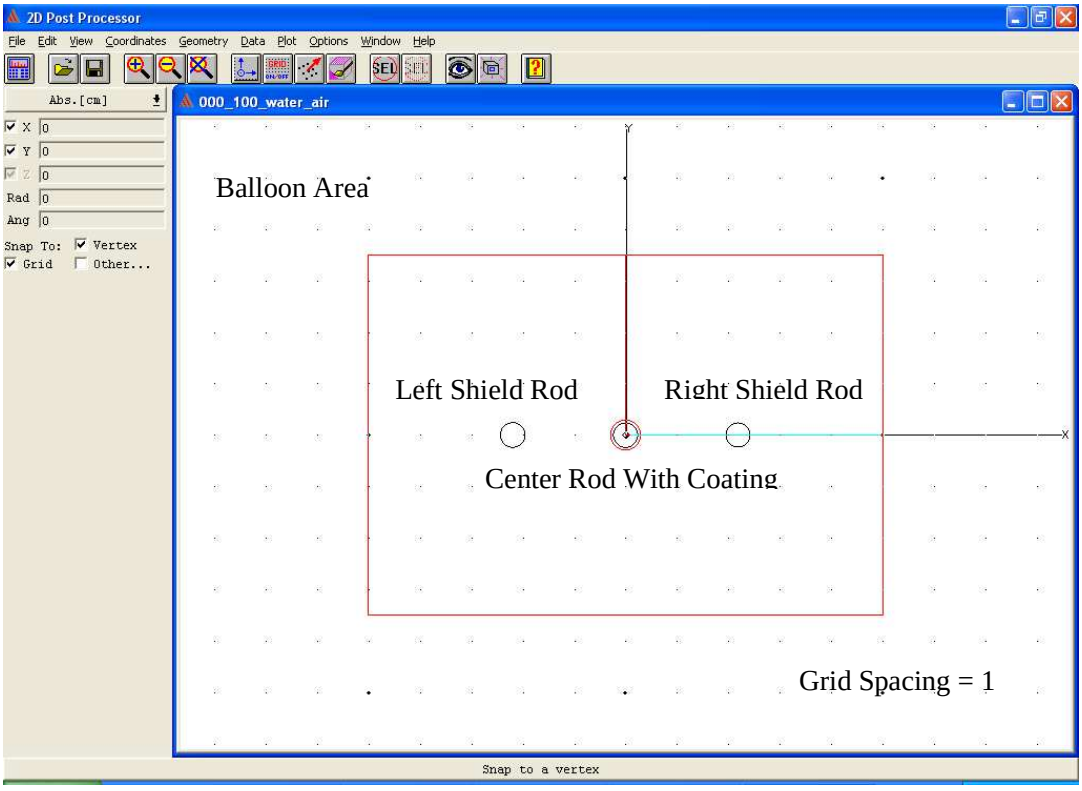

Fig. 6.01 Ansoft Maxwell 2D Model Configuration

The Φ and E field were modeled for the NC and CCRC probes immersed in air, polyolefin or water using the respective dielectric constants of K_{air} = 1, K_{coat} = 3.3 and K_{water} = 81. As well, models were designed to examine the difference in Φ and E field for a CCRC probe completely immersed in water. An input voltage of 0.5 V was applied to the center conducting rod only; the shield rods were

set at 0 V to represent a grounded connection, typical of an unbalanced twin wire transmission line. The 0.5 V was selected based on the potential difference measured across the center conducting rod and one of the shield rods of the CS605 TDR probe using a Mastercraft Digital Multimeter. This voltage also corresponds to the short circuit condition for a TDR probe such that $Z_L \approx 0\Omega$.

To determine the effect of the polyolefin coating on the electric field intensity between the center conducting rod and the ground shield rods, the same model was used with dielectric constants that represented the θ_v levels used in the water air immersion method. These dielectric constants were calculated using water air dielectric mixing model. For each dielectric constant or θ_v, a transect of the electric field intensity, E, was drawn from the center of the center-conducting rod through the center of the ground shield rods to a distance 0.05 m from the center of the center-conducting rod. An E transect modeled for the NC probe and the CCRC probe.

6.3 Results

The Φ generated by a NC probe immersed in air (Fig. 6.02) conforms to the dimensionless electric potential distribution for the three-rod probe that was presented by Zegelin et al. (1989). The model showed no change in Φ when the NC probe was immersed in water or polyolefin. However, a distinct change occurred in Φ when the CCRC probe was used, especially when the probe is completely immersed in water (Fig. 6.03).

The modeled E field generated for the NC probe immersed in air formed a different pattern than Φ (Fig. 6.04). For the NC probe, an elliptical pattern was evident for E with the highest E occurring adjacent to the center rod. E was more concentrated along the axis between the two shield rods (Fig. 6.04), which is opposite in orientation to Φ. The distribution in E did not change with immersion in water or polypropylene. An increase in E occurred around the inner circumference of the shield rods facing the center rod. A distinct difference in E occurs for the CCRC probe, especially

when the probe is completely immersed in water (Fig. 6.05). For the CCRC probe, E was found to be concentrated within the polyolefin coating material.

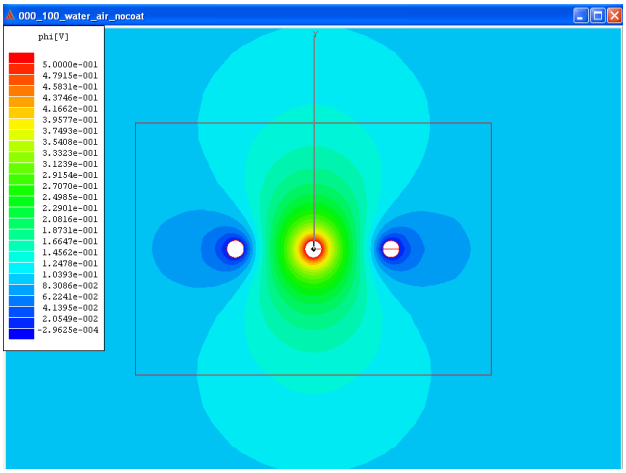

Fig. 6.02 Φ Field for Three Rod NC TDR Probe in Air, Water and Polyolefin

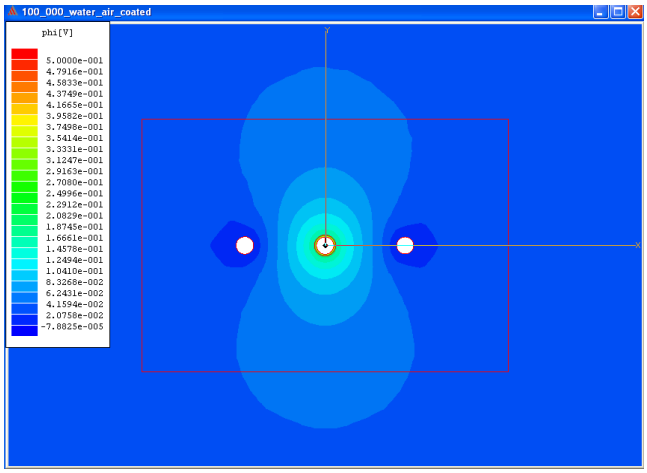

Fig. 6.03 Φ Field for Three Rod CCRC TDR Probe Completely Immersed Water

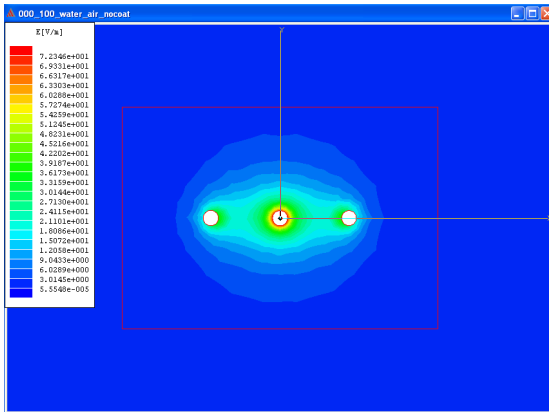

Fig. 6.04 E Field for Three Rod NC TDR Probe in Air, Water or Polyolefin

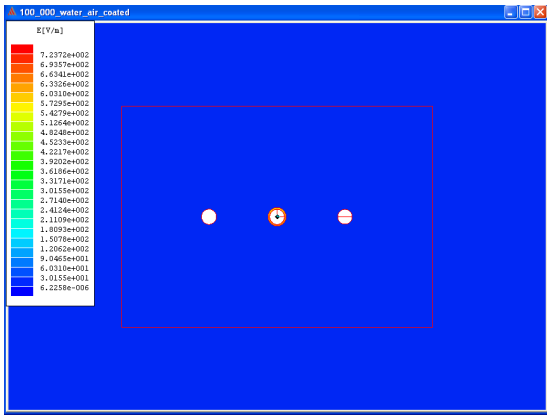

Fig. 6.05 E Field for Three Rod CCRC TDR Probe Completely Immersed Water

The polyolefin coating on the CCRC probe appears to have a dampening effect on Φ and E in the sample region while Φ and E seem to be more concentrated within the coating material. The insulating effect of the polyolefin coating substantially alters the Φ and E fields generated by the TDR probe. The effect of the polyolefin coating becomes more pronounced with increasing θ_v.

The E transect for the NC probe was the same at all θ_v levels (Fig. 6.06). A rapid decrease in E was seen to occur with distance from the center-conducting rod, reaching a minimum value at a distance of 0.0125 m. This was followed by an increase in E to the ground shield rod after which a gradual decrease occurred. In contrast, the E cross section for the CCRC probe was not the same for

the different θ_v levels (Fig. 6.07). The CCRC probe E transect followed the same pattern as the NC probe transect, however a drastic increase in the electric field intensity occurred within a distance of 0.6 mm from the surface of the center-conducting rod. As well, the increase in E at this distance was seen to increase as θ_v increased. The increase in the electric field intensity was confined within the polyolefin coating.

Outside of the polyolefin coating, a decrease in the electric field intensity was noted over the CCRC probe cross section. The decrease in the electric field intensity of the CCRC probe was seen to increase with an increase in θ_v. The one exception was $\theta_v = 0.000\ m^3\ m^{-3}$, i.e. air, where there was a decrease in the electric field intensity within the polyolefin coating and the electric field intensity along the cross section outside of the polyolefin coating of the CCRC probe was generally equivalent to the cross section of the NC probe.

The decrease in the electric field intensity with increasing θ_v corresponds with the earlier finding that $\Delta K_a^{0.5}$ between the NC and CCRC probes increases with increasing θ_v. The significant increase in electric field intensity within the polyolefin coating with increasing θ_v suggests that the containment of the electric field intensity within the polyolefin coating is a contributing factor in the observed reduction of TDR measured $K_a^{0.5}$ using the CCRC probe.

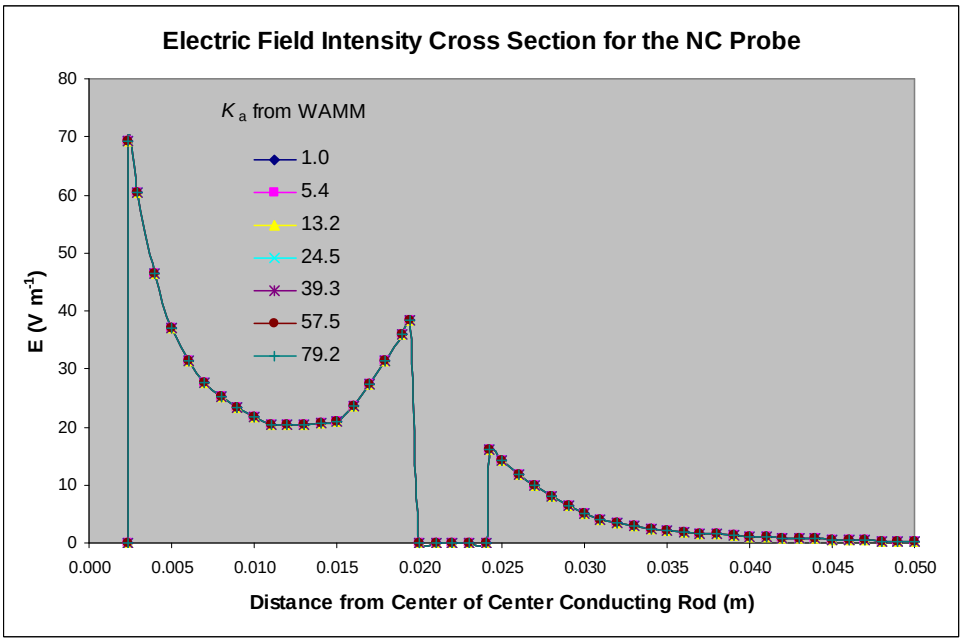

Fig. 6.06 Electric Field Intensity Cross Section for the NC Probe
K_a values were calculated to match water air immersion θ_v values using the WAMM

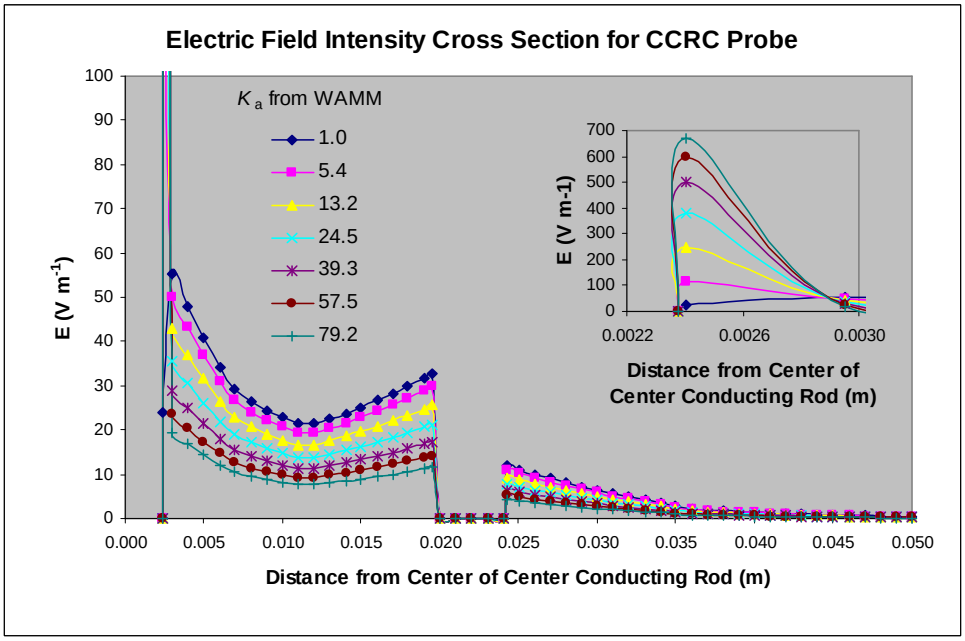

Fig. 6.07 Electric Field Intensity Cross Section for the CCRC Probe
K_a values were calculated to match water air immersion θ_v values using the WAMM

Chapter 7
Conclusions

The application of a 0.00053 m polyolefin coating to the center-conducting rod of the CS605 probe increased the capability of the probe to measure θ_v in highly saline solutions. The CCRC probe made TDR θ_v measurement possible at EC_{soln} levels as high as 1.06 S m^{-1} compared to a maximum EC_{soln} of 0.132 S m^{-1} for the NC TDR probe. However, the application of a polyolefin coating to the center-conducting rod eliminated the ability of the CCRC probe to effectively measure the electrical conductivity of the solution. Using a GAP probe, with a 0.01 m long gap at the center of the polyolefin coating that exposed a section of the stainless steel center rod, made it possible to measure the electrical conductivity of a solution. However, the GAP probe was only capable of measuring θ_v when EC_{soln} was less than 0.558 S m^{-1}. There has to be direct contact between the metal surface of the TDR probe rods and the sample to make EC measurement possible as the nonconductive property of the polyolefin coating acts as an insulator between the probe rods and the sample being measured.

The EC measured using the GAP probe was contained within the small section of the exposed metal surface of the center-conducting rod, i.e. the actual area sampled was only $1/30^{th}$ of the total area measured by the CS605 TDR probe. Any sizeable gradient in the EC of the soil being measured along the length of the probe would not be seen using the GAP probe coating configuration used here and result in an incorrect EC measurement. Increasing the size of the gap would alleviate this problem, however an increase in the size of the gap would lower the maximum EC concentration that the probe could effectively measure. However, the size of the gap can be tailored to the expected range of electrical conductivity, i.e. low EC concentrations could use larger gaps and high EC concentrations could use smaller gaps. The possibility of using several small gaps spaced at intervals

along the length of the polyolefin coating has been presented as a viable alternative (pers. comm. *D. Rudolph*) and certainly deserves further study.

An increase in EC_{soln} did not affect the TDR measurement of θ_v. No difference was found in measured $K_a^{0.5}$ when EC_{soln} was increased. However, the ability to measure θ_v was limited to the maximum EC_{soln} levels noted above for each respective TDR probe.

The straightforward relationship between Z_L^{-1} vs. EC_{soln} was found to perform effectively as a calibration method for the determination of EC_{soln} using TDR compared to the Giese-Tiemann method which could not be used when $EC_{soln} \geq 0.132$ S m^{-1}. The cell constant method was considered to be unacceptable as a means of determining EC in highly saline soils due to the fact that the cell constant K was not a constant value.

The linear relationship between NC $K_a^{0.5}$ vs. CCRC and GAP $K_a^{0.5}$ was in agreement with other research results using soils. The linear relationship between $K_a^{0.5}$ vs. θ_v for the CCRC probe in sand-water mixtures demonstrated that the response of a coated TDR probe in soil would be linear. The linear relationship between $K_a^{0.5}$ vs. θ_v for the CCRC probe in both the water-air immersion method and sand-water mixtures were in agreement with results reported in the literature. Equivalency between NC $K_a^{0.5}$ values and WAMM predicted $K_a^{0.5}$ values indicated that the water-air immersion method provides a suitable methodology for TDR research. Although these results indicate a linear relationship between $K_a^{0.5}$ as measured with the coated probe and $K_a^{0.5}$ of the soil, a definitive test of the coated probe response in a series of soils with a range of homogenous water contents should be conducted. The water-air immersion method will inherently result in a linear relationship between $K_a^{0.5}$ vs. θ_v, regardless of the media properties or probe coating properties, i.e. dielectric constant and thickness.

The very strong linear relationship between $K_a^{0.5}$ vs. θ_v supports the premise of using $\alpha = 0.5$ in dielectric mixing models when using non-coated probes. The polyolefin coating affected TDR

measured $K_a^{0.5}$ values significantly with the CCRC and GAP probes yielding $K_a^{0.5}$ values considerably lower than NC $K_a^{0.5}$ values except for measurements taken in air. The fact that the difference between $K_a^{0.5}$ ($\Delta K_a^{0.5}$) measured using the NC probe and $K_a^{0.5}$ measured using the CCRC and GAP probes increased with increasing water content indicated that the polyolefin coating had a more pronounced effect when the CCRC and GAP probes were exposed to materials of higher dielectric constant.

The variation in the thickness of the polyolefin coating applied to the center-conducting rod showed enough variation in measured $K_a^{0.5}$ to warrant a separate calibration for each application of a coating to the TDR probe. Each separate TDR probe should be calibrated individually even if the same polyolefin tubing material is used to coat each TDR probe.

The material surrounding the probe head had a measurable effect on the TDR waveforms with a substantial difference seen in the waveform traces when the NC probe head was surrounded by water instead of air. As well, a discrepancy in the probe head offset (l_{off}) value was found for the NC probe when the probe head was completely immersed in air compared to complete immersion in deionized water. The effect of an increase in the dielectric constant of the material surrounding the probe head was not just limited to the immediate area of the probe head but was seen to affect the entire TDR waveform. The stable position of ρ_{apex} and the greater definition of the TDR waveform, especially the position of the second reflection point ρ_2, suggest that the use of a high dielectric constant material in the construction of the probe head would improve TDR $K_a^{0.5}$ measurement.

The modeled electrostatic fields generated by a TDR probe were greatly affected when the center-conducting rod was coated with polyolefin. A decrease in potential and electric field intensity was seen to occur in the region outside of the polyolefin coating. The decrease in potential and electric field intensity was greater when the dielectric constant of the material surrounding the CCRC probe was increased. The decrease in electric field intensity outside of the polyolefin coating was in direct contrast to the significant increase in electric field intensity within the polyolefin coating and

the increase in electric field intensity within the polyolefin coating increased as the dielectric constant of the material surrounding the CCRC probe increased.

A common element was found between the increase in $\Delta K_a^{0.5}$ for the NC and CCRC probes and the increase in the dielectric constant of the material surrounding the probe. In essence, the coating on the center-conducting rod has extended the probe head along the entire length of the center rod. Even though the geometry and dimensions are different as well as the fact that the dielectric constant of the probe head material and the polyolefin coating are not equivalent, the entire center-conducting rod is covered in the similar manner as the rod sections contained within the probe head. The effect on TDR measurement noted using the CCRC probe also exists for the dielectric constant measurement of the rod sections in the probe head, which was evident from the different shapes of the TDR waveforms and calculated l_{off} values for the probe head surrounded by either air or water.

The same dampening of the electrostatic fields would occur in the region outside of the probe head but to a larger extent since the thickness of the probe head is significantly greater than that of the CCRC polyolefin coating and the probe head material fills the entire volume between the center conducting rod and the ground shield rods. The effect on $K_a^{0.5}$ measurement would be similar to that found when the thickness of the polyolefin coating on the center-conducting rod was increased.

The application of a polyolefin coating on the center-conducting rod of a three rod TDR probe with a gap in the coating at the midsection of the rod can be used as an effective means to extend the capability of measuring water content and electrical conductivity in saline environments where regular TDR probes would be ineffective. Examining the effect of a polyolefin coating on TDR measurement also provides an alternative approach to the understanding of the working principles of TDR.

Appendix A
TDR EC Formulations

Relationship between voltage and ρ

[1] $\rho = \frac{V_r}{V_0} = \frac{V_r - V_0}{V_0}$

[2] $V_r = \rho * V_0 \quad 1/\rho = V_0/V_r$

[3] $\rho = \frac{Z_L - Z_c}{Z_L + Z_c} = \frac{V_r}{V_0}$

[4] $V_0 * (Z_L - Z_c) = V_r * (Z_L + Z_c)$

[5] $V_0 * (Z_L - Z_c) = \rho V_0 * (Z_L + Z_c)$

[6] $V_0Z_L - V_0Z_c = \rho V_0Z_L + \rho V_oZ_c$

[7] $V_0Z_L - \rho V_0Z_L = V_0Z_c + \rho V_0Z_c$

[8] $Z_L * (V_0 - \rho V_0) = Z_c * (V_0 + \rho V_0)$

[9] $Z_L * [V_0(1 - \rho)] = Z_c * [V_0(1+ \rho)]$

[10] $Z_L = \frac{Z_c * V_0 * (1+ \rho)}{V_0 * (1 - \rho)}$

[11] $Z_L = \frac{Z_c * (1 + \rho)}{(1 - \rho)}$

Conversion between voltage and ρ values

The forms are simply the inverse of each other: due to arithmetic the final step in the LHS cannot be attained for the RHS

$$\rho = \frac{V_r - V_0}{V_0}$$

$$\frac{(1-\rho)}{(1+\rho)} = \frac{1 - \frac{V_r - V_0}{V_0}}{1 + \frac{V_r - V_0}{V_0}} \qquad \frac{(1+\rho)}{(1-\rho)} = \frac{1 + \frac{V_r - V_0}{V_0}}{1 - \frac{V_r - V_0}{V_0}}$$

$$\frac{(1-\rho)}{(1+\rho)} = \frac{V_0}{V_0} * \frac{1 - \frac{V_r - V_0}{V_0}}{1 + \frac{V_r - V_0}{V_0}} \qquad \frac{(1+\rho)}{(1-\rho)} = \frac{V_0}{V_0} * \frac{1 + \frac{V_r - V_0}{V_0}}{1 - \frac{V_r - V_0}{V_0}}$$

$$\frac{(1-\rho)}{(1+\rho)} = \frac{V_0 - \cancel{V_0} * \frac{V_r - V_0}{\cancel{V_0}}}{V_0 + \cancel{V_0} * \frac{V_r - V_0}{\cancel{V_0}}} \qquad \frac{(1+\rho)}{(1-\rho)} = \frac{V_0 + \cancel{V_0} * \frac{V_r - V_0}{\cancel{V_0}}}{V_0 - \cancel{V_0} * \frac{V_r - V_0}{\cancel{V_0}}}$$

$$\frac{(1-\rho)}{(1+\rho)} = \frac{V_0 - (V_r - V_0)}{V_0 + (V_r - V_0)} \qquad \frac{(1+\rho)}{(1-\rho)} = \frac{V_0 + (V_r - V_0)}{V_0 - (V_r - V_0)}$$

$$\frac{(1-\rho)}{(1+\rho)} = \frac{V_0 - V_r + V_0}{\cancel{V_0} + V_r - \cancel{V_0}} \qquad \frac{(1+\rho)}{(1-\rho)} = \frac{\cancel{V_0} + V_r - \cancel{V_0}}{V_0 - V_r + V_0}$$

$$\frac{(1-\rho)}{(1+\rho)} = \frac{2V_0 - V_r}{V_r} \qquad \frac{(1+\rho)}{(1-\rho)} = \frac{V_r}{2V_0 - V_r}$$

$$\frac{(1-\rho)}{(1+\rho)} = \frac{2V_0}{V_r} - 1$$

EC_{GT} Thin Section Calculation

THIN SECTION

$$EC_{GT} = \frac{\varepsilon_0 * c}{l_r} * \frac{Z_{TDR}}{Z_0} * \frac{2V_0 - V_{inf}}{V_{inf}}$$

$$EC_{GT} = \frac{\varepsilon_0 * c}{l_r} * \frac{Z_{TDR}}{Z_0} * \frac{(1 - \rho_{inf})}{(1 + \rho_{inf})}$$

$$Z_{TDR} = Z_0 * K^{0.5} * \frac{V_{min}}{2V_0 - V_{min}}$$

$$Z_{TDR} = Z_0 * K^{0.5} * \frac{(1 + \rho_{min})}{(1 - \rho_{min})}$$

$$EC_{GT} = \frac{\varepsilon_0 * c}{l_r} * \frac{\cancel{Z_0} * K^{0.5}}{\cancel{Z_0}} * \frac{(1 + \rho_{min})}{(1 - \rho_{min})} * \frac{(1 - \rho_{inf})}{(1 + \rho_{inf})}$$

$$EC_{GT} = \frac{\varepsilon_0 * c}{l_r} * K^{0.5} * \frac{(1 + \rho_{min})}{(1 - \rho_{min})} * \frac{(1 - \rho_{inf})}{(1 + \rho_{inf})}$$

$$\frac{\varepsilon_0 * c}{l_r} = \frac{8.85E\text{-}12 * 3.0E+08}{l_r} = 0.008848$$

$$EC_{GT} = 0.008848 * K^{0.5} * \frac{(1 + \rho_{min})}{(1 - \rho_{min})} * \frac{(1 - \rho_{inf})}{(1 + \rho_{inf})}$$

Appendix B
Response of Coated TDR Probes Used for Water Content Measurement

A review of the literature provided three examples of the TDR response for a three-rod TDR probe with the center rod coated (CCRC) probe used to measure water content in different soils. In each case, regression lines were determined using data transposed from the graphs reported. The graphs used for transposed data are presented below with the corresponding linear regression analysis.

All three studies displayed a very strong linear relationship between water content and the travel time or $K_a^{0.5}$ for a three-rod CCRC probe. The regression results are in agreement with the very strong linear relationship that was measured using the Water-Air Immersion and Sand-Water Mixtures methods.

Mojid, M.A., Wyseure, G. C. L. and Rose, D. A., 1998

The Use of Insulated Time-Domain Reflectometry Sensors to Measure Water Content in Highly Saline Soils. Irrigation Science, 18:55-61.

In this study, two different polyethylene-coating materials were used and designated as Material 1 and Material 2. The results are listed as their Fig. 2. Data transposed from Fig. 2 corresponds with the symbol "□". The regression analysis undertaken was based on the results presented for Material 1 (Fig. 2 Reproduced). The regression analysis yielded a linear regression equation of:

[1] Apparent dielectric constant = 0.795 * Soil dielectric constant + 2.328 $r^2 = 0.997$

Fig. 2 Mojid et al., 1998

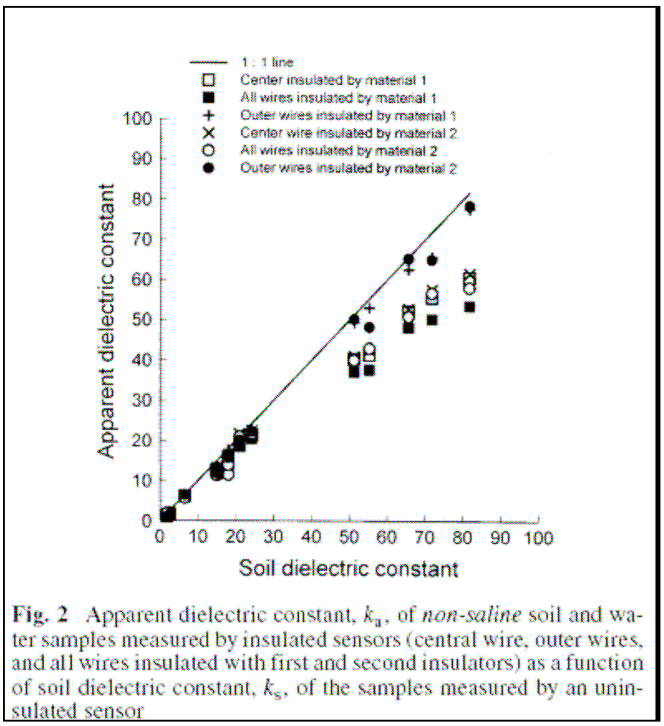

Fig. 2 Apparent dielectric constant, k_a, of *non-saline* soil and water samples measured by insulated sensors (central wire, outer wires, and all wires insulated with first and second insulators) as a function of soil dielectric constant, k_s, of the samples measured by an uninsulated sensor

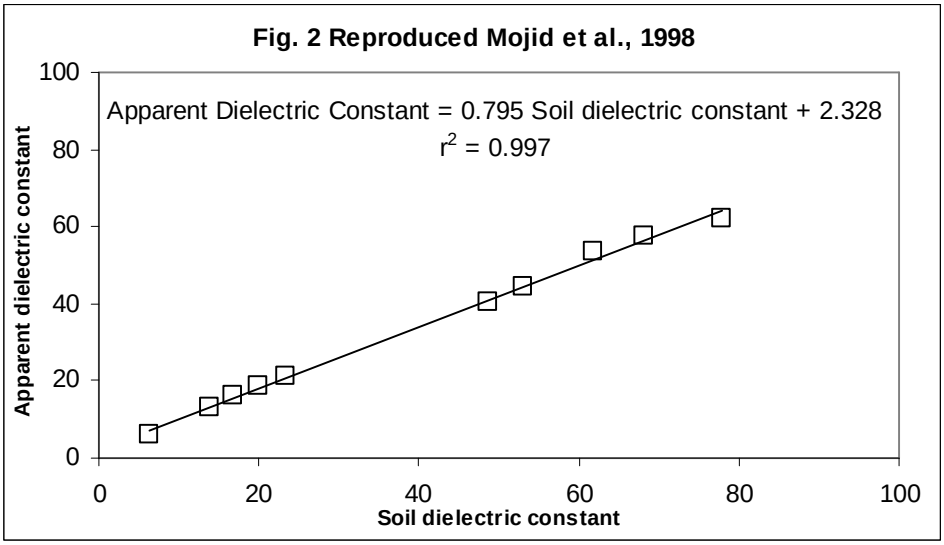

Persson, M., Bendz, D. and Flyhammer, P., 2004

Time-Domain Reflectometry Probe for Water Content and Electrical Conductivity Measurements in Saline Porous Media. Vadose Zone Journal, 3:1146-1151.

In this study, the center rod of the TDR probe was coated using two different types of heat shrink material: polyolefin and polyvinylidene fluoride. Results are presented as their Fig. 4. Data transposed from Fig. 4 corresponds with the symbol "+". The regression analysis undertaken was based on the results presented for K_{ap} (lower left quadrant of Fig. 4) that used a polyolefin heat shrink coating. The regression analysis (Fig. 4 Reproduced) yielded a second order polynomial regression equation of:

[2] $K_{ap} = 0.010\ (\text{Water content})^2 + 0.121\ (\text{Water content}) + 2.909 \qquad r^2 = 0.994$

Converting K_{ap} values to $K_{ap}^{0.5}$ values (Fig. 4A Reproduced) yielded a linear regression equation of:

[3] $K_{ap}^{0.5} = 0.085\ \text{Water content} + 0.1433 \qquad r^2 = 0.994$

Fig. 4 Persson et al., 2004

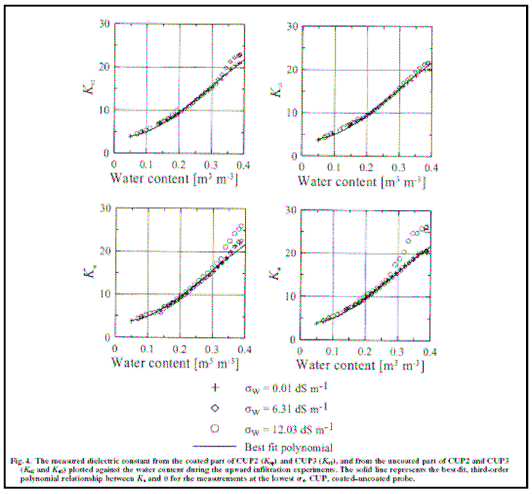

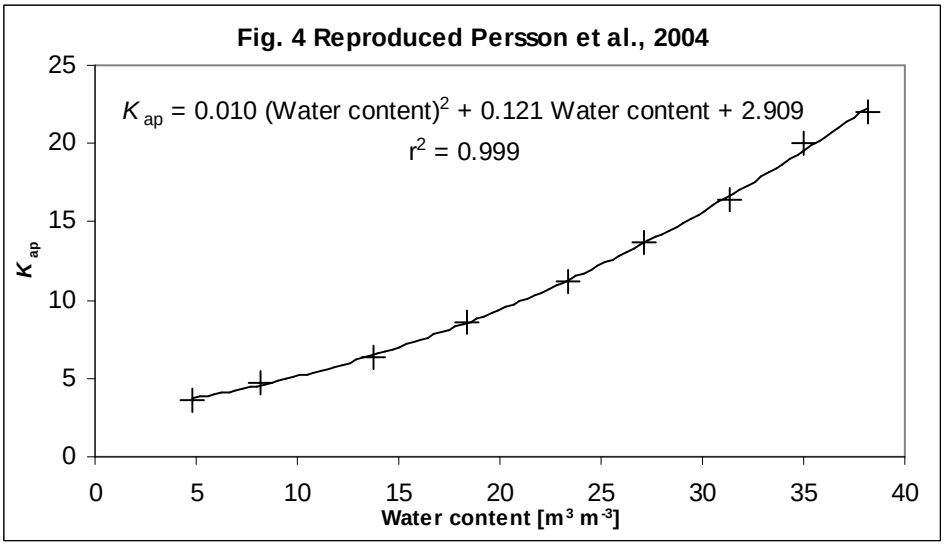
Fig. 4 Reproduced Persson et al., 2004
K_{ap} = 0.010 (Water content)^2 + 0.121 Water content + 2.909
r^2 = 0.999
K_{ap}
Water content [m^3 m^{-3}]
0
5
10
15
20
25
30
35
40

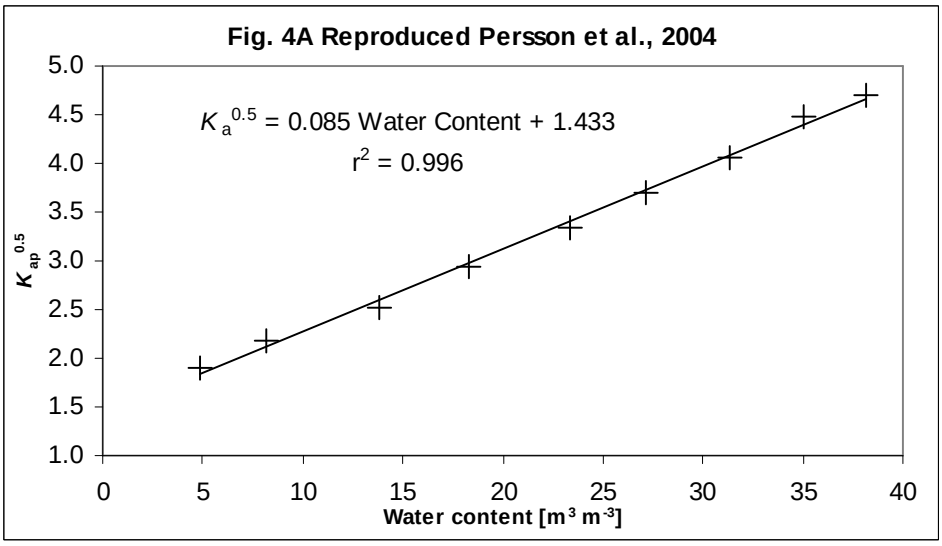
Fig. 4A Reproduced Persson et al., 2004
$K_a^{0.5}$ = 0.085 Water Content + 1.433
r^2 = 0.996
$K_{ap}^{0.5}$
Water content [m^3 m^{-3}]
1.0
1.5
2.0
2.5
3.0
3.5
4.0
4.5
5.0
0
5
10
15
20
25
30
35
40

Staub, M., Laurent, J., Morra, C., Stoltz, G., Gourc, J., and Quintard, M., 2008

Calibration of Time-Domain Reflectometry Probes to Measure Moisture Content in Municipal Solid Waste in Laboratory-Scale Cells. Geo-Environmental Engineering, Kyoto, Japan, June 2008.

In this study, the type of material used for the coated probe was not mentioned, however a Campbell Scientific CS605 probe was used. Results are presented as their Fig. 5. Data transposed from Fig. 5 correspond with the symbol "◊". The regression analysis undertaken was based on the results presented for Volumetric MC with an EC of 0 mS cm^{-1}. The regression analysis (Fig. 5 Reproduced) yielded a linear regression equation of:

[4] Volulmetric MC = 9.992 Travel Time – 39.864 $r^2 = 0.996$

Converting Travel Time to $K_a^{0.5}$ and plotting $K_a^{0.5}$ vs. Volumetric MC (Fig. 5A Reproduced) gives a very strong linear relationship with a regression equation of:

[5] $K_a^{0.5} = 0.050$ Volumetric MC + 1.998 $r^2 = 0.996$

Fig. 5. Staub et al., 2008

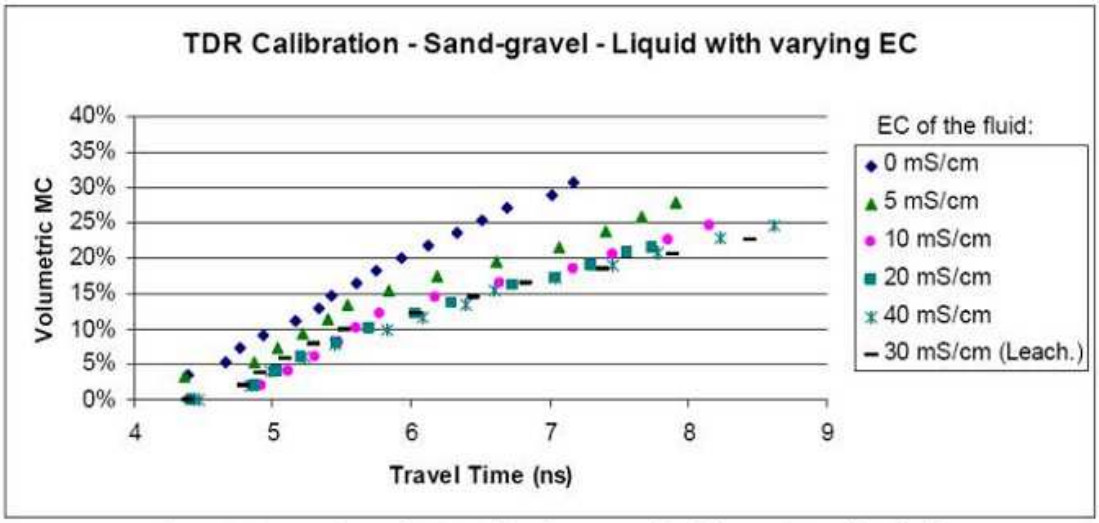

Figure 5: Comparison of TDR calibration curves for different ECs of the fluid.

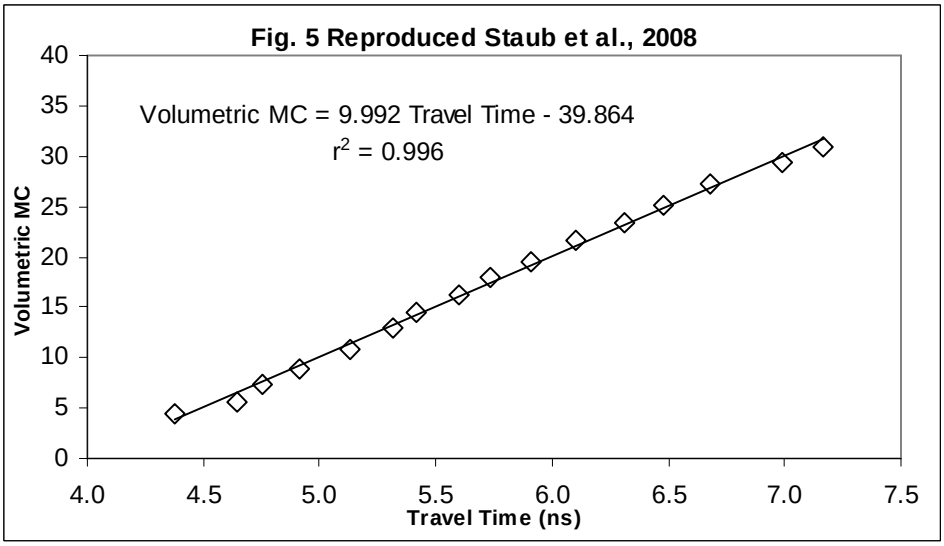
Fig. 5 Reproduced Staub et al., 2008
Volumetric MC = 9.992 Travel Time - 39.864
r2 = 0.996
Volumetric MC
Travel Time (ns)
40
35
30
25
20
15
10
5
0
4.0
4.5
5.0
5.5
6.0
6.5
7.0
7.5

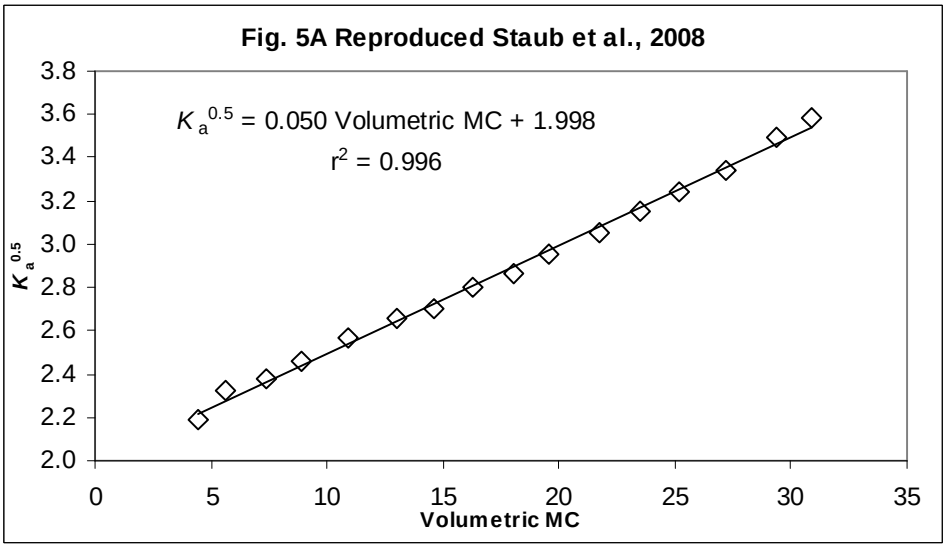
Fig. 5A Reproduced Staub et al., 2008
Ka0.5 = 0.050 Volumetric MC + 1.998
r2 = 0.996
Ka0.5
Volumetric MC
3.8
3.6
3.4
3.2
3.0
2.8
2.6
2.4
2.2
2.0
0
5
10
15
20
25
30
35

Bibliography

Annan, A. P. 1977a. Time-domain reflectometry – air-gap problem in a coaxial line. *Geological Survey of Canada*, Report of Activities, Part B, Paper 77-1B:55-58

Annan, A. P. 1977b. Time-domain reflectometry – air-gap problem for parallel wire transmission lines. *Geological Survey of Canada*, Report of Activities, Part B, Paper 77-1B:59-62

Ansoult, M., de Backer L. W. and Declercq, M. 1984. Statistical relationship between dielectric constant and water content in porous media. *Soil Science Society of America Journal*, 48:47-50

Becker, R. 2004. Spatial time domain reflectometry for monitoring transient soil moisture profiles. Ph.D. Thesis, Institut fur Wasser und Gewasserentwicklung – Bereich Wasserwirtshchaft und Kulturtechnick, Mitteilungen Heft 228, Universitat Karlsruhe

Becker, R., Huebner, C. and Stacheder, M. 2006. Electromagnetic simulation of time domain reflectometry probes: simplified approaches to assess calibration curves, sensitivity, field extent and transient response. *Proceedings TDR 2006*, Purdue University, West Lafayette, USA, Sept. 2006, Paper ID35, 17p, https://engineering.purdue.edu/TDR/Papers

Birchak, J. R., Gardner, C. G., Hipp, J. E. and Victor, J. M. 1974. High dielectric constant microwave probes for sensing soil moisture. *Process IEEE*, 62(1):93-98

Blonquist, J. M., Jones, S. B. and Robinson, D. A. 2005. Standardizing Characterization of Electromagnetic Water Content Sensors: Part 2. Evaluation of Seven Sensing Systems. *Vadose Zone Journal*, 4:1059-1069

Campbell Scientific Inc., 2005. TDR100

Clarkson, T. S., Glasser, L., Tuxworth, R. W. and Williams, G. 1977. An appreciation of experimental factors in time-domain spectroscopy. *Advanced Molecular Relaxation Interaction Processes*, 10:173-202

Dalton, F. N. and Van Genuchten, M. Th. 1986. The time-domain reflectometry method for measuring soil water content and salinity. *Geoderma*, 38:237-250

Dalton, F. N., Herkelrath, W. N., Rawlins, D. S. and Rhoades, J. D. 1984. Time-domain reflectometry: simultaneous measurement of soil water content and electrical conductivity with a single probe. *Science*, 224:989-990

Dasberg, S. and Dalton, F. N. 1985. Time domain reflectometry field-measurements of soil-water content and electrical-conducitivity. *Soil Science Society of America Journal*, 49:293-297

Dascher, D. J. 1996. Measuring parasitic capacitance and inductance using TDR. *Hewlett Packard Journal*

Dobson, M. C., Ulaby, F. T., Hallikainen, M. T. and El-Rayes, M. A. 1985. Microwave dielectric behavior of wet soil. II: Dielectric mixing models. *IEEE Transactions, Geoscience Remote Sensing GE-23*(1):35-46

Fellner-Feldegg, H. 1969. The measurement of dielectrics in the time domain. *Journal of Physical Chemistry*, 73(3):616-623

Ferre, P. A., Rudolph, D. L. and Kachanoski, R. G. 1996. Spatial averaging of water content by time domain reflectometry: Implications for twin rod probes with wand without dielectric coatings. *Water Resources Research*, 32(2):271-279

Ferre, P. A., Knight, D. L., Rudolph, D. L. and Kachanoski, R. G. 1998. The sample areas of conventional and alternative time domain reflectometry probes. *Water Resources Research*, 34(11):2971-2979

Frohlich, H. 1986. Theory of Dielectrics Dielectric Constant and Dielectric Loss Second Edition. *Oxford University Press*, New York, U.S.A.

Fujiyasu, Y., Pierce, C. E., Fan, L. and Wong, C. P. 2004. High dielectric insulation coating for time domain reflectometry soil moisture sensor. *Water Resources Research*, 40, W04602, doi:10.1029/2003WR002460

Giese, K. and Tiemann, R. 1975. Determination of the complex permittivity from thin-sample time domain reflectometry improved analysis of the step response waveform. *Advances in Molecurlar Relaxation Processes*, 7:45-59

Heimovaara, T. J., Huisman, J. A., Vrugt, J. A. and Bouten, W. 2004. Obtaining the spatial distribution of water content along a TDR probe using the SCEM-UA Bayesian inverse modeling scheme. *Vadose Zone Journal*, 3:1128-1145

Heimovaara, T. J., and Bouten, W. 1990. A computer controlled 36-channel time domain reflectometry system for monitoring soil water contents. *Water Resources Research*, 26(10):2311-2316

Herkelrath, W. N., Hamburg, S. P. and Murphy, F. 1991. Automatic, real-time monitoring in a remote field area with time domain reflectometry. *Water Resources Research*, 27(5):857-864

Hook, W. R. and Livingston, N. J. 1996. Errors in converting time domain reflectometry measurements of propagation velocity to estimates of soil water content. *Soil Science Society of America Journal*, 59:35-41

Jackson, H. W. 1976. Introduction to Electric Circuits Fourth Edition. *Prentice-Hall Inc.*, Engelwood Cliffs, New Jersey, U.S.A

Jones, S. B., Blonquist, J. M., Robinson, D. A., Rasmussen, V. P. and Or, D. 2005. Standardizing Characterization of Electromagnetic Water Content Sensors: Part 1. Methodology. *Vadose Zone Journal*, 4:1048-1058

Kellner, E. and Lundin, L. 2001. Calibration of time domain reflectometry for water content in peat soil. *Nordic Hydrology*, 32(4/5):315-332

Knight, J. H. 1992. Sensitivity of time domain reflectometry measurements to lateral variations in water content. *Water Resources Research*, 28(9):2345-2352

Knight, J. H., Ferre, P. A., Rudolph, D. L. and Kachanoski, R. G. 1997. A numerical analysis of the effects of coatings and gaps upon relative dielectric permittivity measurement with time domain reflectometry. *Water Resources Research*, 33(6):1455-1460

Ledieu, J., De Ridder, P. De Clerck, P. and Dautrebande, S. 1986. A method of measuring soil moisture by time-domain reflectometry. *Journal of Hydrology*, 88:319-328

Miyamoto, T. and Maruyama, A. 2004. Dielectric coated water content reflectometer for improved monitoring ofnear surface soil moisture in heavily fertilized paddy field. *Agricultural Water Management*, 64:161-168

Mojid, M. A., Wyseure, G. C. L. and Rose, D. A. 1998. The use of insulated time domain reflectometry sensors to measure water content in highly saline soils. *Irrigation Science*, 18:55-61

Mojid, M. A. and Cho, H. 2002. Response of the core and shield rods of time-domain reflectometry probe to transverse soil-water content heterogeneity. *Journal of Hydrology*, 262:21-27

Nadler, A., Abraham, G. and Peretz, I. 1999. Practical aspects of salinity effect on TDR-measured water content: A field study. *Soil Science Society of America Journal*, 63:1070-1076

Nichol, C., Beckie, R. and Smith, L. 2002. Evaluation of uncoated and coated time domain reflectometry probes for high electrical conductivity systems. *Soil Science Society of America Journal*, 66:1454-1465

Noborio, K. 2001. Measurement of soil water content and electrical conductivity by time domain reflectometry: a review. *Computers and Electronics in Agriculture*, 31:213-237

Or, D., Jones, S. B., VanSharr, J. R., Humphries, S. and Koberstein, L., 2004. *WinTDR Soil Software Analysis User's Guide WinTDR Version 6.1* – Fall 2004

Paquet, J. M., Caron, J. and Banton, O. 1993. In situ determination of the water desorption characteristics of peat substrates. *Canadian Journal of Soil Science*, 73:329-339

Pepin, S., Plamondon, A. P. and Stein, J. 1992. Peat water content measurement using time domain reflectometry. *Canadian Journal of Forest Research*, 22:543-540

Pepin, S., Livingston, N. J. and Hook, W. R. 1995. Temperature-dependent measurement errors in time domain reflectometry determinations of soil water. *Soil Science Society of America Journal*, 59:38-43

Persson, M. and Berndtsson, R. 1998. Texture and electrical conductivity effects on temperature dependency in time domain reflectometry. *Soil Science Society of America Journal*, 62:887-893

Persson, M., Bendz, D. and Flyhammar, P. 2004. Time-domain reflectometry for water content and electrical conductivity measurements in saline porous media. *Vadose Zone Journal*, 3:1146-1151

Robinson, D. A., Jones S. B., Wraith, J. M., Or, D. and Friedman, S. P., 2003a. A review of advances in dielectric and electrical conductivity measurement in soils using time domain reflectometry. *Vadose Zone Journal*, 2:444–475

Robinson, D. A., Schaap, M., Jones, S. B., Friedman, S. P. and Gardner, C. M. K., 2003b. Considerations for Improving the Accuracy of Permittivity Measurement using Time Domain Reflectometry: Air-Water Calibration, Effects of Cable Length. *Soil Science Society of America Journal*, 67:62-70

Roth, K., Schulin, R., Fluhler, H. and Attinger, W. 1990. Calibration of time domain reflectometry for water content measurement using a composite dielectric approach, *Water Resources*

Research, 26(10), 2267-2273, 1990

Roth, C. H., Malicki, M. A. and Plagge, R. 1992. Empirical evaluation of the relationship between soil dielectric constant and volumetric water content as the basis for calibrating soil moisture measurements by TDR. *Journal of Soil Science*, 43:1-13

Schaap, M. G., Robinson, D. A., Friedman, S. P. and Lazar, A. 2003. Measurement and modeling of the TDR signal propagation through layered dielectric media. *Soil Science Society of America Journal*, 67:1113-1121

Shibchurn, A., Van Geel, P. J. and Kennedy, P. L. 2005. Impact of density on the hydraulic properties of peat and the time domain reflectometry (TDR) moisture calibration curve. *Canadian Geotechnical Journal*, 42: 279-286

Staub, M., Laurent, J., Morra, C., Stoltz, G., Gourc, J. and Quintard, M. 2008. Calibration of time-domain reflectometry probes to measure moisture content in municipal solid waste in laboratory-scale cells. *Geo-Environmental Engineering*, 199-205

Sun, Z. J., Young, G. D., McFarlane, R. A. and Chambers, B. M. 2000. The effect of soil electrical conductivity on moisture determination using time-domain reflectometry in sandy soil. *Canadian Journal of Soil Science*, 80:13-22

Topp, G. C., Davis, J. L. and Annan, A. P., 1980. Electromagnetic determination of soil water content: measurements in coaxial transmission lines. *Water Resources Research*, 16(3): 574-582

Topp, G. C., Davis, J. L. and Annan, A. P., 1982. Electromagnetic determination of soil water content using TDR: I. Applications to wetting fronts and steep gradients. *Soil Science Society of America Journal*, 46:672-678

Topp, G. C. and Davis, J. L. 1985. Measurement of soil water content using time-domain reflectometry (TDR): A Field Evaluation. *Soil Science Society of America Journal*, 49:19-24

Topp, G. C., Yanuka, M., Zebchuk, W. D. and Zegelin, S. 1988. Determination of electrical conductivity using time domain reflectometery: soil and water experiments in coaxial lines. *Water Resources Research*, 24(7):945-952

Whalley. W. R. 1993. Considerations on the use of time-domain reflectometry (TDR) for measuring soil water content. *Journal of Soil Science*, 44:1-9

Wyseure, G. C. L., Mojid, M. A. and Malik, M. 1997. A. Measurement of volumetric water content by TDR in saline soils. *European Journal of Soil Science*, 48:347-354

Zegelin, S. J., White, I. and Jenkins, D. R. 1989. Improved field probes for soil water content and electrical conductivity measurement using time domain reflectometry. *Water Resources Research*, 25(11):2367-2376